DWLBC REPORT

Groundwater Recharge Investigations in the Eastern Mount Lofty Ranges, South Australia

2007/20

Government of South Australia
Department of Water, Land and Biodiversity Conservation

Groundwater Recharge Investigations in the Eastern Mount Lofty Ranges, South Australia

Eddie Banks, Tania Wilson, Graham Green and Andrew Love

Knowledge and Information Division
Resource Investigation Group
Department of Water, Land and Biodiversity Conservation

June 2007

Report DWLBC 2007/20

Knowledge and Information Division Resource Investigation Group
Department of Water, Land and Biodiversity Conservation
25 Grenfell Street, Adelaide
GPO Box 2834, Adelaide SA 5001
Telephone National (08) 8463 6946
International +61 8 8463 6946
Fax National (08) 8463 6999
International +61 8 8463 6999
Website www.dwlbc.sa.gov.au

Disclaimer

The Department of Water, Land and Biodiversity Conservation and its employees do not warrant or make any representation regarding the use, or results of the use, of the information contained herein as regards to its correctness, accuracy, reliability, currency or otherwise. The Department of Water, Land and Biodiversity Conservation and its employees expressly disclaims all liability or responsibility to any person using the information or advice. Information contained in this document is correct at the time of writing.

ISBN 978-1-921218-62-0

Preferred way to cite this publication

Banks, EW, Wilson, T, Green, G & Love, AJ 2006, *Groundwater recharge investigations in the Eastern Mount Lofty Ranges, South Australia,* Report DWLBC 2007/20, Government of South Australia, through Department of Water, Land and Biodiversity Conservation, Adelaide.

FOREWORD

South Australia's unique and precious natural resources are fundamental to the economic and social wellbeing of the state. It is critical that these resources are managed in a sustainable manner to safeguard them both for current users and for future generations.

The Department of Water, Land and Biodiversity Conservation (DWLBC) strives to ensure that our natural resources are managed so that they are available for all users, including the environment.

In order for us to best manage these natural resources, it is imperative that we have a sound knowledge of their condition and how they are likely to respond to management changes. DWLBC scientific and technical staff continue to improve this knowledge through undertaking investigations, technical reviews and resource modelling.

Rob Freeman
CHIEF EXECUTIVE
DEPARTMENT OF WATER, LAND AND BIODIVERSITY CONSERVATION

CONTENTS

LIST OF FIGURES

LIST OF TABLES

EXECUTIVE SUMMARY

The Mount Lofty Ranges provide important surface water and groundwater resources for domestic, industrial and agricultural purposes. Development and implementation of the Water Allocation Plan for the Eastern Mount Lofty and Western Mount Lofty Ranges will ensure that current and future use of these resources are sustainable and that the environment is also recognised as a user of the resource.

Technical investigations are being conducted to determine the various components of the water balance, which are essential to the development of the Water Allocation Plan. The most important components that need to be quantified in the groundwater balance are vertical recharge and discharge rates, and horizontal flow velocities. Determining these components in fractured rock aquifers is extremely difficult because the groundwater is stored in, and moves through, fractures and joints in what is essentially impervious rock.

The primary aim of this investigation is to assist in the development of water allocation policy by estimating the recharge rate to the fractured rock aquifer system at selected sites in the Burra Creek, Angas River and Finniss River Catchments, respectively the Burra, Bull Creek and Ashbourne investigation sites. This will provide sound knowledge with which to estimate recharge rates at a catchment scale and assist in the development of a conceptual model of the fractured rock aquifer systems in these three catchments.

Groundwater solutes within the shallow and deep aquifer systems at the Burra, Bull Creek and Ashbourne sites are primarily derived from marine aerosols that have been concentrated by evapotranspiration prior to recharge. There is no evidence of any significant contribution from mineral weathering and water–rock interaction to the groundwater samples, which are dominated by sodium and chloride ions.

At the Burra investigation site there is a local, shallow flow system with a perched watertable overlying a deeper flow system divided by a semi-confining layer of clay and weathered slate between 33–45 m. In the shallow flow system, vertical circulation of groundwater is particularly slow compared to the deeper flow system, which appears to be recharged more rapidly as indicated by the chlorofluorocarbon apparent-age gradient. Carbon-14, hydrochemistry and isotope results indicated that there is connection between the shallow and deep systems. Horizontal flow in the deep system was typically less than 2 m/y at the time of sampling.

At the Bull Creek site there is good hydraulic connection between the shallow regolith zone and the fractured rock aquifer system below. The chlorofluorocarbon and carbon-14 data showed that there is a linear age gradient increasing with depth, which suggests that direct recharge is the predominant mechanism at the site. Modern groundwater (<40 years) was measured to at least 20 m depth, whilst at 60 m the groundwater has a carbon-14 uncorrected age of about 1500 years. At about 15 m, the groundwater exhibits a strong transpiration signature implying active uptake of water by vegetation at this depth. Horizontal flow at the site was less than 3 m/y below 20 m depth at the time of sampling.

Similar to the Burra site, Ashbourne is characterised by two aquifer flow systems — a local shallow system to about 25 m, separated from an underlying deeper fractured rock system by a 15 m thick confining layer. Chlorofluorocarbon and carbon-14 results were consistent and showed that groundwater in the shallow system is less than 40 years old, whilst groundwater in the deeper system is much older (~1500 years) with a strong vertical connection between fractures. Groundwater in the shallow system has a much higher salinity than the deeper system and indicates processes of transpiration and mechanisms of direct recharge. Horizontal flow measurements made at the site were typically less than 2 m/y, at the time of sampling, between 20–90 m depth.

Assuming only two-thirds of the resource can be extracted, according to the chlorofluorocarbon-12 recharge estimates, ~10, 12 and 15 mm/y is available for allocation in the Burra Creek, Angas and Finniss River Catchments. The amount of water available to each user will need to be determined in accordance with the Water Allocation Plan.

1. INTRODUCTION

1.1 FRACTURED ROCK AQUIFERS

The Mount Lofty Ranges (MLR) provide important surface water and groundwater resources for domestic, industrial and agricultural purposes locally, as well as metropolitan Adelaide's reticulated water supply. Development and implementation of the Water Allocation Plan (WAP) for the Eastern Mount Lofty Ranges (EMLR) and Western Mount Lofty Ranges (WMLR) will ensure that current and future uses of these resources are sustainable and that the environment is also recognised as a user of the resource.

Currently, technical investigations are being conducted to determine the various components of the water balance, which are essential to the development of the WAP. The long-term sustainability of the groundwater resource requires careful estimates of the magnitude of all components of the groundwater budget. The most important components that need to be quantified are vertical recharge and discharge rates, and horizontal flow velocities. Determining these components in fractured rock aquifers (FRA) is extremely difficult because the groundwater is stored in, and moves through, fractures and joints in what is essentially impervious rock. Traditional investigation techniques applied to sedimentary systems have limited applicability to FRA systems. However, several techniques developed recently have been applied to the FRA in the Clare Valley (Cook et al. 1999; Cook & Simmons 2000; Love et al. 2002, in prep.). These techniques were successful in estimating the components of the groundwater budget and provided sound knowledge in understanding some of the complexities of FRA to develop a conceptual model of the groundwater flow system.

A similar approach has been used in this investigation of the Burra Creek Catchment (BCC), Angas River Catchment (ARC) and Finniss River Catchment (FRC) as well as other regions in the MLR. The techniques include borehole downhole geophysics, geological fracture mapping, aquifer tests and vertical profiling of groundwater chemistry, isotopes and radioactive tracers. Downhole geophysics was used to indicate physical properties, lithology and porosity of the rock formations. Fracture location, orientation and groundwater flow can also be determined using downhole geophysics. Structural mapping of surface outcrop provided details of fracture spacing and their dominant orientations. Aquifer tests provided information on fracture aperture. Groundwater chemistry, specifically chlorofluorocarbon and carbon-14 analyses, provides information on the groundwater age. From this estimated age it is possible to make inferences about the recharge rate; generally, young ages will indicate relatively high recharge rates and conversely old groundwater ages indicate lower recharge rates.

1.2 AIMS AND OBJECTIVES

The following investigation aims to provide technical information to support the successful implementation of the WAP for the EMLR. Specifically, this investigation will:

- determine the recharge rate to the FRA system at the Burra, Bull Creek and Ashbourne investigation sites in the BCC, ARC and FRC, respectively

- estimate horizontal flow at Burra, Bull Creek and Ashbourne investigation sites in the BCC, ARC and FRC
- provide sound knowledge to estimate recharge rates at a catchment scale
- assist in the development of a conceptual model of the FRA system in the BCC, ARC and FRC.

2. EMLR CATCHMENTS

2.1 BURRA CREEK CATCHMENT

The BCC covers an area of ~937 km^2 (Figs 2.1, 2.2). It is in the northernmost extent of the greater MLR, extending from the eastern side of the ranges and across the flat plains of the Murray Basin where the Burra Creek discharges into the River Murray at the township of Morgan. Creeks are typically ephemeral, with Burra Creek as the only permanent water source in the northern section of the catchment. The township of Burra is in the northern arm of the catchment, which is characterised by sparsely vegetated undulating hills up to 850 m in elevation. Extensive vegetation clearing for the development of pasture and livestock grazing in the last hundred years and the operation of the historic copper mine in the Burra township have had a considerable impact on the hydrological cycle. Clearing of vegetation associated with these activities is likely to have increased potential groundwater recharge to the catchment.

2.1.1 CLIMATE

The climate in the Burra region is characterised by hot dry summers and cool wet winters. The average annual rainfall is ~300–500 mm/y in the northwestern arm of the catchment compared to less than 300 mm/y across the low, flat plains in the eastern reach of the BCC. The decrease in rainfall from the western margin to the eastern part of the catchment is strongly correlated to the changes in topography and the effects of orographic relief on rainfall patterns (Fig. 2.2). The majority of the rainfall occurs between the months of late April–May through to September.

2.1.2 GEOLOGY

The geology of the BCC is dominated by sequences of the Burra Group, specifically the Skillogalee Dolomite, Woolshed Flat Shale, Undalya Quartzite, Saddleworth Formation and Mintaro Shale.

Deposition of the Burra Group sediments occurred during the Adelaidean between 850 and 540 million years ago. The shallow marine sediments of the Skillogalee Dolomite were deposited in a fault-controlled rift basin within the Adelaide Geosyncline. Subsequent marine transgressions resulted in deposition of deeper water sediments, such as the overlying Woolshed Flat Shale, Undalya Quartzite and Saddleworth Formation. Deformation and low-grade metamorphism occurred during the Cambro-Ordovician Delamerian Orogeny. This orogenic event resulted in north–south-trending folds with plunge reversals along the fold axes. A north–south-trending fault developed in the Skillogalee Dolomite and, with hydrothermal fluids migrating along this structure, resulted in focusing of copper mineralisation associated with the Burra Mine (Gravestock & Gatehouse 1995).

Figure 2.1 Burra, Angas and Finniss Catchment Locations

Burra Creek Catchment
Finniss Catchment
Angas Catchment
Eastern Mount Lofty Ranges
Western Mount Lofty Ranges
Major towns
Major streams
Catchment boundaries

Produced By: Mount Lofty Ranges Team
Knowledge and Information Division
Department of Water, Land and Biodiversity Conservation

Datum: Geocentric Datum of Australia 1994 (GDA 94).

Date: 17th July 2006

N

0 10 20 30 40 50 km

Government of South Australia
Department of Water, Land and Biodiversity Conservation

M:\Projects_GWMt_Lofty_Ranges\EMLR 2006\Angas\Angas_State_location.mxd 17 July 2006 E. Banks

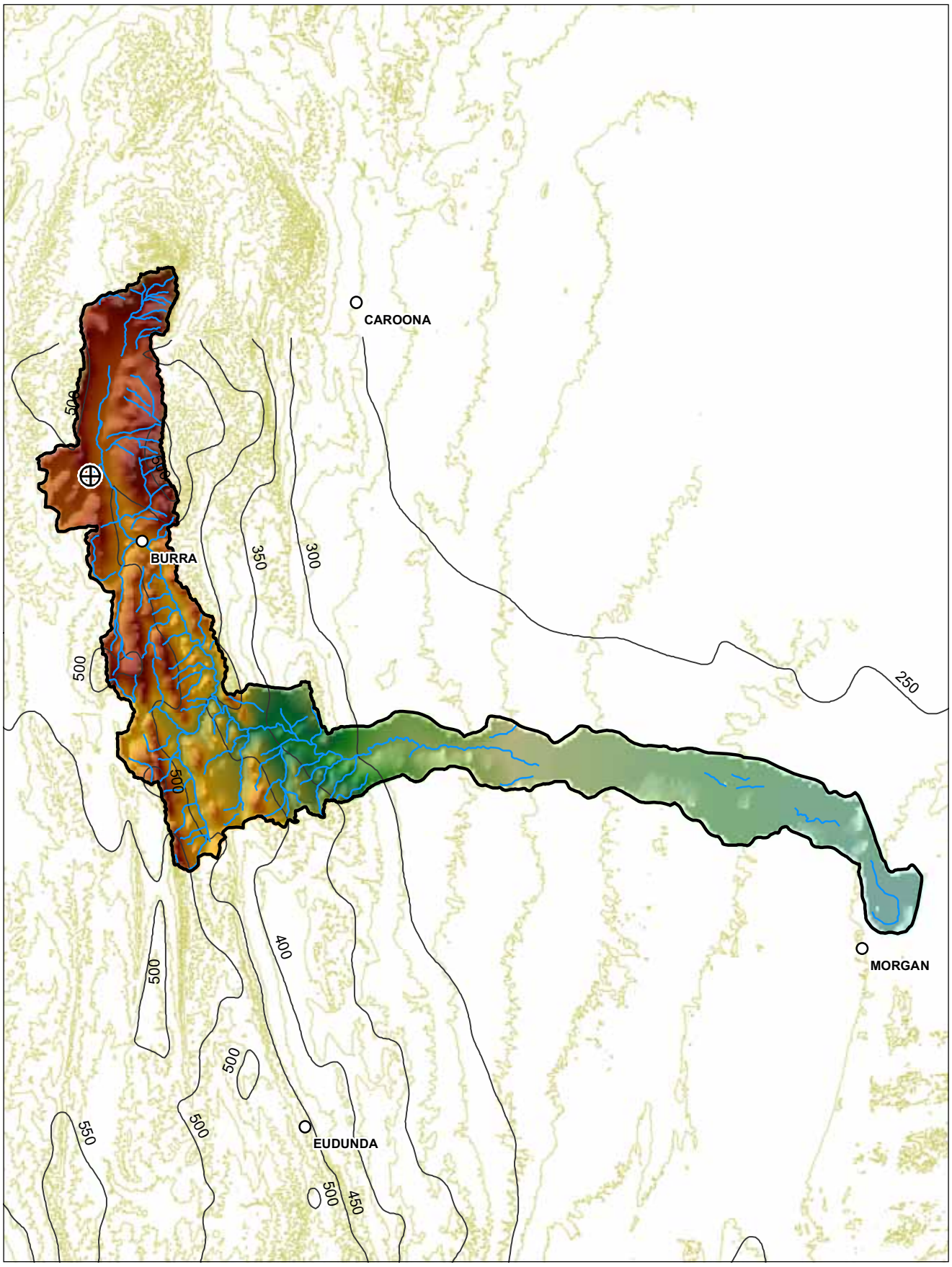

Elevation (m ASL)

Value

High : 850

Low : 10

Catchment boundaries

Burra investigation site

Annual rainfall isohyets (50 mm)

Topographic contours (40 m)

Streams

Towns

0 5 10 15 20 25 km

Fig 2.2 Burra Creek Catchment

Produced By: Mount Lofty Ranges Team
Knowledge and Information Division
Department of Water, Land and Biodiversity Conservation

Datum: Geocentric Datum of Australia 1994 (GDA 94).

Date: July 2007

N

Government of South Australia
Department of Water, Land and Biodiversity Conservation

M:\Projects_GW\Mt_Lofty_Ranges\EMLR 2006\Burra\Work_temp\Burra_location.mxd 18 July 2006 G. Green

Locally, the investigation site in the BCC is situated in the Saddleworth Formation of the Burra Group (Fig. 2.3). Slate, and minor metasandstone, of unknown thickness dominates the geology at this site. A shallow regolith zone overlies these Adelaidean sequences.

The slate is pale olive to light grey in colour and exhibits a well-developed slaty cleavage. Minor muscovite is observed throughout the slate. Minor quartz vein material and pyrite mineralisation occur at depths exceeding 60 m. Weathering within the slate is observed to depths of ~33 m. Iron staining is common throughout along cleavage and fracture surfaces to depths of 60 m. Minor dendritic manganese is observed at shallow depths associated with the upper weathered zone.

Overlying the slate is a regolith zone extending to a depth of ~16 m, within which the basal section (8–16 m) consists of silty clay with minor weathered slate fragments. Minor silcrete lenses are observed between 8 and 10 m and are of limited spatial distribution. These lenses appear to result in localised perched watertables. These sediments are overlain by ~8 m of clay. Detailed lithological drilling logs are included in Appendix B.

2.1.3 HYDROGEOLOGY

The BCC can be considered to have two distinct hydrogeological sections. A western limb, orientated from north to south at the western side of the catchment is characterised by a FRA system formed within metasiltstone and slate of the Saddleworth Formation in the sequences of the Burra Group. A distinct southern limb is orientated east to west along the southern end of the catchment. This southern limb is characterised by a topographically lower sedimentary valley system in a section of the sedimentary clay and sand formations of the lower Murray Group sediments (Fig. 2.3). It is inferred that the FRA system of the western limb discharges into the sedimentary system of the southern limb, although there is some debate as to whether the sedimentary system receives water from a local or regional aquifer system. This investigation addresses only the FRA in the upper BCC, as there are currently no suitably constructed wells in the sedimentary system to apply the specialised hydrogeological techniques used in this study.

Figure 2.4 shows a map of groundwater potentiometric surface elevation (m AHD) for the BCC. Groundwater head elevation tends to mirror the land surface elevation and is highest in the northwestern end of the catchment, where the surface topography is highest, and lowest in the eastern part of the catchment, where the surface topography descends to the lower elevation of the River Murray basin. The direction of groundwater flow is from high to low potentiometric elevation.

The potentiometric surface contours provide a more detailed analysis of groundwater flow direction; the generalised groundwater flow direction is at 90° to the contour lines. It can be seen that in the upper northern and western parts of BCC, where topography is relatively steep, flow is generally from north to south and towards valley bottoms in the middle of the catchment, where it may either discharge to streams and/or receive recharge from losing streams. In the southern and eastern parts of the catchment, flow is generally in an easterly direction, possibly discharging from FRA systems of the upper catchment into sedimentary aquifers of the lower catchment.

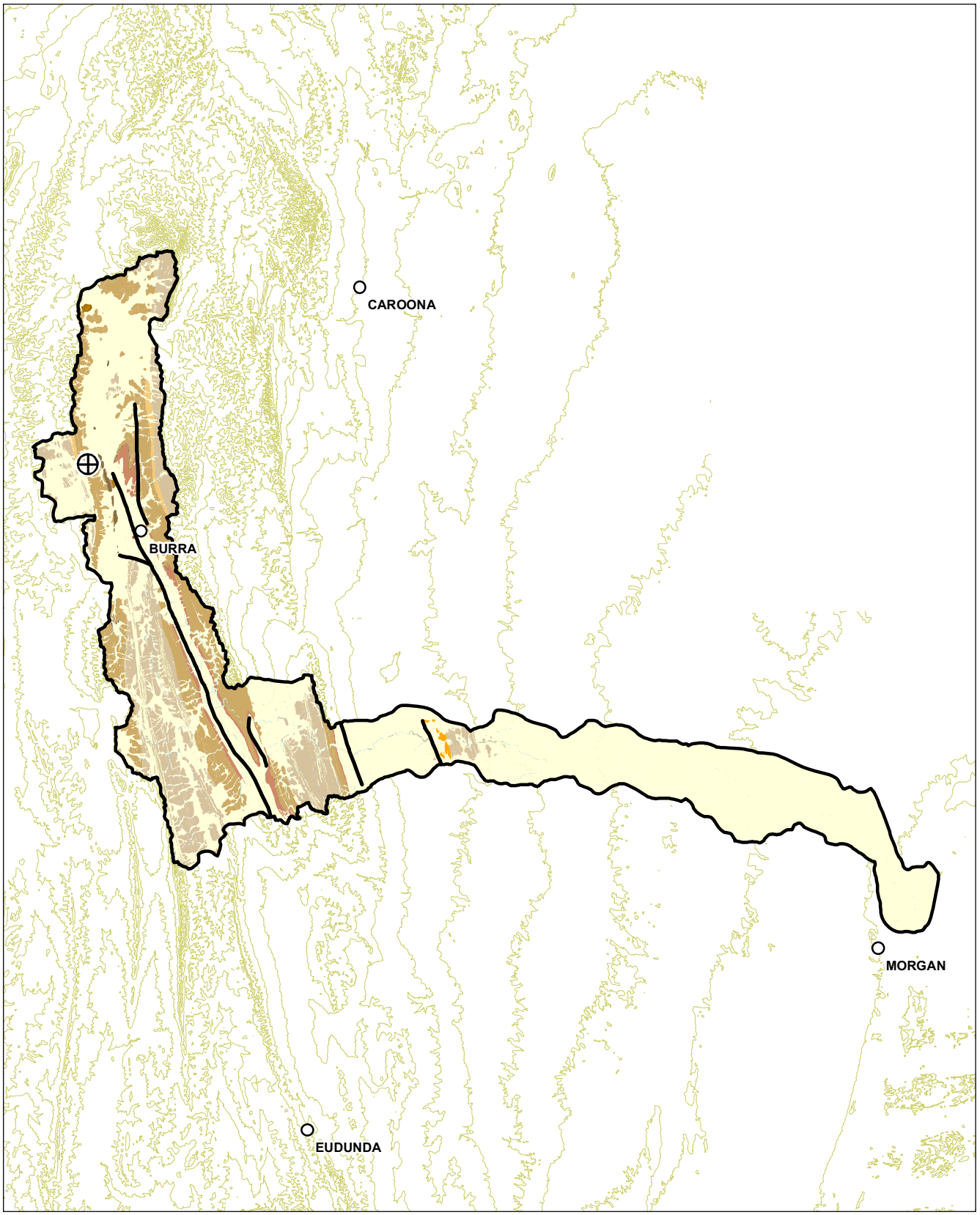

Geology

- Undifferentiated Quaternary and Tertiary sediments
- Wilpena Group
- Umberatana Group
- Mintaro Shale
- Saddleworth Formation
- Undalya Quartzite
- Woolshed Flat Shale
- Skillogalee Dolomite
- Rhynie Sandstone
- Callanna Group

- Towns
- Burra investigation site
- Streams
- Contour (40 m)
- Major Faults
- Catchment boundary

Figure 2.3 Burra Creek Catchment Geology

Produced By: Water Information Group
Knowledge and Information Division
Department of Water, Land and Biodiversity Conservation

Datum: Geocentric Datum of Australia 1994 (GDA 94).

Date: 18th July 2006

N

0 5 10 15 20 25 km

Government of South Australia
Department of Water, Land and Biodiversity Conservation

M:\Projects_GWMI_Lofty_Ranges\EMLR 2006\Burra\Burra_Geology.mxd 18 July 2006 G. Green

Figure 2.4 also shows salinity, as indicated by electrical conductivity (EC), of bore water within the BCC. The majority of bores are located in the northern part of the western limb of the BCC, and are generally in close proximity to surface water features, where the watertable is at a shallower depth. Bore water EC ranges from ~265 μS/cm to over 20 000 μS/cm. No observable trends in groundwater salinity occur throughout the catchment, but there are localised areas of high groundwater EC compared to the rest of the catchment. These are in the southern limb of the catchment, on the slopes between the upper and lower parts of the catchment, and in the easternmost reach of the catchment, close to the River Murray.

2.1.3.1 Groundwater Potentiometric Surface Map of the Burra Creek Catchment

The groundwater potentiometric surface shown in Figure 2.4 was created by using the ARC GIS inverse difference weighted (IDW) interpolation function to calculate groundwater head elevations in 2546 boreholes within and surrounding the BCC area. Many of the groundwater extraction bores within the study area have not been surveyed for surface elevation and do not have data for reduced standing water levels (RSWL). To obtain an approximation of the RSWL for bores that do not have these data available, the GIS coverage of bores within the study area was overlain on a Digital Elevation Model (DEM) of the study area to obtain a surface elevation of each bore. The latest standing water level (SWL) measurement for each bore was then subtracted from the derived surface elevation to determine an approximate RSWL.

The potentiometric surface elevations indicated by the bores are supplemented by ground surface elevation data derived from the elevation of points along creeks throughout the catchment and within 6 km of the catchment boundary. The mid-point of each stream reach within the study area was overlain on the DEM and an elevation was assigned. While it is recognised that the elevation of the stream reach mid-points do not necessarily represent groundwater elevations, they provide an approximation of groundwater elevation along valley bottoms. It is assumed that groundwater surface elevations mirror the land surface topography and that the stream bed is a point of either recharge or discharge of groundwater and is located close to groundwater surface elevation.

The groundwater surface contours shown are constructed according to the IDW surface interpolation. The interpolated surface was constructed from a network of points that extended to a distance beyond the boundaries of the catchments; however, the illustrated surface has been clipped to the extent of the BCC area.

The map can only be taken as an approximation of the groundwater potentiometric surface elevations. There are several reasons for inaccuracies in the potentiometric surface derived by the method described:

1. The derivation of borehole surface elevation by overlaying borehole positions on a DEM relies on the accuracy of the DEM at all points. As the DEM is constructed from an interpolation of a grid of points of measured elevation, it cannot be expected to depict an accurate elevation at all points.
2. The SWL measurements and RSWL data are valid for the point in time that the measurement was made. Groundwater level is expected to change both seasonally and over longer time periods as the aquifers respond to changes in groundwater extraction rates and recharge. The dates of SWL or RSWL measurements in the database of

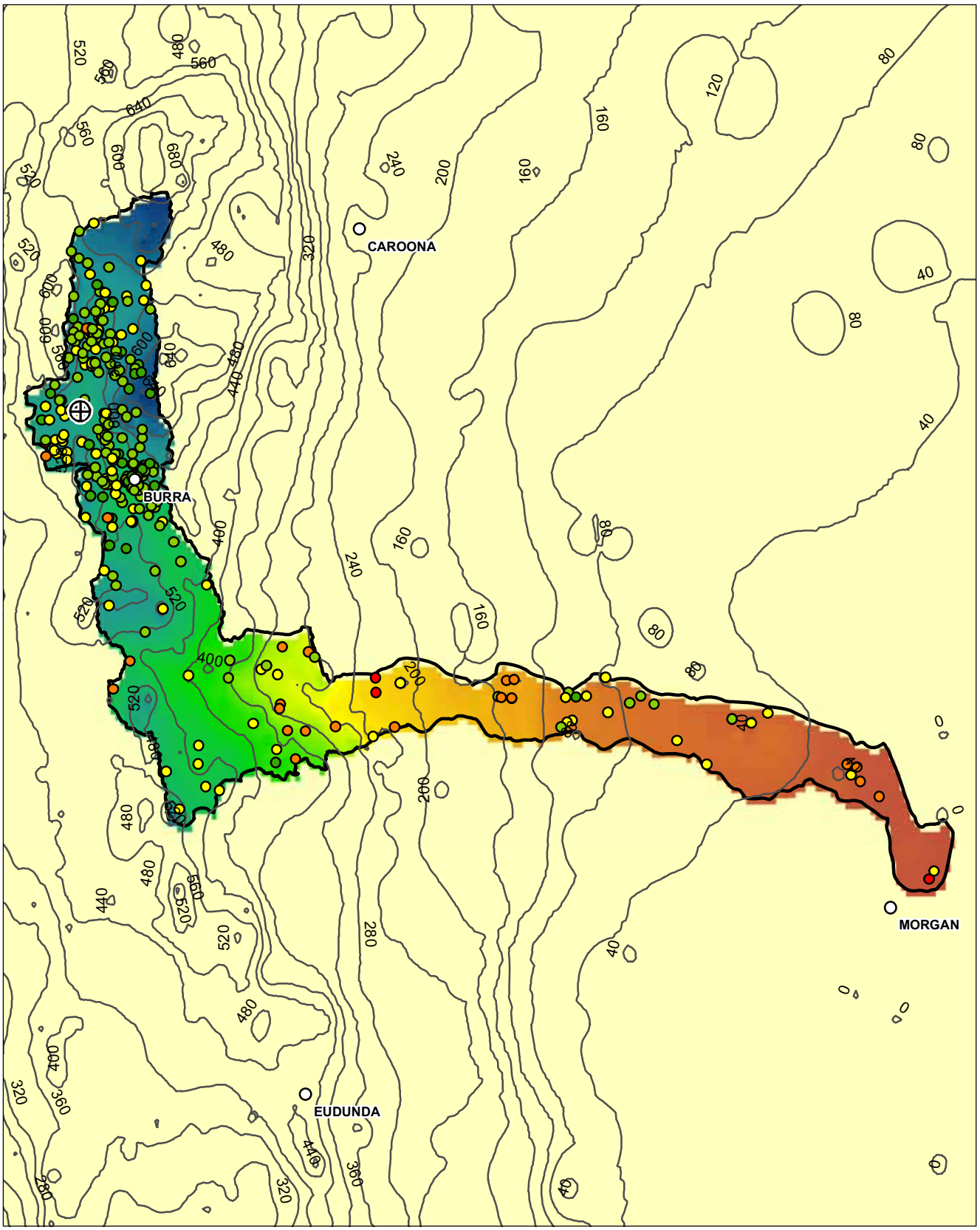

Figure 2.4 Burra Creek Catchment Groundwater Potentiometric Surface

Bore water EC (uS/cm)

- 250 - 2500
- 2501 - 5000
- 5001 - 10000
- 10000 - 15000
- 15000 +

Burra Creek catchment boundary

Groundwater potentiometric surface elevation (m AHD)

High : 660

Low : 0

Groundwater potential contours (40 m)

Burra Investigation Site

Produced By: Mount Lofty Ranges Team
Knowledge and Information Division
Department of Water, Land and Biodiversity Conservation

Datum: Geocentric Datum of Australia 1994 (GDA 94).

Date: August 2006

N

0 5 10 15 20 km

Government of South Australia
Department of Water, Land and Biodiversity Conservation

M:\Projects_GW\Mt_Lofty_Ranges\EMLR 2006\BurraWork_temp\Mamre_Upper_Pot_Contours.mxd 17 August 2006 G. Green

boreholes used for the groundwater potentiometric surface cover a range of 30 years. For the purposes of constructing the potentiometric surface, all boreholes in that database with SWL measurements prior to 1976 were excluded.

3. The derived map presents the groundwater surface as a continuous surface over the whole study area. In reality, groundwater may exist in numerous discrete aquifers such that at any point in the landscape there may be more than one true groundwater potentiometric level, depending on the arrangement of unconfined and confined aquifers underlying that point.
4. The derived groundwater potentiometric surface is an interpolation of individual points with varying degrees of spatial separation. The derived surface is a 'best fit' approximation of a continuous surface passing through, or close to, the measured elevations at these points.

In view of these sources of inaccuracy in the derived potentiometric surface, the map should not be used to determine a definitive groundwater head elevation at any particular point within the study area. The purpose of the map is to give an indication of relative groundwater head elevations such that the general directions of groundwater flow through the study area can be envisaged.

2.2 ANGAS RIVER AND FINNISS RIVER CATCHMENTS

The ARC covers an area of ~200 km^2 (Figs 2.1, 2.5). The catchment runs in a southeasterly direction and ranges in elevation from 450 m along the western boundary to about 50 m at the southeastern tip where the Angas River flows intermittently across the flat plains into Lake Alexandrina. The major land uses in the catchment are dairying, irrigated pasture and livestock grazing, and some viticulture (Zulfic & Barnett 2003).

The FRC covers an area of 375 km^2 and is adjacent to the ARC (Figs 2.1, 2.5). Along its western boundary the elevation is ~400 m above sea level, decreasing to ~20 m in the lower reaches of the Finniss River where it discharges into Lake Alexandrina behind Hindmarsh Island. As with the ARC, the major land uses in the FRC are livestock grazing and dairying as well as forestry and conservation areas. Along some of the wider alluvial valleys there is horticultural and vegetable development.

2.2.1 CLIMATE

The ARC has cool wet winters and typically hot dry summers. The long-term average annual rainfall for the ARC, measured at the township of Macclesfield, is 733 mm/y. Rainfall is winter dominant, falling between the months of April and October, and decreases significantly from the western margin to the lower eastern reaches of the ARC where the average is less than 450 mm/y.

The investigation site in the FRC is just outside the township of Ashbourne where there has been 117 years of climate data collection. The average annual rainfall at Ashbourne is 674 mm, which is in the middle of the catchment and in between the rainfall stations at Meadows and Finniss where the average annual rainfall is 877 and 488 mm, respectively (Zulfic & Barnett 2003). Similar to the ARC, the rainfall is winter dominant, falling between April and October. Savadamuthu (2003) reported the long-term rainfall records from the

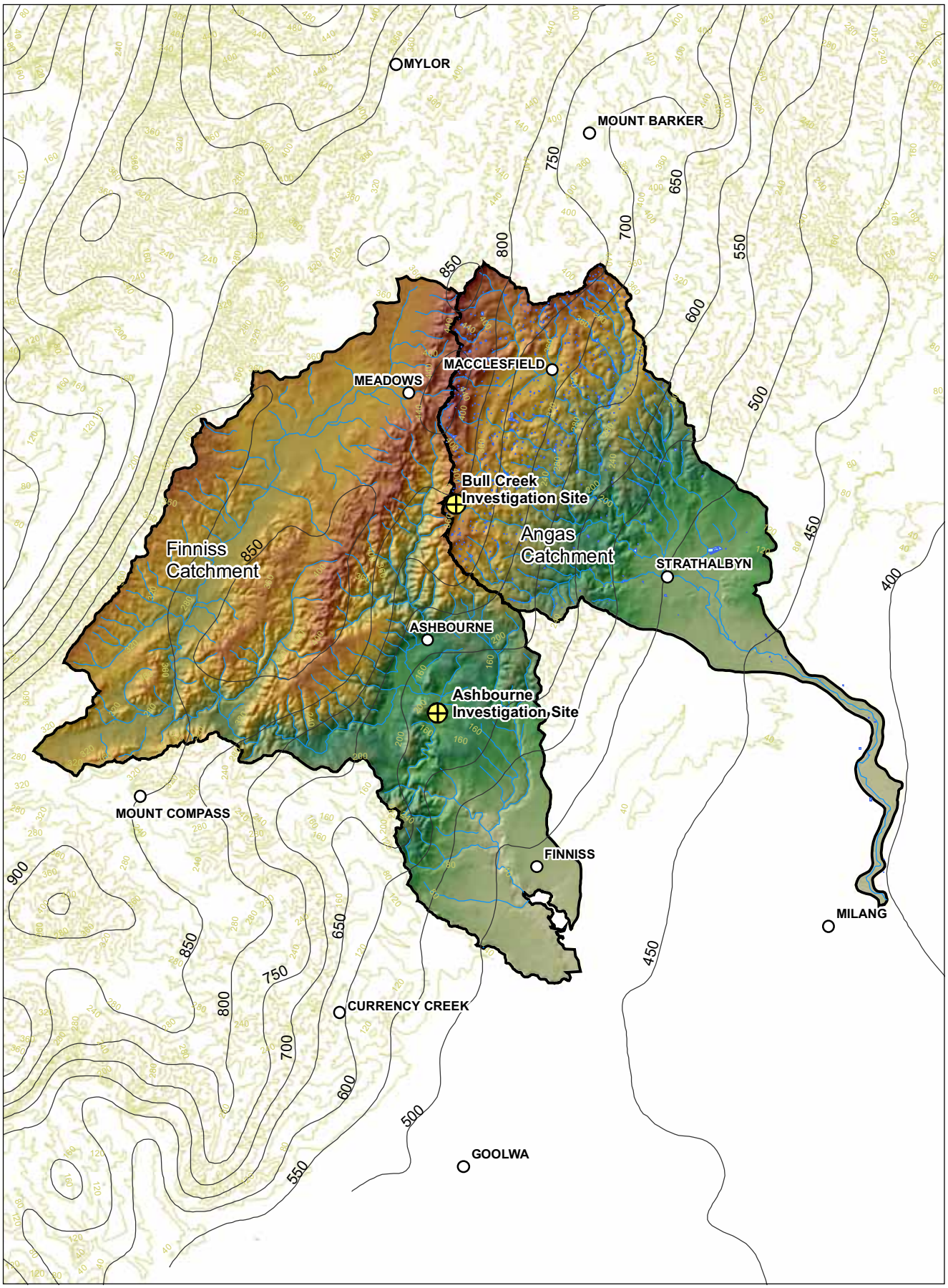

Elevation (m ASL)

Value

High : 500

Low : 0

Groundwater investigation site

Catchment boundaries

Town

Farm dams

Annual rainfall isohyets (50 mm)

Topographic contours (40 m)

Streams

Figure 2.5 Catchments of the Angas and Finniss Rivers

Produced By: Mount Lofty Ranges Team
Knowledge and Information Division
Department of Water, Land and Biodiversity Conservation

Datum: Geocentric Datum of Australia 1994 (GDA 94).

Date: 17th July 2006

N

0 2 4 6 8 10 km

Government of South Australia
Department of Water, Land and Biodiversity Conservation

M:\Projects_GW\MLR_LofY_Ranges\EMLR 2006\Angas\Angas_Finniss_location.mxd 17 July 2006 G. Green

Upper Finniss sub-catchment showing an overall decreasing trend in annual rainfall, with the decline being more pronounced in the last 20 years. It was also noted that runoff from this catchment is highly variable and dependent on rainfall, with a runoff coefficient of 0.17 (17%), which is relatively high in comparison to other catchments in the EMLR. The FRC also has one of the highest farm dam densities in the EMLR, which substantially reduces surface flows through the catchment.

2.2.2 GEOLOGY OF THE ANGAS AND FINNISS RIVER CATCHMENTS

On a regional scale, the geology of the ARC and FRC is highly variable and includes a significant portion of the stratigraphic sequence associated with the Adelaide Geosyncline. Outcrops of basement inliers, namely the Barossa Complex, occur within the FRC. Outcropping stratigraphic sequences of the Neoproterozoic Burra Group, Umberatana Group and Wilpena Group occur, as well as the Cambrian Kanmantoo Group. Deformation associated with the Cambro-Ordovician Delamerian Orogeny has resulted in the development of a north–south-trending, south-plunging anticline–syncline pair that is spatially associated with these catchments (Gravestock & Gatehouse 1995).

On a local scale, the investigation site in the ARC is within the Adelaidean Wilpena Group, specifically the Brachina Formation. Light grey metasiltstone with a well-developed cleavage characterises the geology. Minor muscovite, pyrite and quartz vein fragments are observed at depths exceeding 20 m. Silicification of the sediments has also occurred at depths greater than 45 m. Weathering is observed to depths of ~25 m, with iron staining on cleavage and fracture surfaces apparent at depths greater than 25 m.

A regolith zone is developed to a depth of ~25 m, which consists of highly weathered, friable metasiltstone in the basal section (4–25 m), overlain by clayey sand. Lithological logs of the regolith zone are provided in Appendix B.

In the FRC, the investigation site is within the Kanmantoo Group, specifically the Tapanappa Formation. Grey, laminated, metasiltstone with a well-developed cleavage and metasandstone dominate the geology. Weathering occurs to a depth of ~30 m, with iron staining on cleavage and fracture surfaces continuing to be observed at depths exceeding 30 m.

A surficial regolith zone extends to ~10 m depth. The basal section (6–10 m) consists of highly weathered and friable metasiltstone, overlain by silty sand and minor gravel. Detailed lithological logs are provided in Harrington et al. (2004).

2.2.3 HYDROGEOLOGY OF THE ANGAS RIVER AND FINNISS RIVER CATCHMENTS

2.2.3.1 Angas River Catchment

Groundwater in the ARC occurs primarily in FRA of the Kanmantoo Group. The lower, southeastern part of the catchment is characterised by unconsolidated sediments typical of the Quaternary clay, sand and gravel deposits of the Murray Basin (Fig. 2.6).

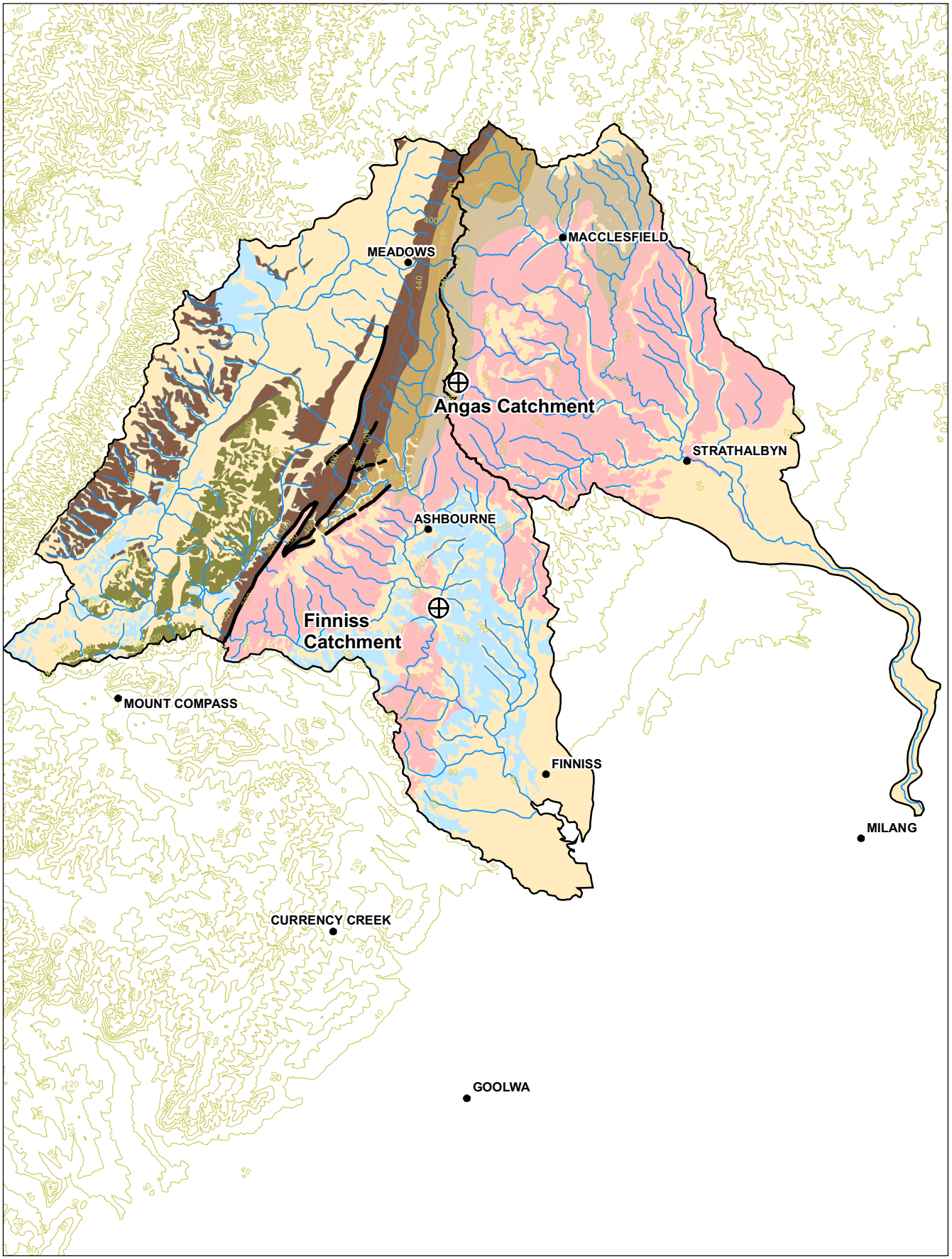

Towns
Groundwater investigation site
Catchment boundaries
Streams
Contour (40 m)
Major Faults

Geology

- Undifferentiated Quaternary and Tertiary sediments
- Cape Jervis Formation
- Kanmantoo Group
- Wilpena Group
- Umberatana Group
- Burra Group
- Barossa Complex

N

0 2 4 6 8 10 km

Figure 2.6

Geology of the Angas and Finniss River Catchments

Produced By: Mount Lofty Ranges Team
Knowledge and Information Division
Department of Water, Land and Biodiversity Conservation

Datum: Geocentric Datum of Australia 1994 (GDA 94).

Date: 17th July 2006

Government of South Australia
Department of Water, Land and Biodiversity Conservation

M:\Projects_GWMt_Lofty_Ranges\EMLR 2006\Angas\Angas_Finniss_Geology.mxd 17 July 2006 G. Green

Figure 2.7 shows a map of groundwater potentiometric surface elevation (m AHD) for the catchments of the Angas and Finniss Rivers. In the ARC, the groundwater potentiometric surface elevation tends to follow the land surface elevation and is highest in the northwestern part of the catchment, where the surface topography is greatest, and lowest in the southeastern part of the catchment, where the surface topography descends to approximately sea level at the northern edge of Lake Alexandrina. Groundwater flow in the catchment is dictated by this descent in the potentiometric head elevation. Hence, groundwater flow throughout the majority of the ARC area is in a southeasterly direction.

As groundwater appears to flow fairly uniformly from northwest to southeast, it is inferred that the FRA system of the upper catchment discharges into the sedimentary system of the lower catchment. However, this investigation addresses only the FRA along the western boundary of the ARC, as there are currently no suitably constructed nested piezometers in the sedimentary system to apply the specialised hydrogeological techniques used within this study.

The majority of bores are located in the northern part of the catchment but there is also a large number of bores close to the Angas River in the lower southeast portion (Fig. 2.7). Bore water EC ranges from ~100 μS/cm to over 25 000 μS/cm; bores of higher salinity appear predominantly in the middle of the catchment on the slopes between the upper and lower parts of the catchment.

2.2.3.2 Finniss River Catchment

Groundwater in the FRC occurs within Permian glacial and fluvioglacial deposits of the Cape Jervis Formation as well as in FRA within the sedimentary and metamorphic rocks of the Kanmantoo Group. The lower, southeastern part of the catchment is characterised by unconsolidated sediments typical of the Quaternary clay, sand and gravel deposits of the Murray Basin (Fig. 2.6).

Figure 2.7 shows the groundwater potentiometric surface elevation (m AHD) for the catchments of the Angas and Finniss Rivers; the same limitations apply to the accuracy and interpretation of the potentiometric surface as were described in section 2.1.3 in relation to the potentiometric surface map of the BCC (Fig. 2.4). Hence the map is intended only to give an indication of relative groundwater head elevations such that the general directions of groundwater flow through the study area can be envisaged.

In the FRC, the potentiometric surface is highest in the northern part of the catchment, where the surface topography is highest, and lowest in the southeastern portion, where the surface topography descends to approximately sea level at the northern edge of Lake Alexandrina. However, in the upper, northwestern part of the catchment, there is a distinct northeast–southwest-trending valley, which causes the groundwater potential gradient and resulting groundwater flow to be in a northwesterly direction in some places. Groundwater in the northwestern side of the catchment may flow in a northwesterly direction and discharge in the adjacent Pedler Creek Catchment.

In the southeastern part of the FRC, groundwater flow is in a southeasterly direction. It is inferred that in this area the FRA system of the upper catchment discharges into the sedimentary system of the lower catchment. However, this investigation addresses only the FRA in the upper FRC, as there are currently no suitably constructed nested piezometers in the sedimentary system to apply the specialised hydrogeological techniques used within this study.

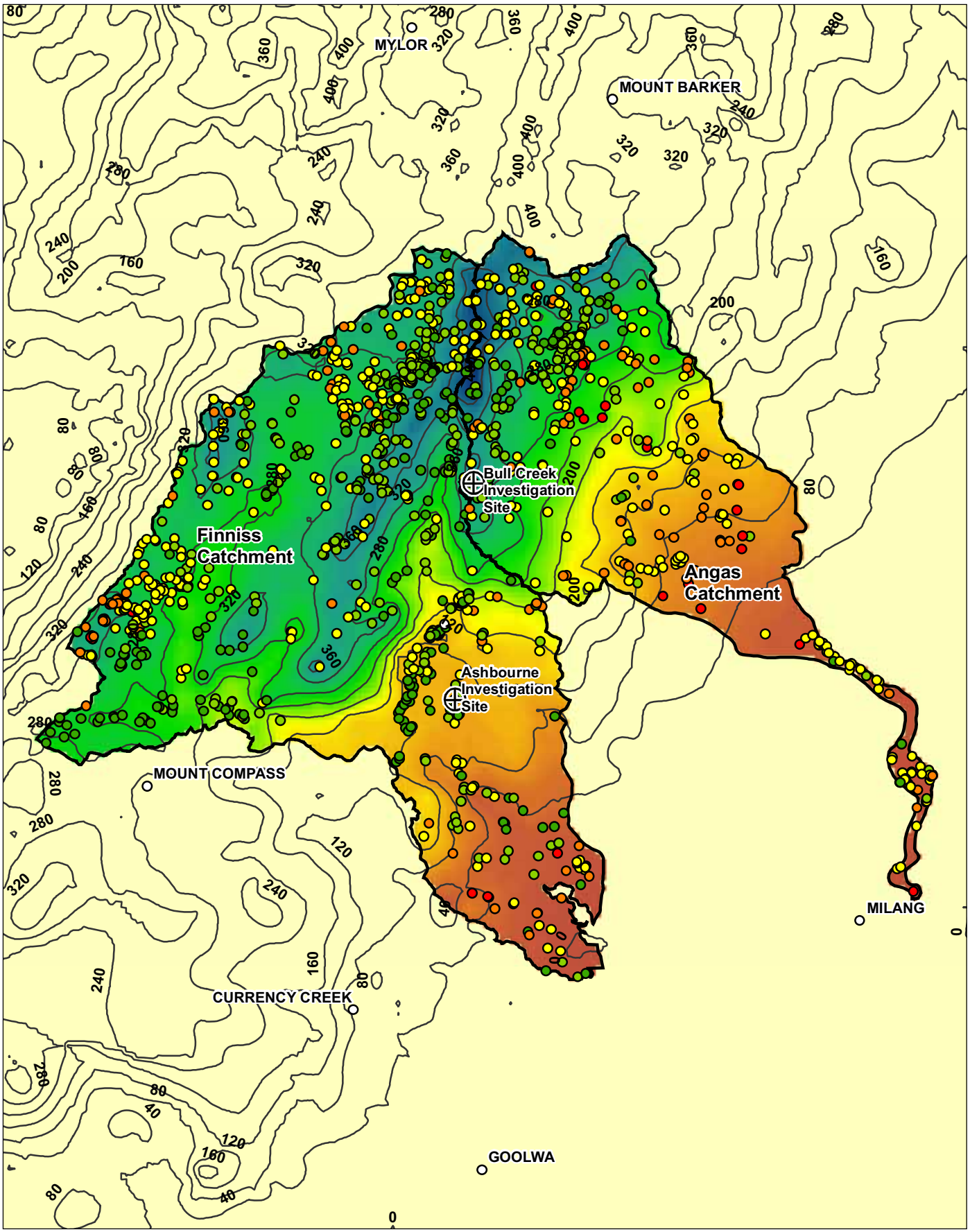

Figure 2.7 Angas and Finniss River Catchments Groundwater Potentiometric Surface

Bore water EC (uS/cm)

- 80 - 1250
- 1251 - 2500
- 2501 - 5000
- 5001 - 10000
- 10000 +

Angas & Finniss River Catchment boundaries

Groundwater potentiometric surface elevation (m AHD)

High : 450

Low : 0

Groundwater potential contours (40 m)

GW Investigation Site

0 2 4 6 8 10 Km

N

Produced By: Mount Lofty Ranges Team
Knowledge and Information Division
Department of Water, Land and Biodiversity Conservation

Datum: Geocentric Datum of Australia 1994 (GDA 94).

Date: 17th August 2006

Government of South Australia
Department of Water, Land and Biodiversity Conservation

The majority of bores are located in the upper, northern and eastern parts of the catchment (Fig. 2.7). Bore water EC ranges from ~200 μS/cm to over 18 000 μS/cm. Within this range, bores with higher salinities (>5000 μS/cm) appear to be mostly situated along the northeastern edge of the catchment, or in the lowest southeastern part, close to Lake Alexandrina.

2.2.3.3 Groundwater Potentiometric Surface Map of the Angas and Finniss River Catchments

The groundwater potentiometric surface shown in Figure 2.7 was created using the ARC GIS IDW interpolation function to calculate groundwater head elevations in 6494 boreholes within and surrounding the FRC and ARC areas.

The same methods and limitations described in section 2.1.3.1 in relation to the potentiometric surface map of the BCC apply to the ARC and FRC (Fig. 2.7). Hence, the depiction of the potentiometric surface is intended only to give an indication of relative groundwater head elevations in order that the general directions of groundwater flow through the study area can be envisaged.

3. DRILLING PROGRAM

Ongoing groundwater recharge investigations throughout the EMLR utilised existing investigation sites drilled in the Marne Catchment and FRC, namely Eden Valley and Ashbourne, respectively. This previous drilling program is described in Harrington et al. (2004) and therefore will not be expanded upon in this report.

Two additional catchments were included in the investigation, with drilling and installation of nested piezometer sites undertaken in the BCC and ARC. The drilling program will be described below, and a description of the geology included for the FRC to complement the content of this report. A detailed geological description for the Marne River Catchment and investigation site at Eden Valley can be sourced from Harrington et al. (2004) and Banks et al. (in prep).

3.1 SITE SELECTION

Potential drilling sites within the BCC and ARC were assessed using several criteria including existing groundwater data, rainfall distribution, topography, structural and geological data. In both catchments, potential sites were identified in areas of high rainfall and low topographic relief to minimise depth to groundwater. Available groundwater data were assessed to provide an indication of depth to water and areas of higher well yield.

The geology was assessed to determine the dominant lithology of each catchment and, within these broad rock types, areas exhibiting appropriate structural characteristics were targeted. Key structural features included steeply dipping to near-vertical bedding and a well-developed bedding plane parallel fracture set. These properties are important for the application of the parallel plate model in groundwater recharge investigations (refer to section 4.5.1). Another important factor in site selection was distance from large-scale faults and shear zones. Increased fracture development is typically associated with faulting and, whilst this may result in local areas of increased recharge, it is not representative of catchment-scale processes. Therefore, sites that were a considerable distance from major fault zones, and met all other requirements, were selected.

3.1.1 BURRA CREEK CATCHMENT

The BCC is dominated by low, undulating hills with minimal vegetation cover. Creeks are typically ephemeral, with Burra Creek as the only permanent water source in the northern part of the catchment. Rainfall is typically low and varies from ~300–500 mm/y, with the highest rainfall occurring along the western margin of the catchment.

Historical groundwater data for the area are limited. Existing wells are predominantly shallow (less than 40 m) and are used for stock and domestic purposes. Characteristic of a FRA environment, the groundwater quality and yields are highly variable, with salinity ranging from 1045–9500 mg/L and yields between 0.1–30 L/s.

The Saddleworth Formation is the major lithological unit throughout the northern part of the catchment. A north–south-trending anticline dominates the catchment. Structural data were selected where bedding dip was greater than 80°, as sub-vertical bedding, combined with cleavage, could provide an increased potential for fracture development. A major north–south-trending fault on which the historic Burra Mine is located occurs within the catchment (Fig. 2.3). Increased fracturing is associated with this highly deformed zone and consequently it is inappropriate for recharge investigations.

At the completion of this assessment, a suitable investigation site was selected in the BCC ~12 km NNW of Burra township along the Booborowie Road (Fig. 2.2).

3.1.2 ANGAS RIVER CATCHMENT

The ARC is characterised by steeper topography and increased vegetation cover. Rainfall varies from 733 mm/y in the north to 450 mm/y in the southeast.

Groundwater data for the catchment indicate that the majority of wells are used for domestic purposes and are typically less than 100 m deep. Yields vary from 0.1–38 L/s, with salinities between 200–10 000 mg/L. A high well density occurs in the vicinity of Macclesfield due to the presence of a marble unit, resulting in high-yielding, good-quality groundwater. This concentration of wells appears to be a local anomaly and, therefore, the area was not considered to be appropriate for recharge investigations.

A north–south-trending syncline, with moderate to steeply dipping limbs, dominates the catchment (Fig. 2.6). The limbs of the syncline are comprised of the older Adelaidean rocks, with younger Kanmantoo Group units located in the centre. Although the Kanmantoo Group dominates the geology of the catchment, it is typically a low-yielding, poor-quality aquifer. As such, it was considered beneficial to the investigation to preferentially target sites in the Adelaidean sequences.

A suitable site was located in the Wilpena Group (Brachina Formation) on Old Bull Creek Road, ~7.5 km southwest of Macclesfield (Fig. 2.5). This site has steeply dipping beds, well-developed sub-vertical fractures and is not adjacent to any significant fault zones.

3.2 DRILLING

John Nitschke Drilling Pty Ltd undertook the drilling program during October and November 2004 in the BCC and ARC. An Edson 6000 Rotary Hammer rig was used to drill two wells at each site — one 8 inch diameter and the other 10 inch diameter. Due to the large diameter and depth of the wells, a second air compressor and drilling foam additive were required on numerous occasions to facilitate the removal of cuttings from the hole. At each site, the wells were drilled as close as possible to each other to increase the potential for intersecting the same fracture sets. This is considered important if attempts are to be made to correlate chemistry data from shallow depths with deeper depths.

Each well was completed with welded steel casing to ensure stability of the upper weathered section. The remainder of the well was left as an open-hole completion to enable electrical conductivity, pH and temperature, geophysical and acoustic televiewer logging, EM

Flowmeter testing and well dilution testing to be conducted. These analyses were conducted to assist in the design of the nested piezometers, which were installed later (refer to section 4.3).

Completion details for wells in all three catchments are provided in Table 3.1.

Table 3.1 Bore completion details for each site in the BCC, ARC and FRC.

Catchment	**Easting**	**Northing**	**Permit number**	**Unit number**	**Depth from surface** (m)	**Diameter** (inches)	**Casing depth** (m)
Burra	302953	6278548	102412	663003296	71.6	10	23
Burra	302952	6278544	102149	663003295	119	8	23
Angas	302954	6278552	102087	662711091	61	10	17
Angas	302953	6278550	102088	662711092	120	8	17
Finniss	297574	6089780	61096	662710779	96	10	6
Finniss	297576	6089786	61097	662710780	49	8	6

4. METHODOLOGY

4.1 INTRODUCTION

The following section describes the methodology used to construct the nested piezometers in order to understand the groundwater recharge mechanisms and flow processes at the Burra, Angas and Finniss investigation sites. The construction of the nested piezometers enabled samples to be taken from discrete depths for a suite of hydrochemical, isotopic and radiogenic tracers to investigate the apparent groundwater age, depth of circulation, vertical flow and horizontal flow rates, and sources of groundwater. Aquifer tests were also conducted to determine some of the physical characteristics of the aquifer systems.

4.2 FIELD INVESTIGATIONS

The Burra, Bull Creek and Ashbourne investigation sites were selected because the local geology and hydrogeology is thought to be representative of the BCC, ARC and FRC, respectively.

Geophysical logs, EM Flowmeter and Hydrolab surveys were recorded in the 8 and 10 inch holes. Hydrolab refers to a YSI® 600XL Series Sonde which is used to measure variations in electrical conductivity, pH and temperature with depth. The Department's Geophysical Technical Services group completed down-hole geophysical surveys for the following parameters:

- *Gamma Log* — Measures natural presence of gamma rays. Aids in defining lithology changes, bed boundaries and clay content.
- *Neutron Log* — Measures the amount of hydrogen around the probe. Can provide an indication of porosity and clay content (in combination with gamma).
- *Density (or gamma-gamma) Log* — Gamma source and gamma receiver measures the electron density, which is a function of the bulk density of the formation.
- *Induction (medium and deep) Log* — The induction tool uses electromagnetics to sense the conductivity (inverse of resistivity) of the adjacent formation. Comparisons between deep and medium results can indicate porosity.
- *Point Resistance (PR) Log* — Changes between a down-hole electrode and a reference surface electrode reflect changes in the formation resistivity. This can represent changes in porosity, water salinity, and fluid connectivity.
- *Calliper Log* — Spring-loaded arms that press against the side of the hole and can indicate well and casing integrity. It can also be used to identify fractures in the lithology intercepted by the well.

In addition to the standard geophysical surveys, the EM Flowmeter was also used under ambient and pumped conditions to determine vertical flow within the wells at discrete intervals sealed by inflatable packers. An Acoustic Televiewer survey was also conducted to provide an orientated, visual indication of fracture distribution within each well.

4.3 PIEZOMETER INSTALLATION

At the Burra, Bull Creek and Ashbourne investigation sites, two piezometer nests were installed in the open 8 inch and 10 inch holes. PVC casing of 50 mm diameter was used with slotted PVC screens positioned at intervals determined by the geophysical and EM Flowmeter surveys. Three shallow piezometers were installed next to the nests at the Burra and Bull Creek sites to provide discrete sampling points from the surficial regolith and weathered bedrock zones. This was not necessary at the Ashbourne site because the 8 and 10 inch holes were geologically stable and only required steel casing to 6 m depth (Table 4.1). A full description of the lithological logs and piezometer locations are provided in Appendix B and C, respectively.

Table 4.1 Construction details of the shallow and nested piezometers at the Burra, Bull Creek and Ashbourne investigation sites. Some details at the Ashbourne site have not yet been collected.

Unit number	Easting	Northing	Sample name	Ground elevation (m ASL)	Piezometer depth from surface (m)	TOC (PVC) above ground (m)	Screen interval from surface (m)	Average RSWL (m ASL)
6630-3340	302954	6278552	BR1	504.03	9.83	0.58	6.83–9.83	498.93
6630-3339	302953	6278550	BR2	504.05	14.80	0.55	11.8–14.8	498.94
6630-3338	302953	6278548	BR3	504.08	19.65	0.66	16.65–19.65	498.92
6630-3327	302952	6278544	BR4	504.27	26.50	0.56	23.5–26.5	498.93
6630-3326	302952	6278544	BR5	504.27	34.60	0.56	31.6–34.6	498.88
6630-3325	302952	6278544	BR6	504.27	47.00	0.57	44–47	498.87
6630-3324	302952	6278544	BR7	504.27	51.50	0.56	48.5–51.5	498.87
6630-3323	302952	6278544	BR8	504.27	61.00	0.55	58–61	498.78
6630-3322	302952	6278544	BR9	504.27	66.00	0.55	63–66	498.78
6630-3321	302951	6278537	BR10	504.26	67.00	0.48	64-67	498.84
6630-3320	302951	6278537	BR11	504.26	75.50	0.48	72.5-75.5	498.82
6630-3319	302951	6278537	BR12	504.26	82.00	0.49	79-82	498.84
6630-3318	302951	6278537	BR13	504.26	92.00	0.48	89-92	498.80
6627-11316	298417	6099529	B1	348.31	11.65	0.59	8.65-11.65	341.56
6627-11315	298417	6099528	B2	348.20	16.88	0.60	13.88-16.88	341.34
6627-11314	298417	6099526	B3	348.11	22.03	0.57	19.03-22.03	341.25
6627-11304	298418	6099514	B4	347.63	25.00	0.32	20-25	341.46
6627-11303	298418	6099514	B5	347.63	31.50	0.32	26.5-31.5	341.53
6627-11302	298418	6099514	B6	347.63	41.00	0.32	35-41	341.59
6627-11300	298418	6099517	B7	347.78	47.00	0.27	41-47	342.53
6627-11299	298418	6099517	B8	347.78	56.00	0.28	50-56	333.60
6627-11301	298418	6099514	B9	347.63	58.00	0.32	52-58	342.35
6627-11298	298418	6099517	B10	347.78	68.00	0.28	62-68	342.20
6627-11297	298418	6099517	B11	347.78	87.00	0.29	81-87	342.65
6627-11290			A1		15	0.60	10-15	8.54
6627-11296			A2		19.00	0.80	13-19	8.96

Unit number	Easting	Northing	Sample name	Ground elevation (m ASL)	Piezometer depth from surface (m)	TOC (PVC) above ground (m)	Screen interval from surface (m)	Average RSWL (m ASL)
6627-11289			A3		27.00	0.60	22-27	8.56
6627-11295			A4		34.00	0.80	29-34	8.93
6627-11288			A5		39.50	0.60	34.5-39.5	8.53
6627-11287			A6		46.60	0.60	41.6-46.6	8.56
6627-11294			A7		49.00	0.80	43-49	8.93
6627-11293			A8		63.00	0.80	58-63	8.84
6627-11292			A9		84.00	0.80	79-84	8.80
6627-11291			A10		92.00	0.80	87-92	8.82

4.4 GROUNDWATER AGES AND DEPTH OF CIRCULATION

4.4.1 MAJOR CHEMISTRY AND ISOTOPES

Prior to sampling the groundwater bores, the static water level was measured from top of casing (TOC) using an electric water level probe. The bores were then purged using a 12-volt Supertwister® submersible pump for the low-flow shallow piezometers and a Grundfos-MP1 submersible pump for the deeper piezometers. A YSI® multi-parameter meter was used to monitor the physical parameters of pH, specific electrical conductivity (SEC), dissolved oxygen (DO), redox and temperature during purging. The meter was calibrated with known standards prior to use in the field. Samples were collected after the physical parameters had stabilised, indicating that the sample was representative of the section of the aquifer sampled. The total alkalinity (assumed to be HCO_3^- for the ranges of pH sampled) was also measured in the field using an HACH titration kit.

Major ion analysis was conducted on the groundwater samples that had been filtered through a 0.45 micron membrane filter in the field. Cations (Na^+, Mg^{2+}, K^+, Ca^{2+}, NH_4^+) and trace elements were acidified with nitric acid (1% v/v HNO_3) to keep the ions in solution and analysed by Inductively Coupled Plasma Emission Spectrometry (ICP-ES). Anions (Cl^-, Br^-, SO_4^{2-} and NO_3^-) were analysed by Ion Chromatography (IC). Samples were also collected and analysed for the stable isotopes of the water molecule — deuterium (δ^2H) and oxygen-18 ($\delta^{18}O$).

Adelaide is the closest rainfall station to the BCC, ARC and FRC, with rainfall isotopic data provided by the International Atomic Energy Agency (IAEA) Global Network of Isotopes in Precipitation (GNIP) service. For this study, only complete annual data sets from the GNIP database were used to derive the weighted average precipitation and the local meteoric water line (LMWL) for Adelaide ($\delta2H = 7.25 \times \delta18O + 7.9$).

Precipitation at any given location will display isotopic variation due to the effects of air temperature, latitude, altitude, amount of rainfall and distance from the water source (Dansgaard 1964). To determine the representative isotopic composition of rainfall, the measured isotopic ratios of individual rainfall events are weighted by the amount of rainfall represented in each event. The weighted average precipitation gives greater influence to the isotopic values that represent the majority of precipitation.

The stable isotopes of the water molecule are conservative tracers (i.e. they remain conservative during passage through the unsaturated zone and record the rainfall signature modified by evapotranspiration) and provide information on physical processes of the hydrological system over time as opposed to a point in time such as the potentiometric surface. They are also not removed from water by exchange processes in most low temperature aquifer systems (Coplen et al. 1999). In particular, they can be used for the delineation of groundwater flow systems, determining the extent of the discharge zone beneath a water body, determining recharge processes, and for quantification of mass balance relationships.

4.4.2 CARBON-14 AND CHLOROFLUOROCARBONS (CFCs)

Groundwater samples were collected for chlorofluorocarbons (CFCs), carbon-14 (^{14}C) and dissolved inorganic carbon ($\delta^{13}C$) analysis to determine the apparent age of the water and provide information on the groundwater flow processes, including depth of circulation and vertical aquifer connection.

CFCs are stable organic compounds that were first manufactured in the 1930s and are solely from anthropogenic sources. Concentrations of CFCs in water vary as a function of the atmospheric partial pressures of CFCs and CFC solubility, which is a function of salinity and temperature, and can be used to determine apparent groundwater age. CFCs can be measured in groundwater that has been recharged since about 1940 or in a mixture of groundwater younger than 1940 with older waters. CFCs have been used as age indicators for groundwater studies since about 1979 (Szabo et al. 1996).

Processes that affect the CFC age include sorption, contamination, microbial degradation, hydrodynamic dispersion and soil gas diffusion in the unsaturated zone. Corresponding errors in apparent CFC ages are ~±2 y for ages less than 20 years, increasing to ±4 y for ages of 30 years. The detection limit for both CFCs is ~5 pg/kg, which equates to an age of ~1961 (Leaney 2006).

Analysis of ^{14}C can be used to support the CFC data and provide information for the older waters that are beyond the capacity of the CFC dating technique. For a radioactive environmental tracer, where radioactive decay is the dominant process causing change in activity and the input activity of the tracer is relatively constant, then the groundwater age (t) can derived by:

$$t = -\lambda^{-1} \ln\left(\frac{A}{A_o}\right) \qquad \textbf{Equation 4.1}$$

where λ is the decay constant [T^{-1}], A is the measured activity and A_o is the estimated initial activity.

One of the complications with interpretation of ^{14}C data is using an appropriate correction model to account for geochemical interactions that modify the initial activity (A_o) of ^{14}C at the time of recharge. The correction models include a chemical mixing model (Tamers 1967), isotopic dilution model (Pearson & Hanshaw 1970) and a complete soil gas exchange model (Fontes & Garnier 1979). The models require input of the chemical and isotopic end members of soil gas $\delta^{13}C$, ^{14}C and partial pressure of CO_2 (pCO_2), and carbonate mineral $\delta^{13}C$ and ^{14}C, which can be measured from samples in the laboratory and also approximated using the computer code PHREEQC by Parkhurst and Appelo (1999). The values used in

this investigation for initial activity (A_o) of soil CO_2 ^{14}C = 85 pmC, soil gas $\delta^{13}C$ = -13‰, carbonate mineral $\delta^{13}C$ = -7.8‰ and carbonate mineral ^{14}C = 0 pmC (Harrington 1999).

4.5 VERTICAL FLOW RATES AND AQUIFER RECHARGE

4.5.1 CARBON-14 AND CHLOROFLUOROCARBONS (CFCs)

Vertical profiles of groundwater age have been used successfully to estimate rates of vertical groundwater flow in sedimentary aquifers (Cook & Bohlke 1999). Assuming that sampling takes place near the watertable, then the horizontal component of groundwater flow will be relatively small and the recharge rate (R) may be approximated by:

$$R = \frac{z\theta}{t} \qquad \textbf{Equation 4.2}$$

where z is the depth below the watertable , t is the groundwater age and θ is the porosity.

There are relatively few established and reliable techniques for estimating vertical flow rates in FRA (Love et al. 2002). One approach for determining vertical flow rates, and hence recharge rates, in a FRA assumes that groundwater flow occurs through vertical, planar, parallel fractures with uniform matrix properties. This assumption also implies a vertical distribution of groundwater ages. Therefore, it is necessary to have knowledge of various aquifer parameters including fracture aperture ($2b$) that is determined from aquifer tests, fracture spacing (from fracture mapping) and estimates of the matrix diffusion coefficient. Where fracture orientation and distribution are more complex, groundwater ages are more likely to represent depth of groundwater circulation than provide information on vertical flow rates (Love et al. 2002).

For a conservative tracer with a constant source and subject to radioactive decay, the concentrations within the fractures can be related to vertical flow within the fractures (V_w) by:

$$V_w = \left[1 + \frac{\theta_m D^{1/2}}{b\lambda^{1/2}} \tanh(BD^{-1/2}\lambda^{1/2})\right] \Big/ \left[\frac{\delta t_a}{\delta z}\right] \qquad \textbf{Equation 4.3}$$

(after Neretnieks 1981)

where V_w is the water velocity in the fracture [LT^{-1}], b is the fracture half-aperture [L], B is the fracture half-spacing [L], θ_m is the matrix porosity [unitless], D is the effective diffusion coefficient within the matrix [L^2T^{-1}], λ is the decay constant [T^{-1}] and $\delta t_a/\delta z$ is the age gradient [TL^{-1}]. The decay constant for ^{14}C is 1.21x 10^{-4}/y. Cook and Simmons (2000) substituted the ^{14}C decay constant with the exponential growth rate for CFC-12 (k= 0.06/y) to determine vertical flow rates from CFC-12 age gradients.

The mean volumetric flow rate through the fracture, Q_v (L^3 T^{-1}) is given by:

$$Q_v = V_w \frac{b}{B} \qquad \textbf{Equation 4.4}$$

(L is length and T is time.)

4.5.2 AQUIFER PUMPING TESTS

Single-well pump tests were conducted on several of the piezometers using the Cooper-Jacob straight-line method (Fetter 2001) to determine the bulk hydraulic conductivity over the length of the screen interval. Pump tests are typically more suited to sedimentary systems, but their application to nested piezometers can provide valuable information on the vertical variation of hydraulic conductivity and can be used to derive other physical characteristics of the aquifer (Cook 2003).

Having determined the bulk hydraulic conductivity over the screened interval from the aquifer tests, the average fracture aperture can be derived from a rearrangement of the following equation:

$$K_b = \frac{\rho g (2b)^3}{12\mu(2B)} \qquad \textbf{Equation 4.5}$$

Rearranging equation 4.5, the equivalent fracture aperture can be determined:

$$2b_{eq} = \left(\frac{12\mu(2B)K_b}{\rho g} \right)^{1/3} \qquad \textbf{Equation 4.6}$$

where K_b is the bulk hydraulic conductivity over the test interval [LT^{-1}], p is the fluid density [ML^{-3}], g is acceleration due to gravity [LT^{-2}], $2b$ is the fracture aperture [L], μ is the dynamic viscosity [$MT.L^{-1}$] and $2B$ is the fracture spacing [L], which we have assumed to be the same as that in nearby outcrops of similar lithological type. (L is length, T is time, M is mass.)

4.5.3 CHLORIDE MASS BALANCE

Groundwater recharge rates can also be estimated using the chloride mass balance (CMB) technique. The method assumes that the only source of chloride in groundwater is via rainfall and that the rate of chloride accession to the landscape is constant and there are no sources or sinks of chloride in the subsurface. The following steady state mass balance equation can be used to estimate recharge (R):

$$R = \frac{(P - RO)}{C_{gw}} C_p \qquad \textbf{Equation 4.5}$$

where P is the mean annual precipitation rate [L], RO is the annual runoff rate [L], C_p is the chloride concentration in the precipitation [ML^{-1}], and C_{gw} is the chloride concentration in groundwater (recharge water) [ML^{-1}].

The CMB technique has been used successfully in sedimentary aquifer systems and has been suggested the most reliable technique for determining recharge rates to FRA systems (Cook 2003). However, the recharge rate determined from CMB should be considered as a minimum because of the addition of other sources of chloride. Changes in environmental conditions (i.e. land clearing) will also impact on the equilibrium of chloride in the fractures with the rock matrix and may take a significant amount of time for the diffusion of salts from the matrix into the fractures to re-equilibrate.

Cook et al. (1996) derived a simple approach to determine the approximate time required for the chloride concentration in the matrix to become the same as in the water flowing through the fractures by:

$$t \geq \frac{(2B)^2}{2D} \qquad \textbf{Equation 4.6}$$

where t is time, $2B$ is the fracture spacing and D is the effective diffusion coefficient for the aquifer matrix. Therefore, assuming $D = 10^{-4}$ m^2/y, for $2B$ = 1 m, t ≥5000 y and for $2B$ = 0.1 m, t ≥50 y.

4.6 HORIZONTAL FLOW VELOCITIES

4.6.1 RADON

Radon (^{222}Rn) is a radioactive, inert gas that is generated from the decay of uranium and thorium series isotopes in the aquifer matrix. It has a half-life of ~3.8 days, is highly soluble in water and its concentration will depend on the mineralogy of the aquifer and the pore space geometry (Love et al. 2002).

Cook et al. (1999) developed a technique to estimate horizontal flow rates by comparing unpurged to purged radon concentrations from piezometers, where a purged sample is assumed to be representative of the concentration of radon in the aquifer. For high horizontal flow rates, the concentration of radon of an unpurged sample, measured over the length of the screen of the piezometer, will be similar to the concentration of a purged sample from the piezometer. If the horizontal flow rate were low then the concentration of radon of an unpurged sample would have decayed to background levels. Hence, the ratio of radon concentration from an unpurged sample to a purged sample will depend on the amount of radioactive decay, which occurs as the water moves through the well under natural flow conditions. Assuming a perfectly mixed well, the groundwater flow rate, q (m/y), is given by:

$$q = \frac{c}{c_0 - c}\frac{\lambda \pi r}{2} \qquad \textbf{Equation 4.7}$$

where c and c_0 are the radon concentrations in the well and in the aquifer respectively, r is the well radius and λ is the decay constant for radon (0.18/d). Groundwater flow rates calculated by this method refer to groundwater flow within the well. Due to hydrodynamic dispersion, the horizontal flow rate within the well will be higher than in the aquifer. To estimate flow within the aquifer, the calculated flow rate needs to be multiplied by a factor of 0.5 for an open well or 0.25 for a piezometer.

5. FIELD INVESTIGATIONS

5.1 BURRA CREEK CATCHMENT

The Burra investigation site is located in the northern arm of the BCC, which is characterised by bald rolling hills of moderate elevation and a higher annual rainfall (>300 mm/y). The 8 and 10 inch holes were drilled in the Saddleworth Formation to 119 and 71 m, respectively. Surface casing for both holes was installed to 23 m depth. These two holes were completed as nested piezometers. Three additional piezometers were constructed next to the nested piezometers, targeting the shallow zone from the ground surface to 20 m depth. The lithological logs for the shallow and deep holes are provided in Appendix B.

5.1.1 FRACTURE ANALYSIS

Due to the absence of useful outcrop, a detailed fracture analysis was not undertaken in the BCC. Average values for fracture aperture and spacing, derived from previous studies conducted in a similar lithology, were utilised for recharge calculations using the parallel-plate model.

5.1.2 ELECTRICAL CONDUCTIVITY, TEMPERATURE AND PH IN OPEN WELLS

Specific electrical conductivity (SEC), temperature and pH were measured using a multiparameter YSI Sonde® for the open 8 and 10 inch holes (Fig. 5.1). EC in the 10 inch hole was at least 1000 μS/cm higher than in the 8 inch hole from about 5–25 m depth, and may be an artefact of the surface casing from ground level to 20 m depth. The two profiles correspond closely from 25 (4600 μS/cm) to 45 m (5400 μS/cm). Below 45 m, the profile in the 10 inch hole is uniform (5400 μS/cm) with increasing depth to the base of the hole whilst the profile in the 8 inch hole steadily decreases from 45 m to a depth of 65 m until it becomes uniform (4000 μS/cm) with increasing depth to the base of the hole.

The temperature profiles in both the 8 and 10 inch holes match closely. Temperature decreases from ~18°C at the watertable to 17°C at about 20 m depth, which corresponds to the base of the casing, and is likely to be a result of poor circulation in the steel casing. From 20 m to the base of each of the holes there is a steady increase in the profiles, with a temperature gradient of 0.02°C/m (Fig. 5.1).

The pH profiles in the 8 and 10 inch holes show a steady increase from a pH of 8 at the watertable to a pH of about 10 at 25 m depth. The pH profiles then decrease to a pH of 7.7 at 40 m and are uniform to the base of the holes. The pH profiles in the first 40 m may reflect poor field sampling technique whereby the probe was not allowed enough time to equilibrate prior to being lowered down the hole. It may also be the effect of the casing from ground level to 20 m depth and the cement plug that was used to seal it which would tend to raise the pH to the observed values (Fig. 5.1).

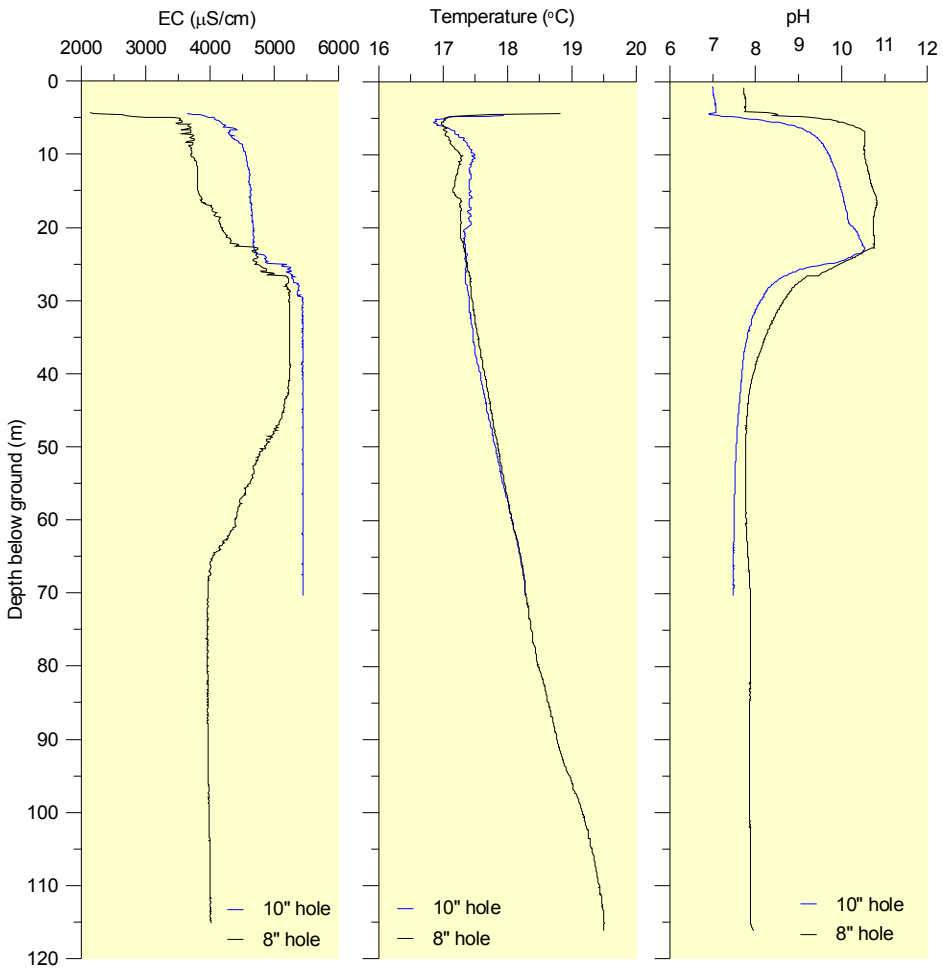

Figure 5.1 **EC, temperature and pH variation with depth in the 8 inch (119 m) and 10 inch (71 m) open holes at the Burra investigation site, March 2005. Both holes are cased to ~23 m.**

5.1.3 GEOPHYSICAL AND EM FLOW SURVEYS IN OPEN WELLS

Figure 5.2 (a) and (b) show the calliper and EM Flowmeter results, respectively, from the 8 inch hole (119 m depth). The calliper log exhibits notable increases in the diameter of the hole at 26, 43, 65, 78 and 103 m depth, indicating potential fractures intersecting the hole. In the EM Flowmeter log, under ambient conditions, there is very little vertical flow in the hole, showing only a slight downward flow (<-0.99 L/min) from 27–92 m and a slight upward flow (<0.012 L/min) from 95–113 m. Under pumped conditions of 11 L/min at the watertable, there is a significant groundwater contribution (>9 L/min) from 20–66 m which corresponds to the likely fracture measured using the calliper log at 65 m depth. From 74–92 m, the groundwater contribution is significantly less (4 L/min) and, below 92 m depth, vertical flow in the hole is less than 0.2 L/min.

Figure 5.2 (c) and (d) show the calliper and EM Flowmeter results, respectively, from the 10 inch hole (71 m depth). The calliper log exhibits notable increases in the diameter of the hole between 62–67 m depth, similar to the calliper log in the 8 inch hole. In the EM Flowmeter log, under ambient conditions, there is very little vertical flow in the hole, showing only a slight downward flow (<-0.36 L/min) from 20–67 m and a slight upward flow (<0.011 L/min) at

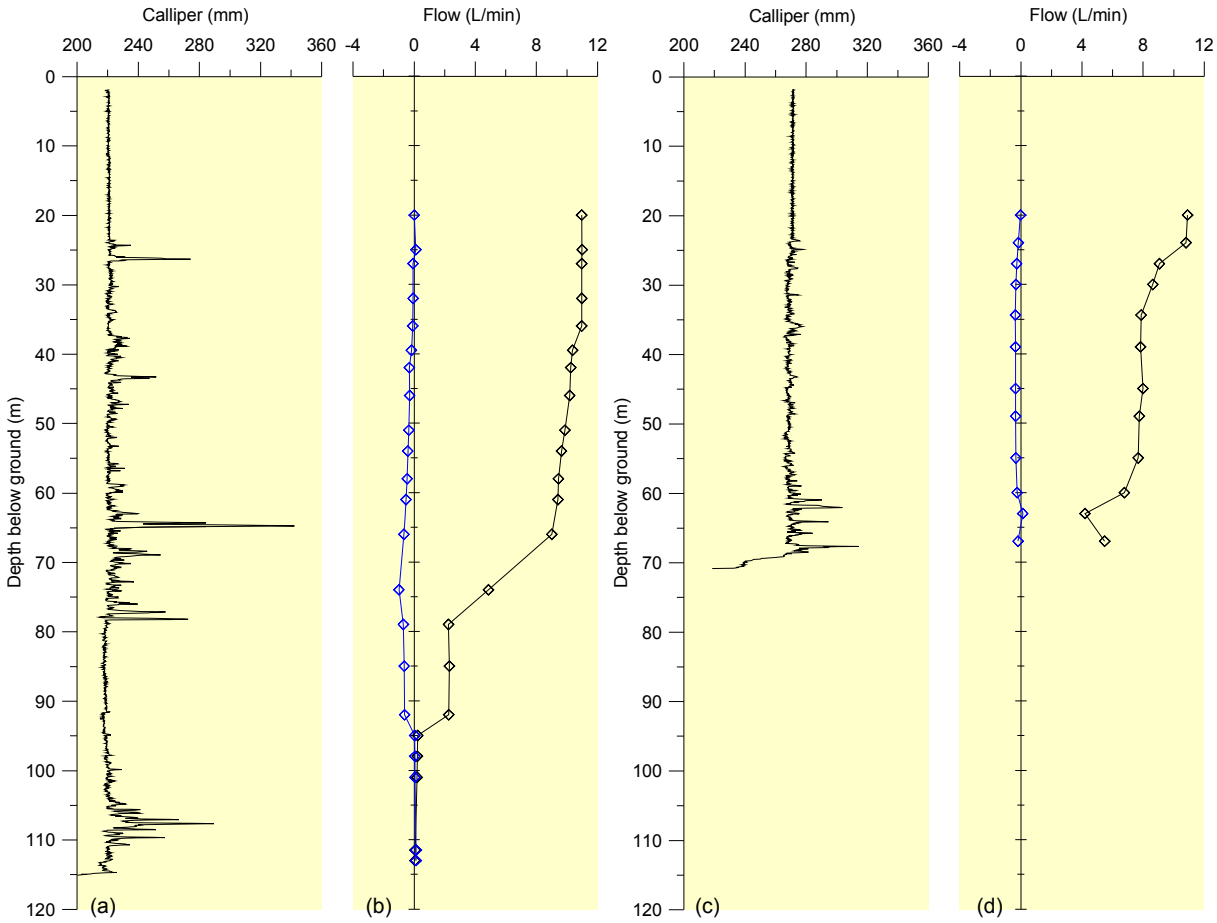

Figure 5.2 **Calliper (a) and EM Flowmeter (b) profiles in the 8 inch open hole (~119 m), and calliper (c) and EM Flowmeter (d) profiles in the 10 inch open hole (~71 m) at the Burra investigation site, March 2005. Diamonds on the flowmeter profile represent intervals where the packers were inflated to measure flow. Both holes are cased to ~23 m.**

63 m depth. Under pumped conditions of 11 L/min at the watertable, there is a significant groundwater contribution (>8.6 L/min) from 20–30 m. From 30–55 m, the groundwater contribution is 7.7–8 L/min and, below 55 m depth, vertical flow in the hole is less than 7.7 L/min.

The results have been used to aid in the definition of strata changes and identify the principal flow zones where the nested piezometer screen intervals have been set. FRA can display highly variable flow rates at different depth intervals due to complex and irregular fracture spacings, apertures and orientations, and hence it is necessary to conduct the geophysical investigations to ensure that the constructed piezometer nests will yield water.

5.1.4 HYDRAULICS

The average watertable elevations measured between October and November 2005 in the nested piezometers are shown in Figure 5.3. The primary y-axis shows the piezometer screen elevation, whilst the secondary y-axis shows the watertable elevation corrected to a reduced standing water level (RSWL) in each of the piezometers. The hydraulic gradient from 8.3–90.5 m is ~0.0016 (0.13 m/82.2 m). There is some variability in the hydraulic head in each of the piezometers, suggesting that some piezometers have poor vertical hydraulic

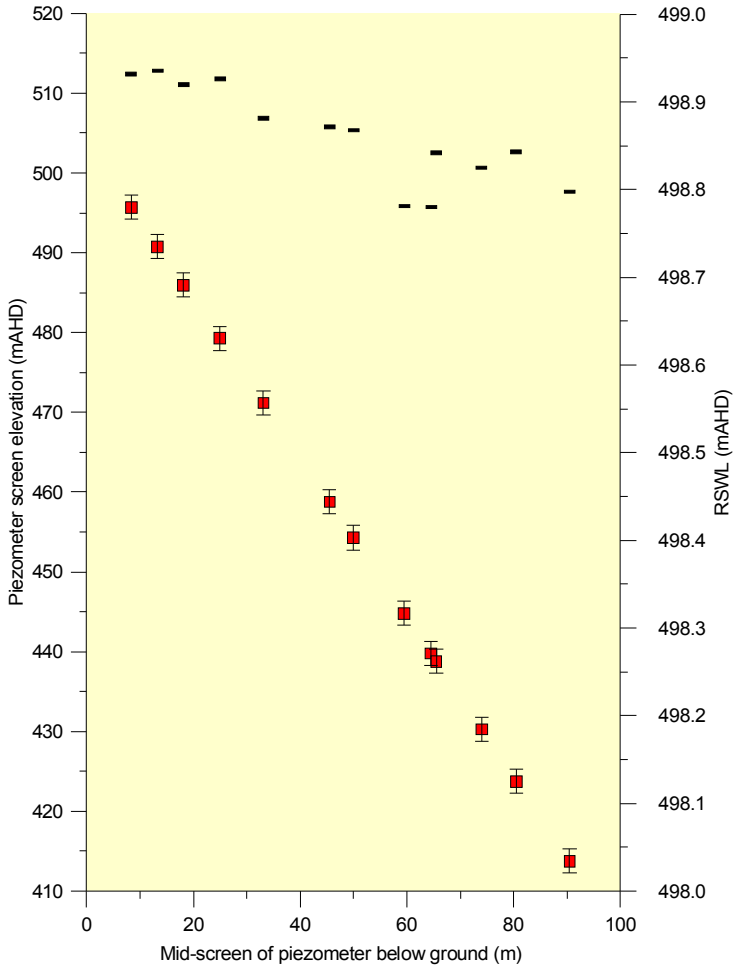

Figure 5.3 Average watertable elevations in the nested piezometers at the Burra investigation site, October–November 2005.

connection whilst others are connected fairly well (i.e. 59.5 and 64.5 m). Between 25–33.1 m there is a significant step in the hydraulic head of about 5 cm, suggesting that there are two distinct flow systems at the site. This supports the field observations during drilling of the shallow piezometers and the 8 inch hole, where a perched watertable was encountered in the shallow clay-rich regolith zone at about 7 m. There was no water cut observed when drilling the 10 inch hole, highlighting that the impeding hydraulic barrier between 25–33.1 m may be discontinuous and semi-confining.

5.2 ANGAS RIVER CATCHMENT

The Bull Creek investigation site is near the western margin of the ARC, in the Wilpena Group (Brachina Formation). The 8 and 10 inch holes were drilled to about 120 and 61 m, respectively. Surface casing for both holes was installed to about 17 m depth. Three additional piezometers were constructed next to the two deep holes targeting the shallow zone from the ground surface to 20 m depth. The lithological logs for the shallow and deep holes are provided in Appendix B.

5.2.1 FRACTURE ANALYSIS

Detailed fracture analyses were undertaken in the ARC to provide values of fracture spacing for use in the parallel-plate model.

Field measurements indicate that the dominant fracture set has an orientation of 013/56 E. This is represented diagrammatically by the stereographic projection of poles to fracture surfaces (Fig. 5.4). The great circle indicates an average bedding orientation and indicates that the dominant fracture set in the region is parallel to bedding. Average spacing between parallel fracture surfaces is 18.3 mm, and frequency analysis indicates that 95% of fracture spacings fall between 5–35 mm (Fig. 5.5).

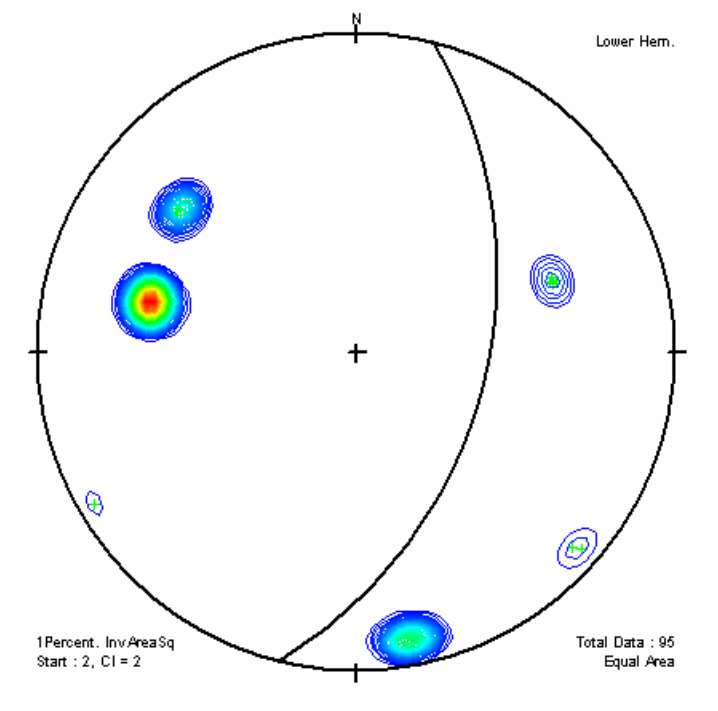

Figure 5.4 Lower Hemisphere Equal Area Stereographic Projection of fracture sets in the ARC (n=95).

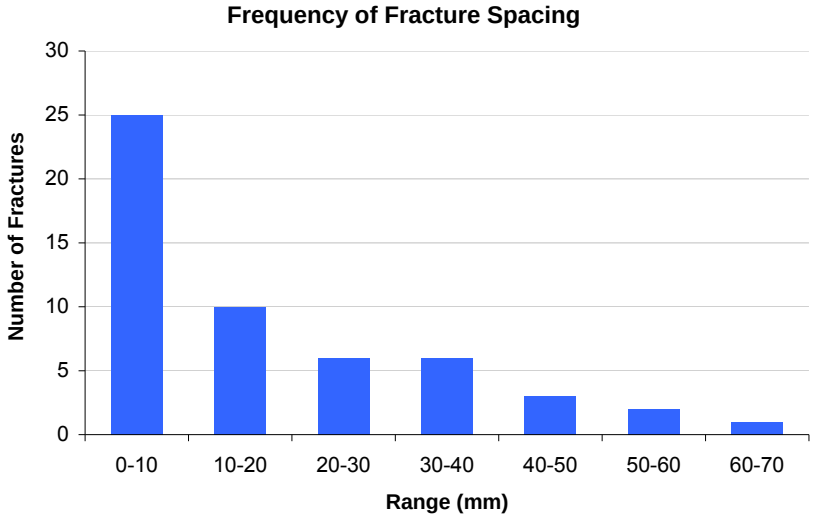

Figure 5.5 Frequency plot of fracture spacings measured over a 1 m interval (n=53).

5.2.2 ELECTRICAL CONDUCTIVITY, TEMPERATURE AND pH IN OPEN WELLS

EC, temperature and pH were measured using Geophysical Technical Service's Hydrolab downhole tool for the open 8 and 10 inch holes (Fig. 5.6). The EC profile in the 10 inch hole was similar to that in the 8 inch hole to 60 m, although it was ~100 μS/cm higher. Similar to the Burra site, there appears to be some influence due to the surface casing on the EC profiles. The profile in the 8 inch hole increases rapidly from 2125 μS/cm at about 53 m to 2300 μS/cm at 56 m depth, where it then becomes uniform to the bottom of the hole. The abrupt change in EC is likely to reflect an active fracture(s) intersecting the hole.

The temperature profiles in both the 8 and 10 inch holes match closely. The profile steadily decreases from about 15.5°C at the base of the surface casing at 17 m to 17.25°C at 120 m, with a temperature gradient of 0.015°C/m (Fig. 5.6). The pH profiles in the 8 and 10 inch holes show a steady decrease from a pH of about 9 at the 17 m depth (base of surface casing) to a pH of about 7.25 at 40 m where it tends to become more uniform with depth, only increasing slightly towards the base of the hole at 120 m (Fig. 5.6).

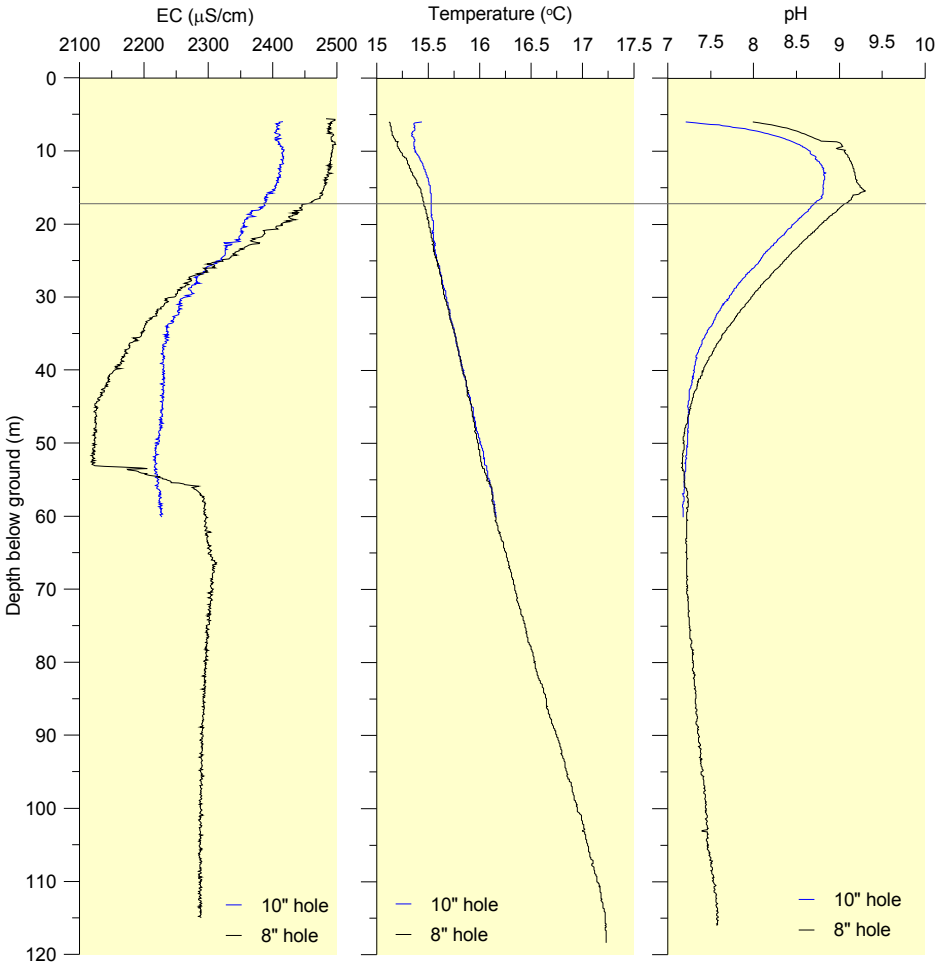

Figure 5.6 **EC, temperature and pH variation with depth in the 8 inch (~120 m) and 10 inch (~61 m) open holes at the Bull Creek investigation site, October 2004. The grey horizontal line represents approximate casing depth.**

5.2.3 GEOPHYSICAL AND EM FLOW SURVEYS IN OPEN WELLS

The calliper logs for the 8 and 10 inch holes show considerable increases in its diameter between the base of the surface casing (~17 m) and 60 m depth, indicating potential fractures intersecting the hole (Fig. 5.7(a),(c)). Below 60 m in the 8 inch hole there is little variation in the calliper log, indicating that there are very few significant fractures intersecting the hole. In the EM Flowmeter log (Fig. 5.7(b)), under ambient conditions, all groundwater flow is in an upward direction, showing noticeable upward flow (0.2–0.3 L/min) between 42–62 m, and 75 and 95 m depth. Under pumped conditions of 1.4 L/min at the watertable (8.25 m below ground), there is a significant groundwater contribution (>0.5 L/min) from 12–25 m. Between 25–49 m, the groundwater contribution is 0.2–0.5 L/min, and below 49 m the flow is less than 0.2 L/min, comparable to flow under ambient conditions. The higher flow between 17–49 m corresponds to the inferred higher fracture density of the calliper log over a similar depth. Due to a ruptured inflatable packer, the EM Flowmeter was not conducted on the 10 inch hole.

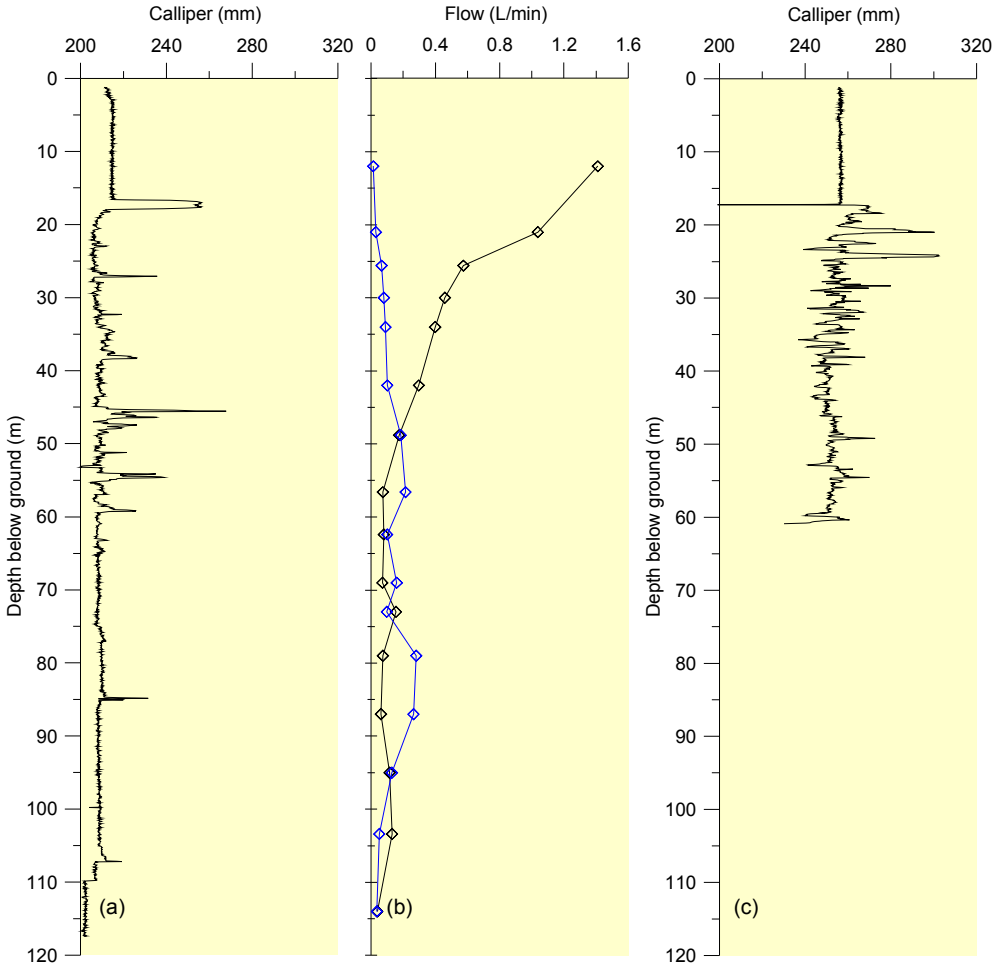

Figure 5.7 **Calliper (a) and EM Flowmeter (b) profiles in the 8 inch open hole (~120 m) and calliper (c) profile in the 10 inch open hole (~61 m) at the Bull Creek investigation site, October 2004. Watertable depth during pumped conditions for the EM Flowmeter was 8.25 m below ground. Diamonds on the flowmeter profile represent intervals where the packers were inflated to measure flow. The 8 inch hole is cased to 16.5 m and the 10 inch hole is cased to 17 m.**

As mentioned in 5.1.3, the calliper and EM Flowmeter results were used to aid in the definition of strata changes and identify the principal flow zones where the nested piezometer screen intervals have been set.

5.2.4 HYDRAULICS

The watertable elevations measured on 28 September 2005 in the nested piezometers at the Bull Creek site are shown in Figure 5.8. The primary y-axis shows the piezometer screen elevation whilst the secondary y-axis shows the watertable elevation corrected to a reduced standing water level in each of the piezometers. The hydraulic gradient from 10.1–20.5 m is ~0.029 (0.3 m/10.4 m), inferring downward flow, and below this depth groundwater flow is upwards. Between 20.5–38 m, the gradient is 0.017 in an upward direction, and from 38–44 m there is a significant step in the watertable elevation of 0.77 m. This suggests that there is poor vertical hydraulic connection between fractures at this depth. The hydraulic gradient from 44–84 m is ~0.01 (0.439 m/40 m), smaller than in the upper part of the aquifer system.

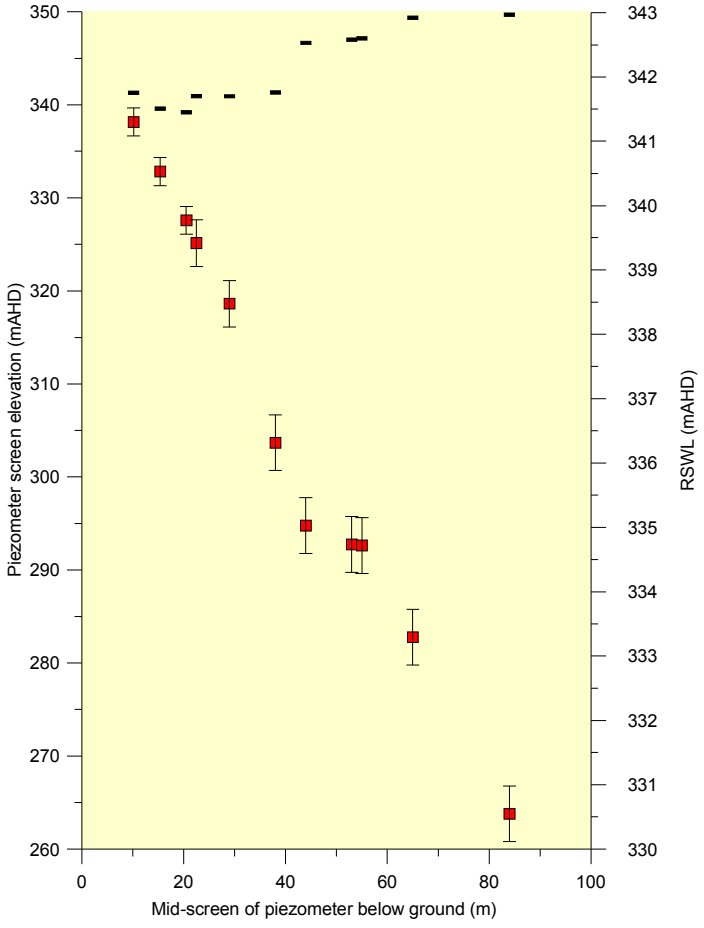

Figure 5.8 Watertable elevations in the nested piezometers at the Bull Creek investigation site, 28 September 2005.

5.3 FINNISS RIVER CATCHMENT

The Ashbourne investigation site is located in the middle of the FRC, where the topography changes from steep, rolling hills of moderate elevation to the low flat plains. The 8 and 10 inch holes were drilled in Kanmantoo Group sediments to 49 and ~97 m depth, respectively. The 8 inch hole was completed with 8.3 m of surface casing and the 10 inch hole with 10.5 m of surface casing.

5.3.1 FRACTURE ANALYSIS

Again, a detailed fracture analysis was undertaken in the FRC to provide fracture spacing information for the parallel-plate model.

Field measurements indicate two dominant fracture sets. The more prevalent is parallel to bedding with an orientation of 030°/82°E; the other dominant set is orientated at 090°/82°E. These are depicted in the stereographic projection of poles to fracture surfaces (Fig. 5.9). The great circle represents an average bedding orientation (030°/82°E). Average spacing of the bedding parallel fracture set is 67.1 mm and frequency analysis indicates that 95% of fracture spacings fall between 33–106 mm (Fig. 5.10).

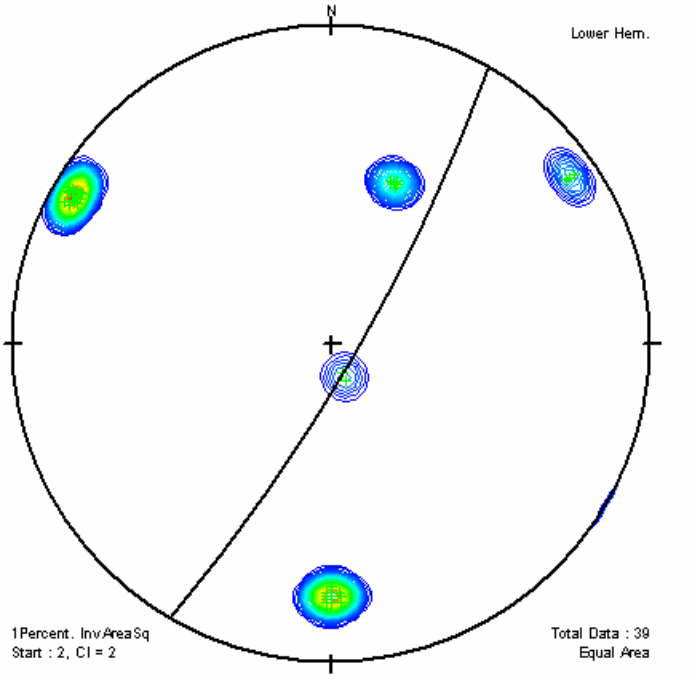

Figure 5.9 Lower Hemisphere Equal Area Stereographic Projection of fracture sets in the FRC (n=39).

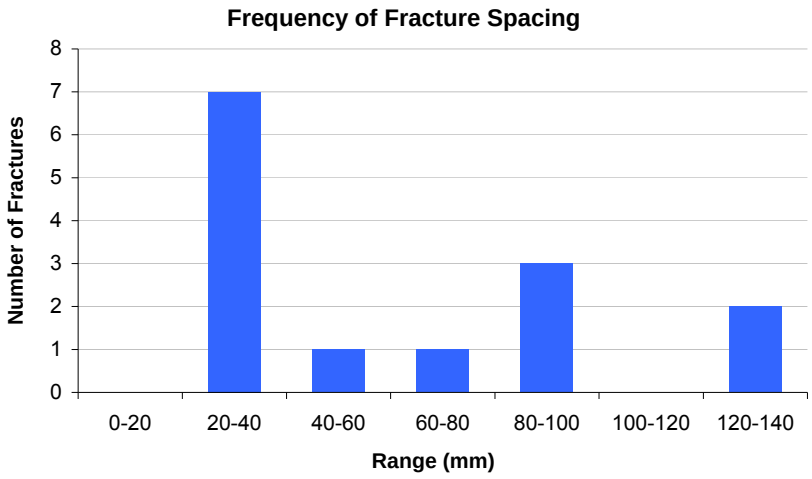

Figure 5.10 Frequency plot of fracture spacings measured over a 1 m interval (n=14).

5.3.2 ELECTRICAL CONDUCTIVITY, TEMPERATURE AND pH IN OPEN WELLS

EC, temperature and pH were measured using Geophysical Technical Service's Hydrolab downhole tool for the open 8 and 10 inch holes (Fig. 5.11). The EC profile in the 8 inch hole is 2700 μS/cm at the base of the surface casing (~8 m), decreasing to ~2450 μS/cm at 47 m. This is 400 μS/cm higher than in the 10 inch hole. There are several noticeable peaks in the profile, occurring at ~22 m and between 30–37 m depth. The abrupt changes in EC are likely to indicate an active fracture(s) intersecting the hole. The profile in the 10 inch hole is uniform over the complete depth of the hole with an EC of ~2250 μS/cm.

The temperature profiles in both the 8 and 10 inch holes match closely. The profile steadily decreases from ~16°C at the base of the surface casing at 8 m to 17.75°C at 95 m, with a temperature gradient of 0.018°C/m (Fig. 5.11). The pH profile in the 8 inch hole increases from less than pH 6 near the base of the casing to a pH close to 7 at 47 m, near the base of the hole. This may be due to the pH probe not being given enough time to equilibrate when lowered down the hole. The pH profile in the 10 inch hole increases from pH 7 at 8 m to 7.7 at 15 m, then decreases to a pH of 7.4 at 60 m and remains uniform to the bottom of the hole (Fig. 5.11).

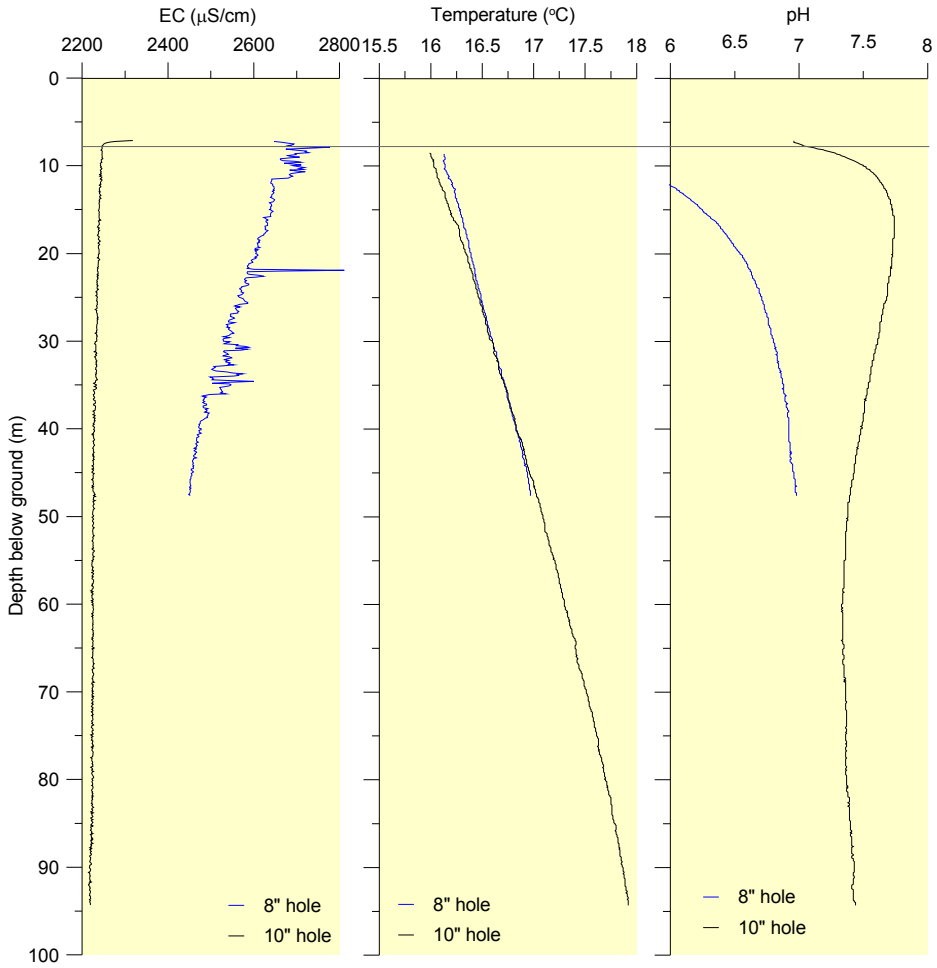

Figure 5.11 EC, temperature and pH variation with depth in the 8 inch (~49 m) and 10 inch (~97 m) open holes at the Ashbourne investigation site, June 2003.

5.3.3 GEOPHYSICAL AND EM FLOW SURVEYS IN OPEN WELLS

The calliper log for the 8 inch hole shows noticeable increases in its diameter at 13, 25, 36 and 43 m (Fig. 5.12(c)). The EM Flowmeter results for this hole show very little to no flow under ambient conditions (Fig. 5.12(d)). Under pumped conditions of 1.75 L/min at the watertable (9 m below ground), there is a significant groundwater contribution (>0.86 L/min) from 15–31 m. From 34–45 m, the flow decreases from 0.72–0.2 L/min, respectively.

The calliper log for the 10 inch hole displays increases in its diameter between 10–20 m, 47 and 69 m depth where potential fractures are likely to be intersecting the hole (Fig. 5.12(a)). The corresponding EM Flowmeter results show minimal to no flow under ambient conditions. Under pumped conditions of 3 L/min at the watertable, there is a considerable groundwater contribution of 2.6 L/min at 14 m, decreasing slightly to 2 L/min at 62 m. From below 62–82 m, the groundwater contribution is 1.6–2 L/min, and below this depth to the base of the hole the contribution is less than 1.6 L/min (Fig. 5.12(b)).

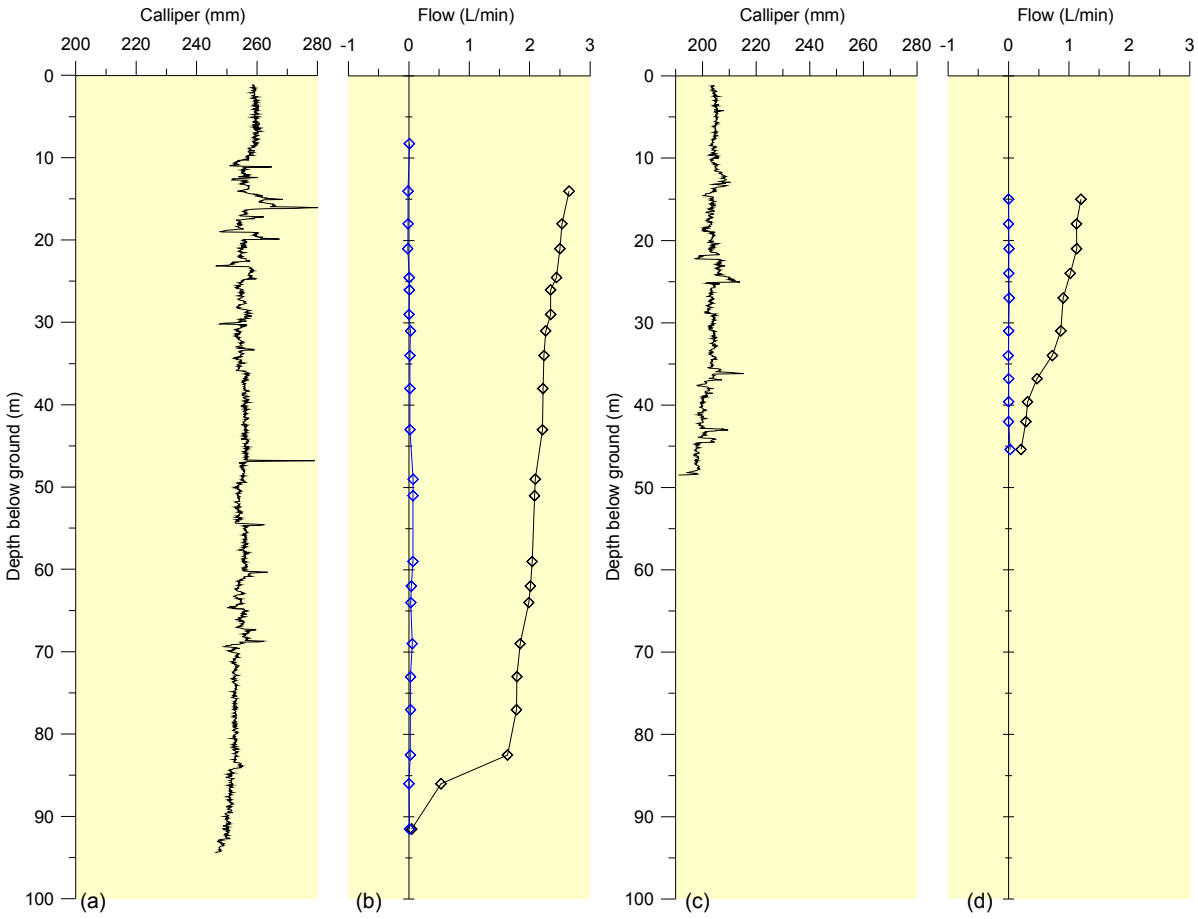

Figure 5.12 **Calliper (a) and EM Flowmeter (b) profiles in the 10 inch open hole (~97 m) and calliper (c) and EM Flowmeter (d) profiles in the 8 inch open hole (~49 m) at the Ashbourne investigation site, June 2003. Water level at time of measurement was 9 m below ground. Diamonds on the flowmeter profile represent intervals where the packers were inflated to measure flow. The 10 inch hole is cased to 10.5 m and the 8 inch hole is cased to 8.3 m.**

5.3.4 HYDRAULICS

The average watertable elevations measured between January and February 2006 in the nested piezometers at the Ashbourne site are shown in Figure 5.13. The primary y-axis shows the piezometer screen depth below ground level whilst the secondary y-axis shows the standing watertable level below ground in each of the piezometers.

The watertable elevations between 12.5–46 m vary by ~0.03 m, and hence the hydraulic gradient is small, with an overall flow gradient trending downwards (Fig. 5.13). There is a step of 0.08 m in the watertable elevations between 46–60.5 m, indicating that there is little vertical connection between the two depths. Below 60 m the hydraulic gradient is typically downwards, although the gradient between 81.5–89.5 m is upward.

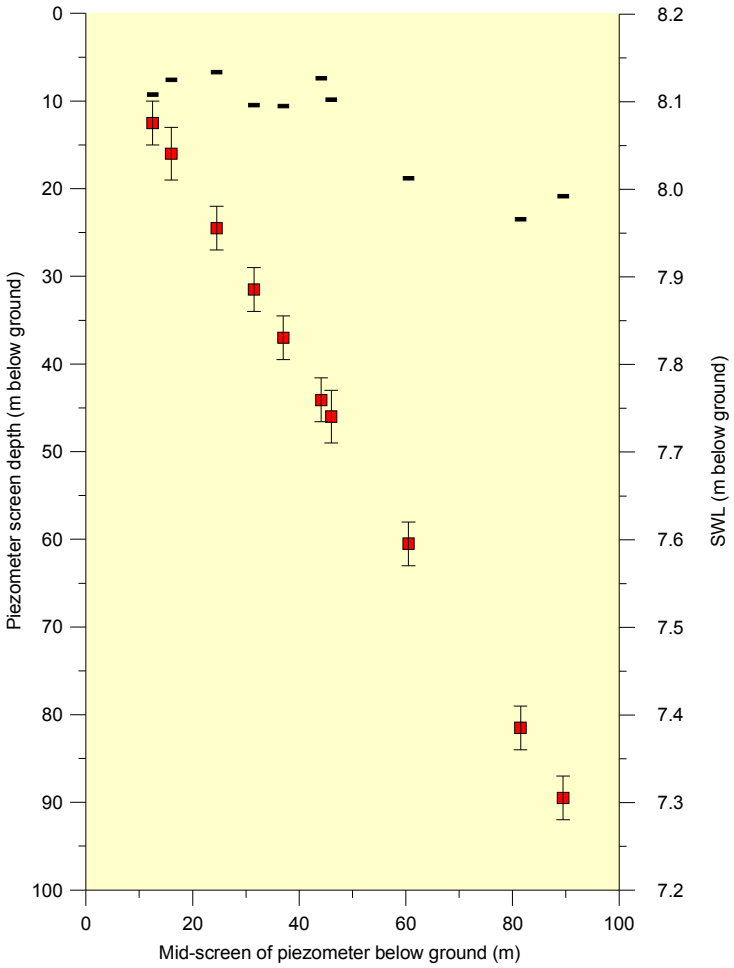

Figure 5.13 Average watertable depths in the nested piezometers at the Ashbourne investigation site, January–February 2006.

6. GROUNDWATER AGES AND DEPTH OF CIRCULATION

This chapter provides an examination and interpretation of the data sets that were used to establish a conceptual model of groundwater recharge mechanisms, vertical circulation and sources to the aquifer systems at the Burra, Bull Creek and Ashbourne investigation sites.

6.1 BURRA CREEK CATCHMENT

6.1.1 MAJOR CHEMISTRY AND ISOTOPES

The groundwater samples and a rainfall sample collected from the Burra investigation site are shown on a Piper plot in Figure 6.1. The majority of groundwater samples are of Na–Mg–Cl type whilst the samples from the piezometers at 25, 33.1 and 65.5 m are of Na–Mg–Ca–Cl type. The rainfall sample collected in March 2006 has a high contribution from bicarbonate and calcium ions, suggesting acquisition from dust particles. The compositions of all groundwater samples predominantly indicate a marine aerosol contribution with minor contribution from the acquisition of continental dust and water–rock interactions.

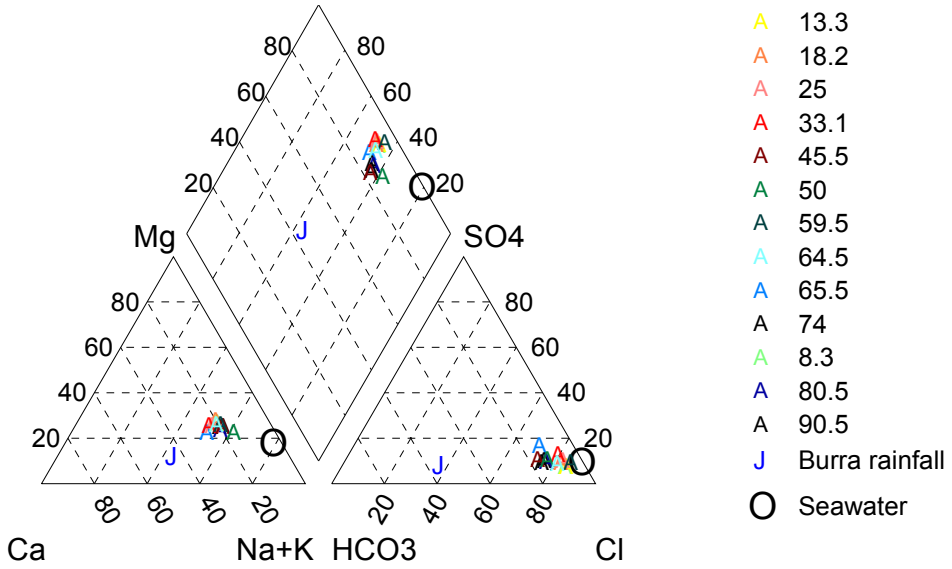

Figure 6.1 Piper plot of groundwater samples collected at the Burra investigation site, October–November 2005. Samples correspond to the mid-screen depth below ground. The Burra rainfall sample was collected in March 2006.

Figure 6.2 shows the measured TDS, chloride (Cl^-), deuterium (δ^2H) and pH profiles with depth at the Burra investigation site. There is a significant change in TDS with depth, from 3320 mg/L at ~8 m to around 2000 mg/L below 60 m. However, the similarity between the Cl^- and TDS depth profiles indicates that there is minimal change in hydrochemical composition with depth. As the concentration of Cl^- increases or decreases, the overall TDS concentration changes in the same proportion. There is also a strong correlation between the deuterium profile and the Cl^- and TDS depth profiles. Where the δ^2H values are more δ^2H-enriched,

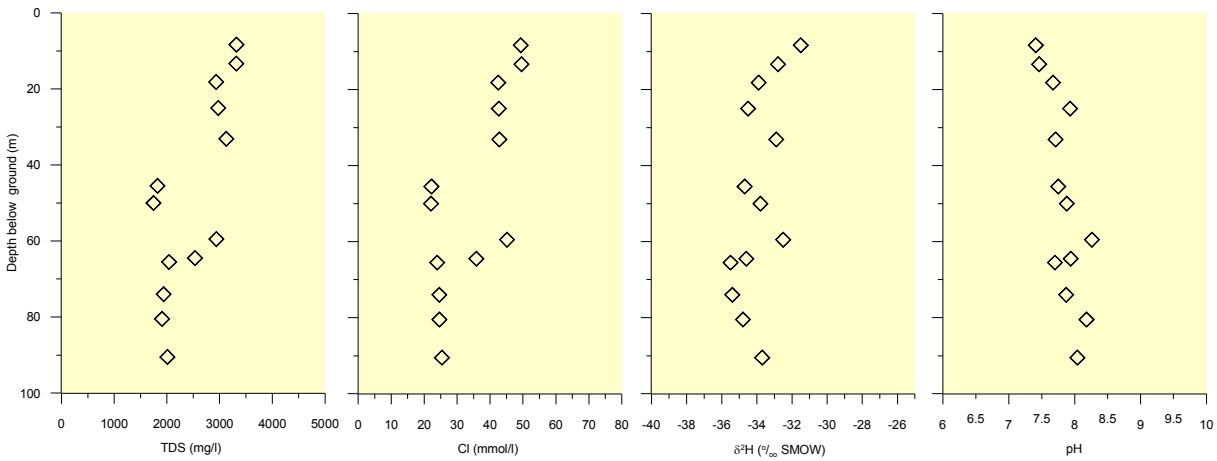

Figure 6.2 TDS, chloride, δ^2H and pH profiles sampled at the Burra investigation site, October–November 2005. The depth shown for each data point represents the mid-point of the 3 m piezometer screen interval.

indicating that greater evaporation has occurred, the Cl^- and TDS values for corresponding depths are higher, also suggesting greater evaporation. There is a similar correlation between more δ^2H-depleted values and lower Cl^- and TDS values.

The correlation between the distribution of the deuterium profile with the TDS and Cl^- profiles suggests that changes in TDS and Cl^- concentration with depth are predominantly a result of differing degrees of evapotranspiration of water prior to groundwater recharge, and not due to any dissolution of minerals after recharge. The higher TDS concentration of the samples from 8.3–33.1 m may represent a shallow local flow system, whilst the TDS concentration of the samples from 45.5–90.5 m depth represent a deeper flow system. The samples collected from 59.5–64.5 m depth are likely to be in connection with the shallow system as indicated by their higher TDS concentrations.

Chloride generally does not participate in common geochemical reactions that occur in aquifers and subsequently behaves as a conservative tracer until saturation is reached (Herczeg & Edmunds 1999). If the observed changes in TDS concentration with depth are solely a result of evaporation prior to recharge, we should expect to see the changes in all of the major inorganic ions remain in the same proportion relative to chloride as they are in seawater. Figure 6.3 shows the concentrations of major ions (Ca^{2+}, Mg^{2+}, Na^+, K^+, SO_4^{2-} and HCO_3^-) against chloride and their proximity to the respective seawater ion/chloride relationship. The rainfall sample plots along the seawater dilution line at very low concentrations.

The plots of the major cations (Ca^{2+}, Mg^{2+}, Na^+, K^+) against Cl^- of the groundwater samples all show linear trends of increasing individual ion concentrations relative to increased Cl^- concentration. However, these trends are not aligned with the seawater dilution line. The ratios of Ca^{2+} and Mg^{2+} to chloride both increase in a linear fashion as Cl^- increases, while the ratios of Na^+ and K^+ relative to chloride decrease as Cl^- increases. This pattern is interpreted as an indication that, prior to recharge, evaporation is occurring in the presence of a cation exchange media, such as a clay-rich soil, in which the relatively high proportion of dissolved Na^+ and K^+ relative to Mg^{2+} and Ca^{2+} causes Na^+ and K^+ to sorb to cation exchange surfaces in place of Ca^{2+} and Mg^{2+}. Hence, as solution concentration increases, more Na^+ and K^+ are removed from solution and absorbed into clays, and Ca^{2+} and Mg^{2+} from feldspars and mafic minerals are released into solution.

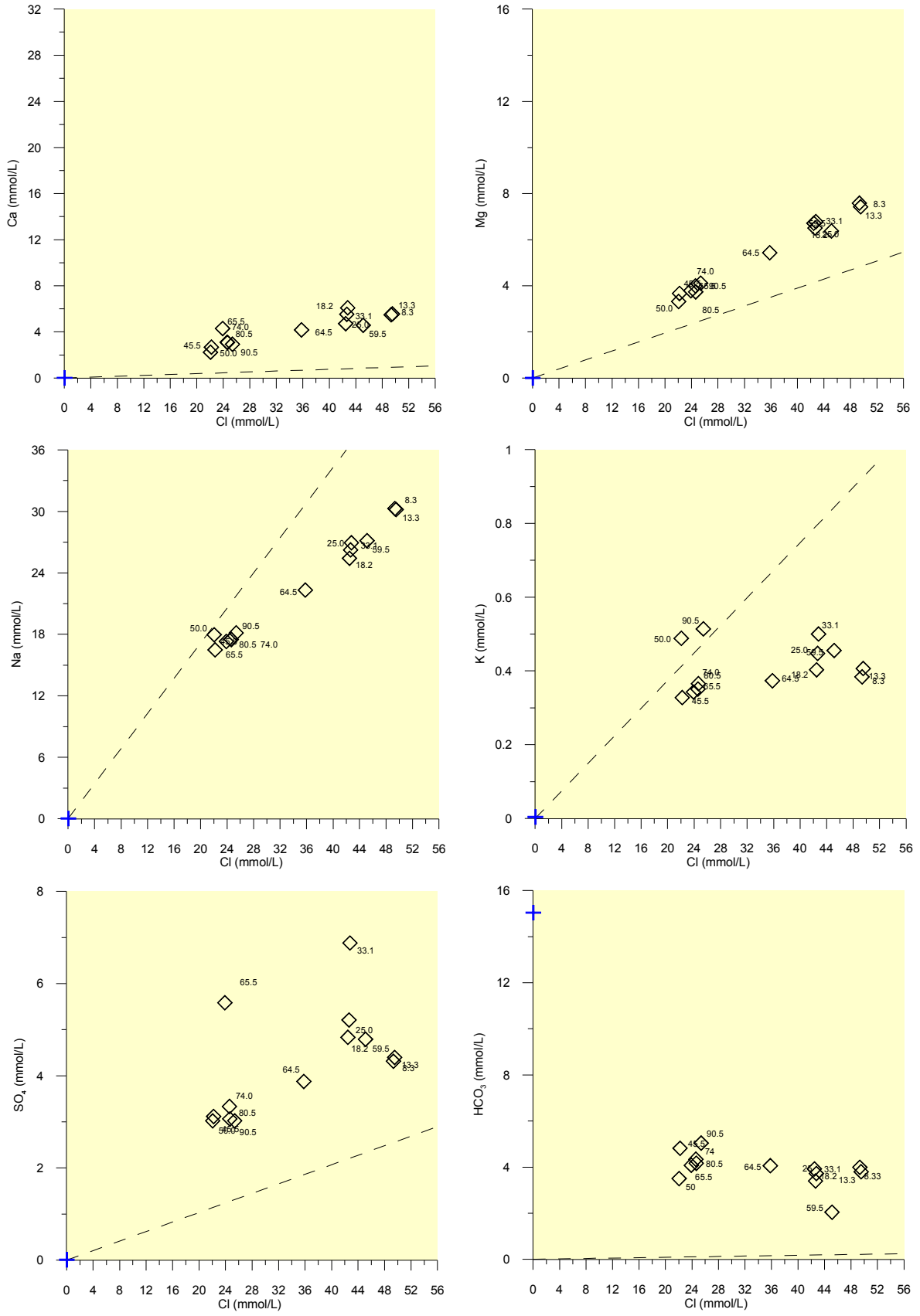

Figure 6.3 **Composition diagrams of major ions versus chloride sampled at the Burra investigation site October–November 2005. The dashed line is the dilution line for seawater and the blue cross is a rainfall sample collected at the site (March 2006). Piezometer mid-screen depths are shown beside each point.**

The data tend to plot in two distinct groups suggesting that they belong to a shallow and deep flow system. As mentioned earlier, the samples from 59.5 and 64.5 m may be in connection with the shallow flow system, which extends from the ground surface to ~33.1 m depth and a deeper flow system below 33.1 m. It is not unreasonable to assume that the different geological features (fracture aperture and spacing, weathered versus unweathered) between about 33.1–45.5 m is the boundary between the two flow systems.

The isotopic signatures of the groundwater samples from the Burra investigation site plot to the left of the mean weighted rainfall for Adelaide (δ^2H = –4.4‰ and δ^{18}O = -23.8‰) and along the local meteoric water line (based on local Adelaide rainfall events; Fig. 6.4). This implies that the groundwater at Burra is of meteoric origin and recharge occurs during the winter months as the isotopic signatures are depleted with respect to the mean. The groundwater samples from the deeper flow system (greater than 45.5 m depth and excluding the samples from 59.5 and 64.5 m depth) represent diffuse recharge, whilst the samples from 8.3, 13.3, 18.2, 25 and 33.1 m depth (upper shallow flow system) represent direct recharge. The shallow flow system is representative of direct recharge processes as there is a slightly δ^2H-enriched signature and higher chloride concentration (Fig. 6.5), indicating that there has been some evapotranspiration in the first few metres of the soil zone during infiltration. The isotopic signature from the deeper system is similar to the shallow system, but the significantly lower chloride concentrations suggest that it may have been recharged more rapidly.

6.1.2 CARBON-14 AND CHLOROFLUOROCARBONS (CFCS)

The CFC-12 concentrations indicate relative groundwater ages. The CFC-12 concentrations are comparatively low between 8.3–18.2 m depth and correspond to groundwater ages greater than 30 years (Fig. 6.6). This may be attributed to slow infiltration and circulation of groundwater in the perched watertable in the shallow system associated with a semi-confining layer of clay-rich regolith material, weathered slate and silcrete. At 25 m, CFC-12 concentrations decrease with depth and are close to or below detection limit (<25 pg/kg) at depths greater than 60 m (Fig. 6.6). Some of the groundwater samples may have been subject to atmospheric contamination due to the presence of CFC-12 below 60 m.

The presence of CFC-12 in samples from depths down to 60 m suggests that the water at these depths is relatively modern (<40 y). The low ^{14}C activities (<40 pmC) at these depths conflict with this finding (Fig. 6.7), suggesting that the ^{14}C concentrations have been affected by geochemical exchange between the water and the rock matrix. The dissolution of the Skillogalee Dolomite, a dominant geological unit in the catchment, would reduce the measured ^{14}C concentrations in the groundwater by mixing with the old (dead) carbon of the dolomite. Thus, the uncorrected ages that were determined from the ^{14}C data will not be considered here in favour of the apparent ages derived from CFC-12 concentrations. However, the ^{14}C data are useful in confirming the distinct change in water characteristics between about 33.1–45.5 m, and the apparent connection between water at 59.5 m depth and water at depths above the 33.1–45.5 m interface observed in the hydrochemistry data. The ^{14}C is ~40 pmC from 8.3–33.1 m depth, which is almost double the measured ^{14}C activity at depths below 33.1 m (Fig. 6.7). The step-like decrease in ^{14}C activity between 33.1–45.5 m depicts an abrupt increase in age of the groundwater. The step-like decrease

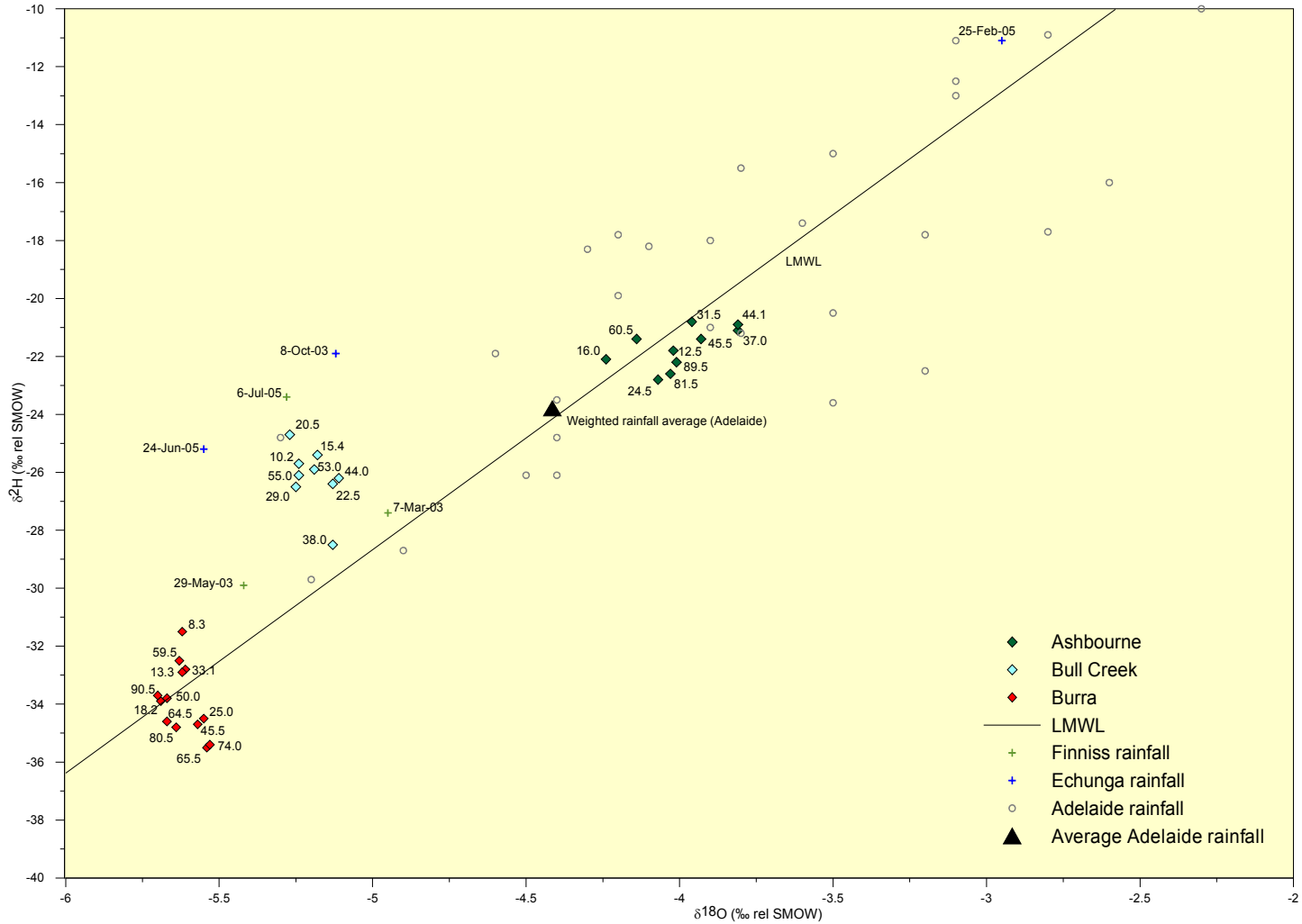

Figure 6.4 **Isotopes δ^2H and $\delta^{18}O$ of the groundwater samples collected at the Burra (October–November 2005), Bull Creek (September 2005–January 2006) and Ashbourne (February 2006) investigation sites. Rainfall samples collected at Finniss stream gauging station (Mar-2003, May-2003, Jul-2005) and Echunga pluviometer (Oct-2003, Feb-2005, Jun-2005). The LMWL for Adelaide is $\delta^2H = 7.7\ \delta^{18}O + 9.9$. The mean weighted rainfall for Adelaide is $\delta^2H = -23.8‰_{VSMOW}$ and $\delta^{18}O = -4.4‰_{VSMOW}$.**

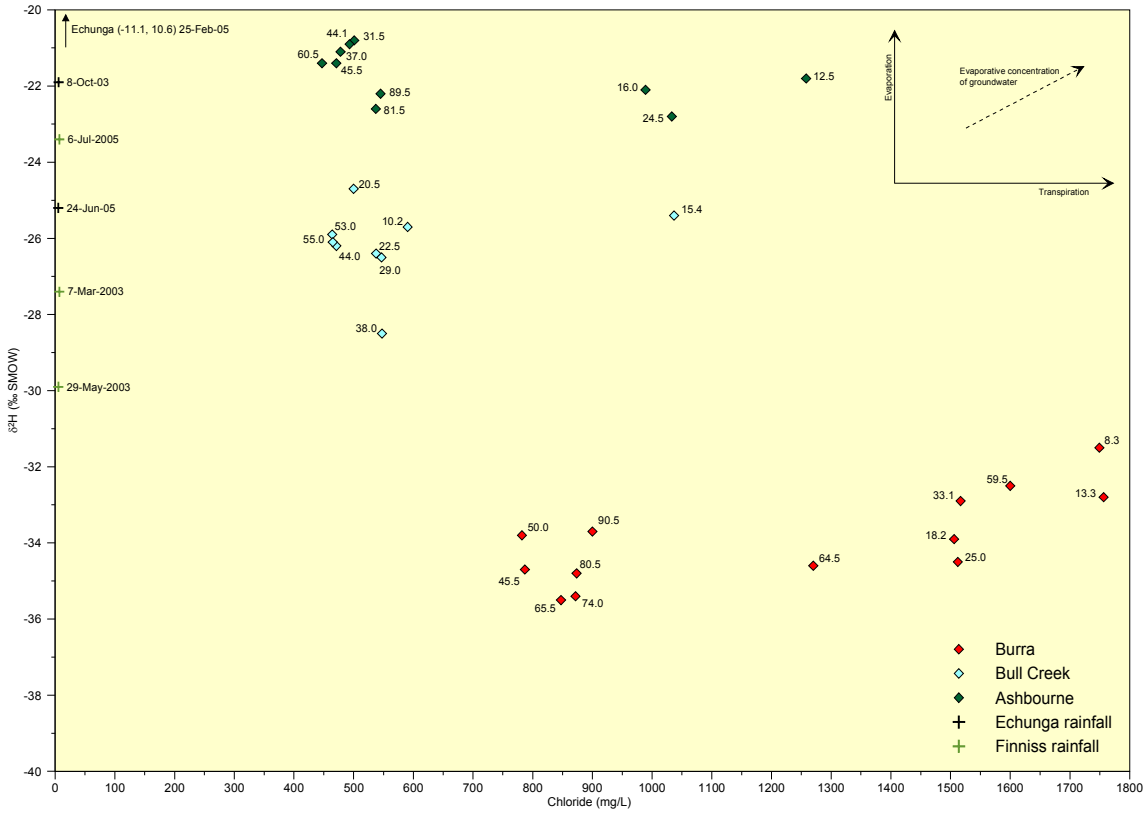

Figure 6.5 **Deuterium (δ^2H) versus chloride of the groundwater samples collected at the Burra (October–November 2005), Bull Creek (September 2005–January 2006) and Ashbourne (February 2006) investigation sites. Rainfall samples collected at Finniss stream gauging station (Mar-2003, May-2003, Jul-2005) and Echunga pluviometer (Oct-2003, Feb-2005, Jun-2005).**

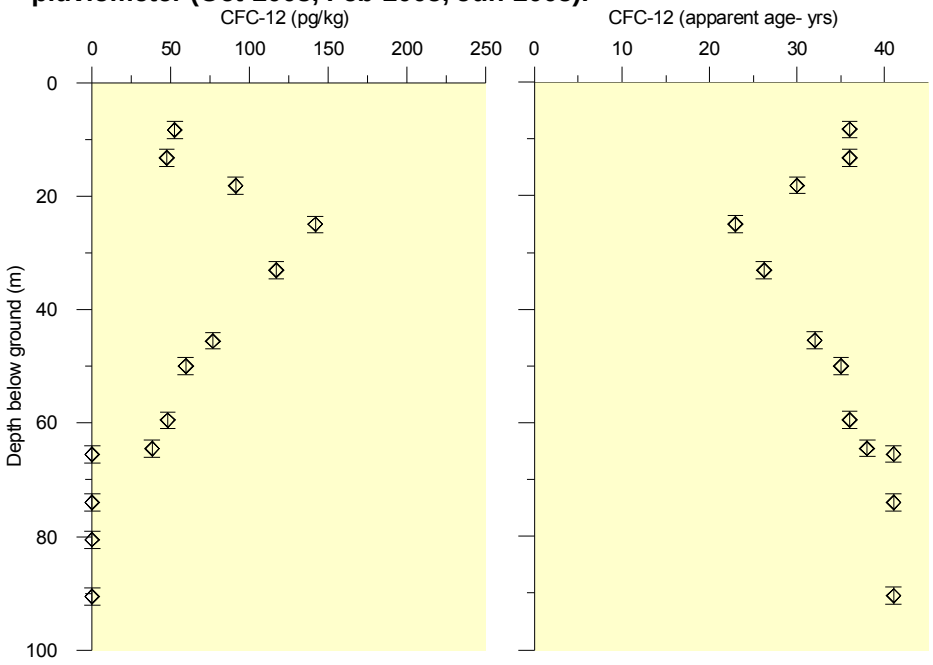

Figure 6.6 **Depth profiles of CFC-12 concentrations and CFC-12 apparent ages of groundwater from the nested piezometers at the Burra investigation site, October–November 2005. The average watertable depth was 5.2 m below ground for October–November 2005 when sampling was completed. The error bars represent the piezometer screen length from which the sample was taken.**

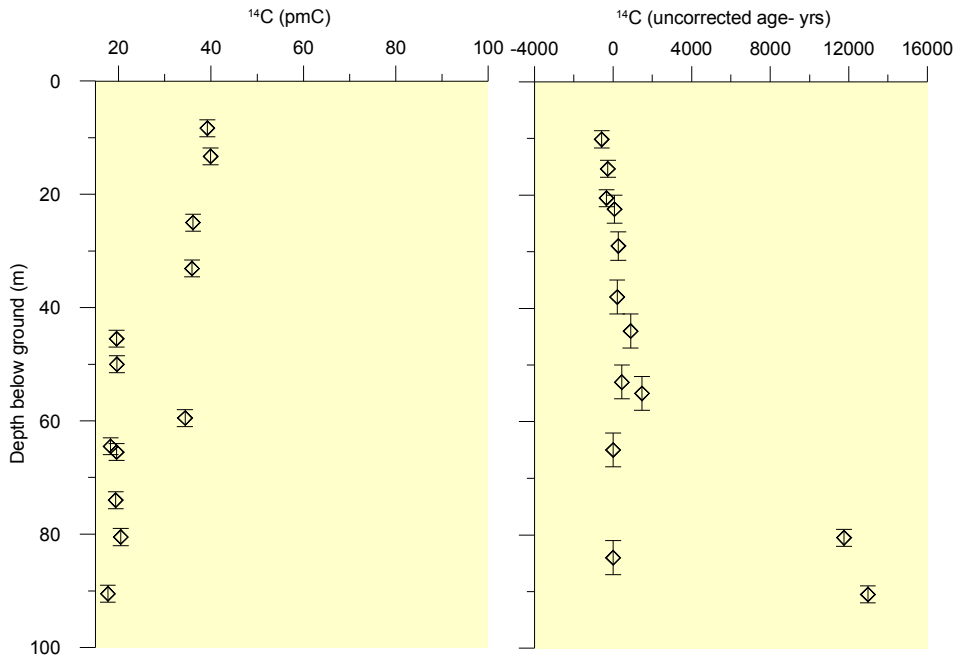

Figure 6.7 Depth profile of ^{14}C activities and ^{14}C uncorrected ages from the nested piezometers at the Burra investigation site, October–November 2005. The average watertable depth was 5.2 m below ground for October–November 2005 when sampling was completed. The error bars represent the piezometer screen length from which the sample was taken.

coincides with the trends observed in the chemistry and isotopic data, which implies a change in the lithology and the existence of a local, shallow flow system and a deeper groundwater flow system.

The apparent ages derived from the CFC data show the water above 18 m depth to be older than water between 18–33 m. As depth increases, the age of water at first decreases, from ~36 years at 8 m to ~23 years at 25 m, and then increases in age from 25 m to 60 m depth with an age/depth gradient of ~0.5 y/m. The reversal of the normal age/depth gradient above 25 m is thought to be due to recirculation of water between the local shallow flow system and the perched aquifer overlying the 33.1–45.5 m interface. The perched aquifer was not present during drilling of the 10 inch hole, suggesting that its existence is spatially variable and the deeper flow system is only semi-confined.

Below 60 m the apparent ages are 35 years or greater. Some samples from below 60 m have CFC-12 concentrations of less than 50 pg/kg, which are interpreted as being greater than 40 years old.

The high uncorrected ^{14}C ages of groundwater samples from the Burra investigation site are due to ^{14}C activities that are unusually low (Table 6.1). Corresponding low $\delta^{13}C$ values detected for these samples suggest that the low ^{14}C activities are due to a high degree of carbonate mineral dissolution. As the $\delta^{13}C$ values of the carbonate minerals contributing carbon to the groundwater are unknown, it was not possible to derive reliable corrected ^{14}C age estimates for groundwater at this investigation site.

Table 6.1 Uncorrected and corrected ^{14}C ages for samples from the Burra investigation site. Corrected ages are derived using the Fontes and Garnier (1979) correction model. Data on the sample $\delta^{13}C$ and HCO_3, and CO_2 molar concentrations are used in the correction model. The values of both the $\delta^{13}C$ and ^{14}C activities of the FRA carbonates and soil CO_2 are also used in the correction model. Values used here were: $\delta^{13}C_{carbonate}$ = -7.8$^o/_{oo}$, $\delta^{13}C_{soilCO2}$ = -13$^o/_{oo}$, $A_{carbonate}$ = 0 pmC, $A_{soilCO2}$ = 85 pmC.

Sample	Depth	A (pmC)	$\delta^{13}C$	HCO_3 (M)	CO_2 (M)	Uncorrected age (y)	Corrected age [F & G model] (y)
BR1	8.3	39.2	-9.50	0.00365	0.00026	6398	-2926
BR2	13.3	39.9	-9.50	0.00346	0.00020	6252	-2720
BR4	25.0	36.1	-9.00	0.00301	0.00007	7081	-3070
BR5	33.1	35.9	-8.70	0.00334	0.00012	7125	-4713
BR6	45.5	19.6	-7.90	0.00448	0.00013	12128	-7389
BR7	50.0	19.6	-8.10	0.00448	0.00013	12111	-5052
BR8	59.5	34.4	-9.10	0.00170	0.00002	7483	-2103
BR9	64.5	18.3	-8.90	0.00366	0.00008	12695	429
BR10	65.5	19.6	-8.20	0.00377	0.00014	12128	-4584
BR11	74.0	19.4	-8.00	0.00399	0.00009	12213	-5551
BR12	80.5	20.5	-7.90	0.00369	0.00004	11757	-6049
BR13	90.5	17.7	-8.70	0.00459	0.00009	12971	-96

6.2 ANGAS RIVER CATCHMENT

6.2.1 MAJOR CHEMISTRY AND ISOTOPES

The groundwater samples collected from the Bull Creek investigation site are shown on a Piper plot in Figure 6.8. Groundwater samples from the piezometers at 10.2, 15.4 and 20.5 m depth are all of Na–Cl type. Samples from the piezometers at 22.5, 29, 38 and 44 m depth are Ca–Na–SO4–Cl type, which is likely to be an artefact from gypsum contamination when Gypset® was used to seal the intervals between the piezometer screens. The sample from 53 m also appears to be contaminated by gypsum, whilst the sample from 55 m is Na–Cl–HCO3 type and is not contaminated because it has a similar composition to the shallow samples.

Samples from the piezometers at 65 and 84 m depth were not collected due to contamination of the groundwater from the piezometer construction process.

Figure 6.9 shows the measured TDS, chloride (Cl^-), deuterium (δ^2H) and pH profiles with depth at the Bull Creek investigation site. The chloride profile is uniform with depth except for a notable increase at 15.4 m. The TDS profile shows an increase at 15.4 m but also an increase between 22.5–53 m. This latter increase is not seen in the chloride profile (chloride ion behaving as a conservative tracer), and is indicative of contamination in these five piezometers from a source other than rock weathering. The δ^2H profile shows no indication of increased evaporation between 22.5–53 m to create an increase in TDS. At 55 m the TDS and chloride are similar, suggesting that this sample is not contaminated, as mentioned earlier in discussing the Piper plot.

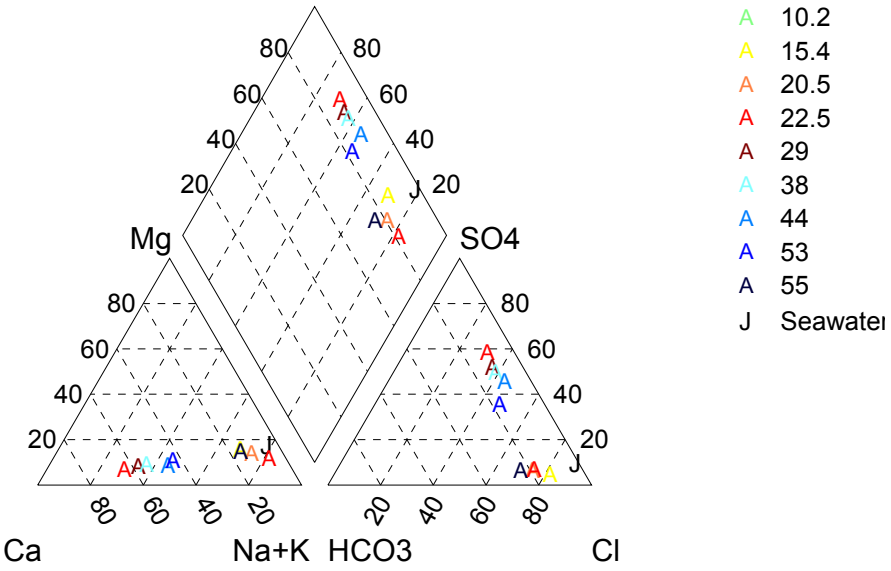

Figure 6.8 **Piper plot of groundwater samples collected at the Bull Creek investigation site, October 2005–January 2006. Samples correspond to the mid-screen depth below ground.**

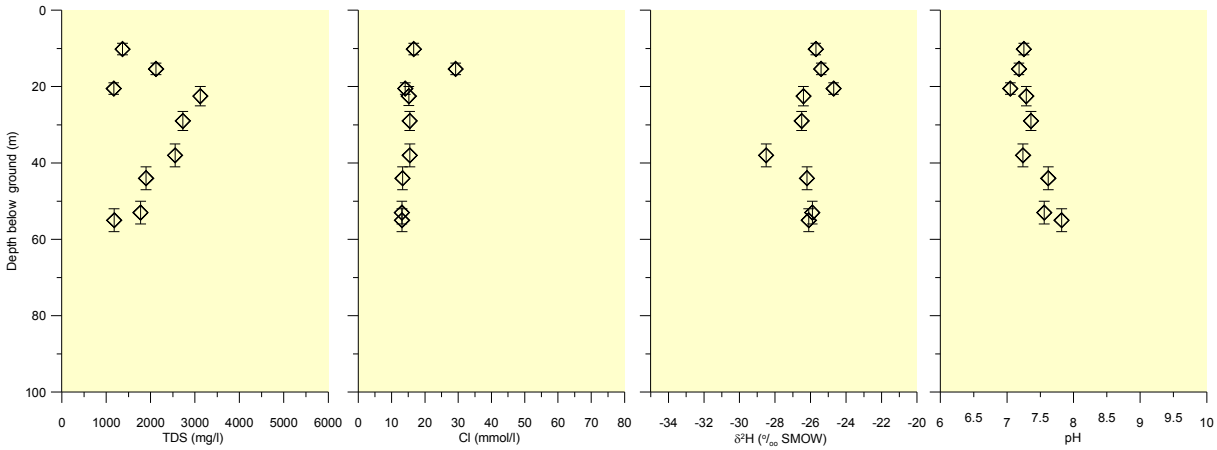

Figure 6.9 **TDS, chloride, d^{2}H, pH and profiles sampled at the Bull Creek investigation site, September 2005–January 2006. The error bars represent the piezometer screen length from which the sample was taken.**

The δ^2H-enrichment with increasing depth between 10.2–20.5 m indicates processes of evaporation and/or transpiration. The chloride profile suggests that at 15.4 m the dominant process is transpiration, resulting in the higher chloride concentration at that depth. From 22.5–55 m the deuterium profile is fairly uniform except for a less δ^2H-enriched sample at 38 m.

The pH profile from 10.2–55 m ranges from 7.1–7.8, typically with higher pH at greater depth.

If the observed changes in TDS concentration with depth are solely a result of evaporation prior to recharge, we should expect to see the changes in all of the major inorganic ions remain in the same proportion relative to chloride as they are in seawater. The graphs in Figure 6.10 show the concentrations of major ions (Ca^{2+}, Mg^{2+}, Na^{+}, K^{+}, SO_4^{2-} and HCO_3^{-}) against chloride and their proximity to the respective seawater ion/chloride relationship. These show that the majority of the samples from 10.2–55 m have a similar composition,

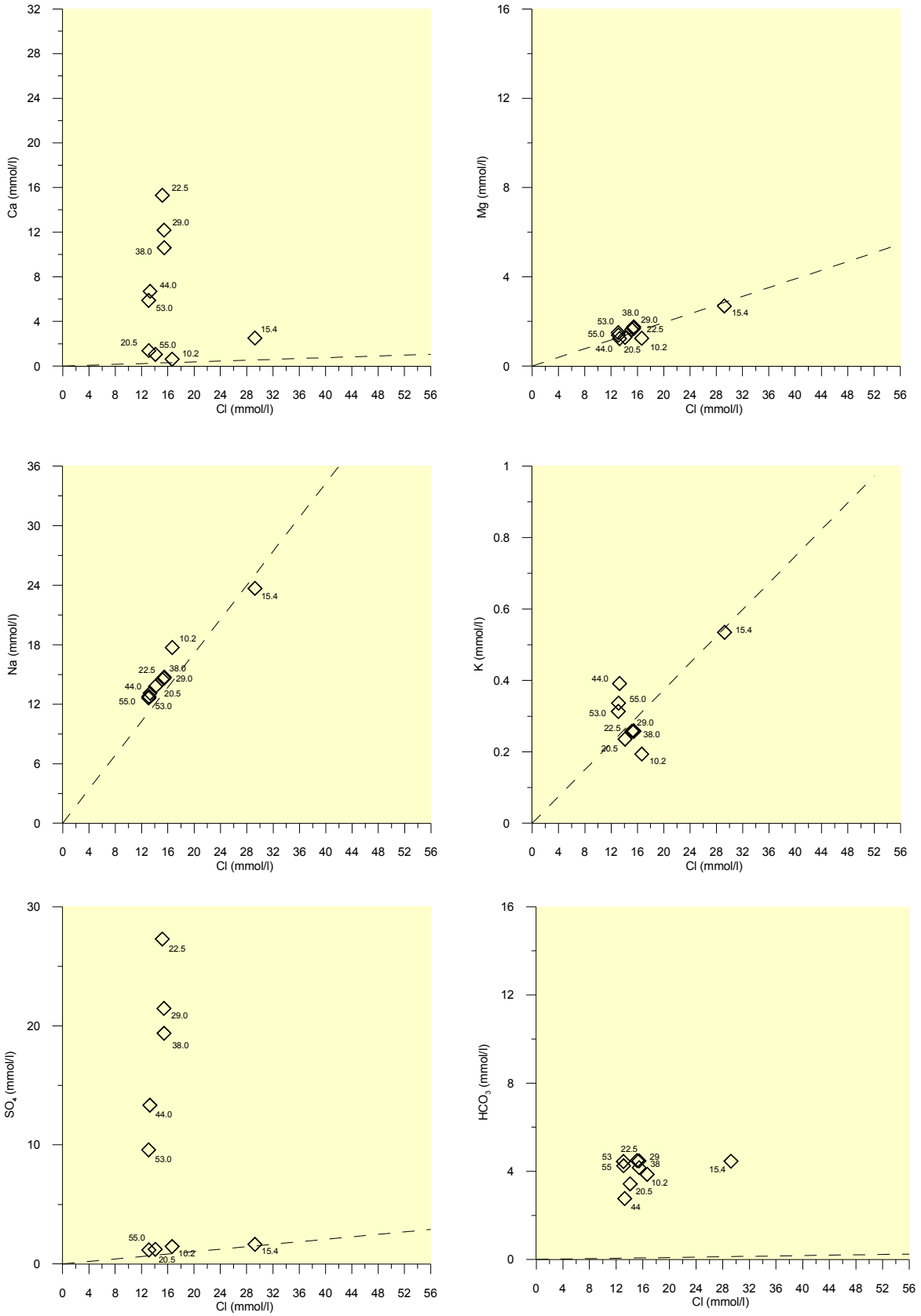

Figure 6.10 Composition diagrams of major ions versus chloride sampled at the Bull Creek investigation site, September 2005–January 2006. The dashed line is the dilution line for seawater. Piezometer mid-screen depths are shown beside each point.

clustering around the seawater dilution line, implying minimal precipitation or dissolution processes between the groundwater and host rock. The graphs of Ca^{2+} and SO_4^{2-} against chloride clearly show contamination in five of the samples from the Gypset® used in the piezometer construction. If the effects of the contamination from Ca^{2+} and SO_4^{2-} ions were removed, all samples would tend to fall close to the seawater dilution line. Only the sample taken at 15.4 m is significantly different from the other samples, lying further along the dilution line at a greater concentration. The absence of a corresponding enrichment of δ^2H supports the view that the greater concentration of the major ions at this depth is due to greater transpiration, rather than greater evaporation.

The hydrochemistry data suggest that the compositions of all samples are dominated to a greater extent by sodium and chloride ions, indicating that the hydrochemical composition of the water is of marine aerosol origin.

The isotopic signatures of the groundwater samples from the Bull Creek investigation site lie above the local meteoric water line but within the range of rainfall for the catchment, as indicated by the $\delta^2H/\delta^{18}O$ signatures for rainfall from Echunga and Finniss (Fig. 6.4). Bull Creek samples plot to the left of the mean weighted rainfall for Adelaide, indicating that groundwater recharge occurs during the winter months. The plot of δ^2H versus chloride (Fig. 6.5) shows that all samples, apart from the 15.4 m sample, have been subject to similar degrees of evaporation and/or transpiration. The high chloride concentration of the sample taken at 15.4 m is likely to be due to transpiration rather than evaporation as there is no significant δ^2H-enrichment compared to the other samples.

Rainfall samples collected from the Echunga pluviometer and Finniss gauging station (nearest representative rainfall samples to ARC and FRC) between March 2003 and July 2005 have isotopic compositions similar to those collected at the GNIP station in Adelaide since 1962. The sample collected from Echunga in October 2003 has a slightly more enriched signature suggesting that it had been subject to secondary evaporation prior to collection.

6.2.2 CARBON-14 AND CHLOROFLUOROCARBONS (CFCs)

The high CFC-12 concentrations (Fig. 6.11) at depths of 10.2 and 15.4 m indicate relatively young groundwater (<25 years). At 20.5 m, the CFC-12 concentration indicates an age of about 40 years, while below this all samples are below reliable detection range, indicating an age of greater than 40 years. The age gradient between 20.5 and 10.2 m can be extended upward to the watertable at a depth of 5 m where a CFC-12 concentration of ~240 pg/kg (present-day surface water CFC-12 concentration) and age of zero years is assumed. Thus a linear age gradient of ~2.7 y/m is apparent across this depth range. Analysis of the ^{14}C activities supports this finding and provides indication of the linearity of the age gradient to greater depths where the groundwater is too old for dating with CFC-12 (Fig. 6.12). The plot of uncorrected ^{14}C ages against depth shows that there is a ^{14}C thermonuclear component in the first three piezometers (negative apparent age), which implies that the water is modern (<40 years), and supports the findings from the CFC data. The uncorrected ^{14}C ages cannot be compared to the CFC-12 ages; however, the ^{14}C data provide confirmation that the linearity of the age gradient extends to a greater depth. The ^{14}C uncorrected age at 60 m is about 1500 years.

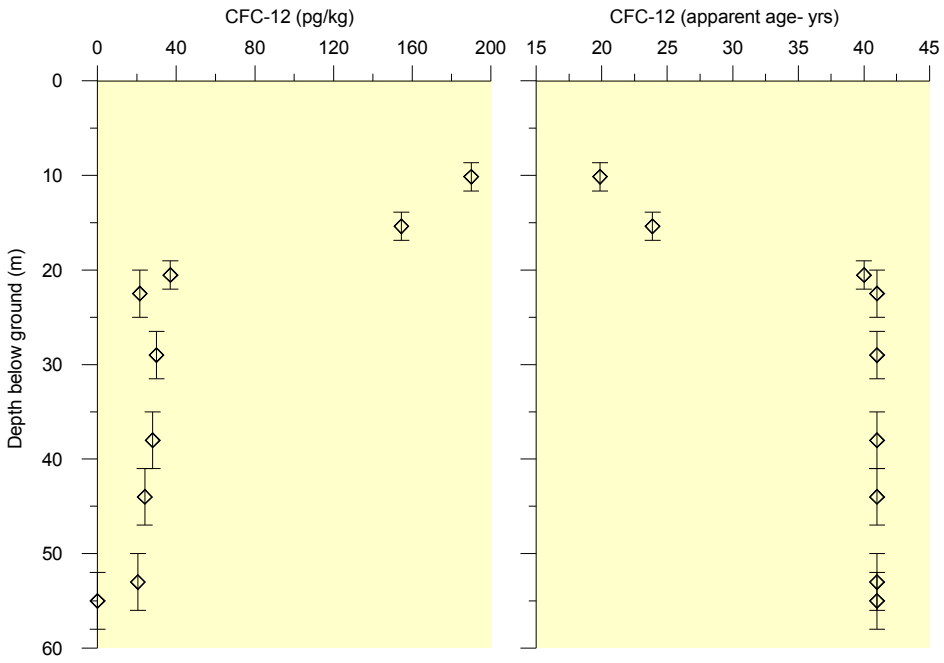

Figure 6.11 Depth profiles of CFC-12 concentrations and CFC-12 apparent ages of groundwater from the nested piezometers at the Bull Creek investigation site. The average watertable depth was 5.7 m below ground for February 2006 when sampling was completed. The error bars represent the piezometer screen length from which the sample was taken.

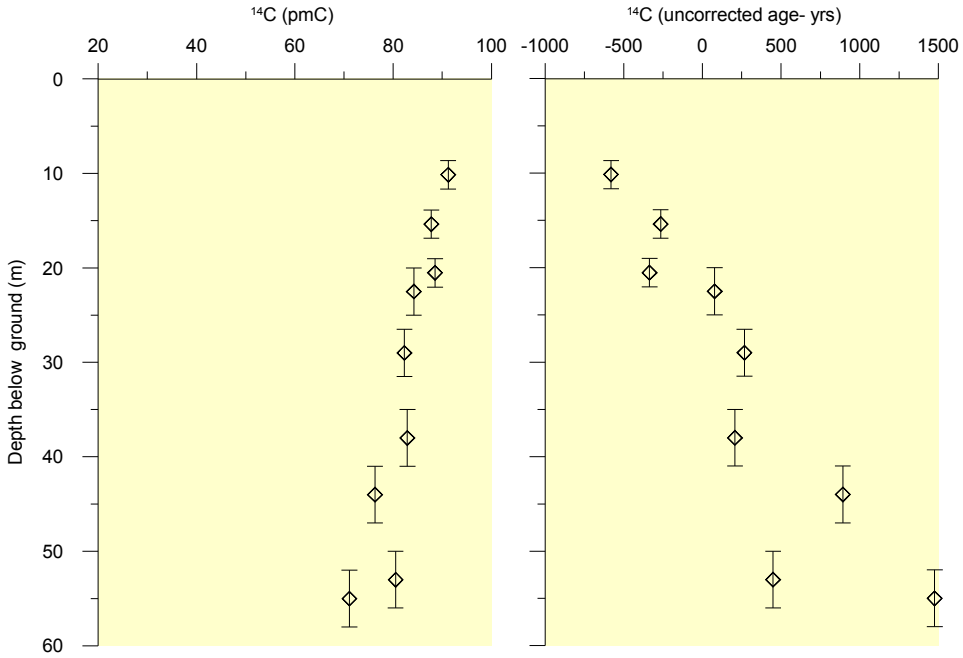

Figure 6.12 Depth profiles of ^{14}C activities and ^{14}C apparent ages from the nested piezometers at the Bull Creek investigation site, February 2006. The error bars represent the piezometer screen length from which the sample was taken.

The position of the 15.4 m sample in the CFC-12 and ^{14}C age/depth relationships supports the hypothesis that the anomaly in the hydrochemistry is due to the water at that depth having undergone a greater degree of transpiration, rather than due to influence from a lateral flow system.

Corrected ^{14}C ages (Table 6.2) show a trend of increasing age with depth. The resolution of the method of age determination and correction is such that the relatively low ages (<500 years) determined for samples down to 20.5 m depth, only indicates that these are samples of modern groundwater. As such, the ages determined here do not conflict with the ages of <40 years determined from the CFC-12 analysis of these samples. At depths below 20.5 m, the ^{14}C ages derived indicate that the carbon within the groundwater progressively increases in age with depth, up to an age in the order of thousands of years at a depth of 55 m.

Table 6.2 Uncorrected and corrected ^{14}C ages for samples from the Bull Creek investigation site. Corrected ages are derived using the Fontes and Garnier (1979) correction model. Data on the sample $\delta^{13}C$ and HCO_3, and CO_2 molar concentrations are used in the correction model. The values of both the $\delta^{13}C$ and ^{14}C activities of the FRA carbonates and soil CO_2 are also used in the correction model. Values used here were: $\delta^{13}C_{carbonate}$ = -7.8$^{o}/_{oo}$, $\delta^{13}C_{soilCO2}$ = -13$^{o}/_{oo}$, $A_{carbonate}$ = 0 pmC, $A_{soilCO2}$ = 85 pmC.

Sample	Depth	A (pmC)	$\delta^{13}C$	HCO_3 (M)	CO_2 (M)	Uncorrected age (y)	Corrected age [F & G model] (y)
B1	10.2	91.2	-15.20	0.00377	0.00037	-581	488
B2	15.4	87.8	-13.10	0.00426	0.00050	-266	-1391
B3	20.5	88.5	-15.10	0.00334	0.00051	-335	312
B4	22.5	84.2	-15.50	0.00429	0.00045	78	1145
B5	29.0	82.3	-15.70	0.00403	0.00024	267	1634
B6	38.0	82.9	-16.10	0.00384	0.00045	207	1619
B7	44.0	76.3	-15.90	0.00256	0.00012	893	2259
B8	53.0	80.5	-16.50	0.00414	0.00020	450	2353
B9	55.0	71.1	-16.90	0.00407	0.00013	1476	3387

6.3 FINNISS RIVER CATCHMENT

6.3.1 MAJOR CHEMISTRY AND ISOTOPES

The groundwater samples collected from the Ashbourne investigation site are shown on a Piper plot in Figure 6.13. The hydrochemical characteristics of these samples are similar to those at the Burra investigation site and are of Na–Mg–Cl type. The compositions of all samples are dominated to a greater extent by sodium and chloride ions indicating that the water is of marine aerosol origin, but there is some contribution from atmospheric precipitation (partial dissolution of dust particles) or acquisition during weathering and water–rock interactions.

Figure 6.14 shows the measured TDS, chloride (Cl^-), deuterium (δ^2H) and pH profiles with depth at the Ashbourne investigation site. The chloride and TDS concentrations are uniform below 30 m depth, and are clearly chemically distinct from samples from 12.5, 16 and 24.5 m depth, which have significantly higher Cl^- and TDS concentrations. The deuterium profile shows samples from these depths to be less enriched than samples from greater depths, suggesting that the greater Cl^- and TDS concentrations observed between 12.5–24.5 m are possibly influenced by greater transpiration prior to recharge.

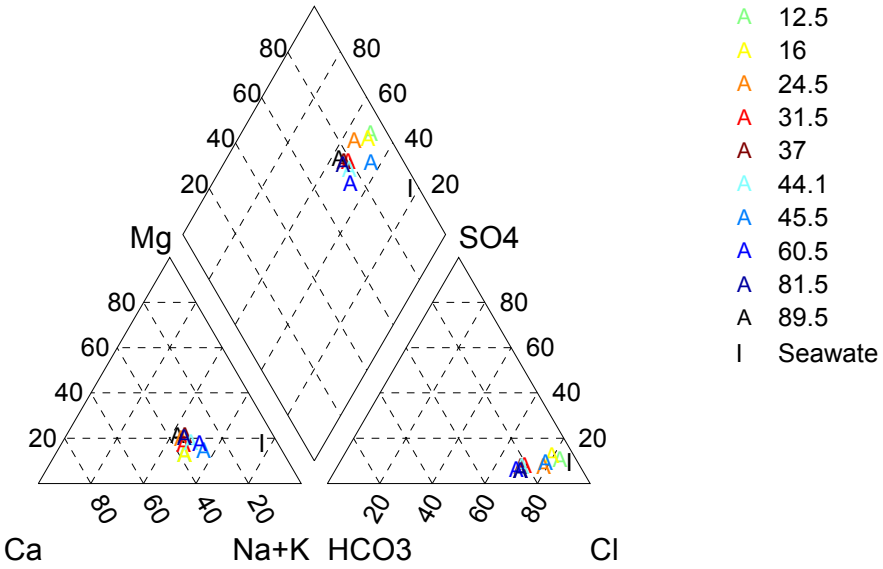

Figure 6.13 Piper plot of groundwater samples collected at the Ashbourne investigation site, February 2006.

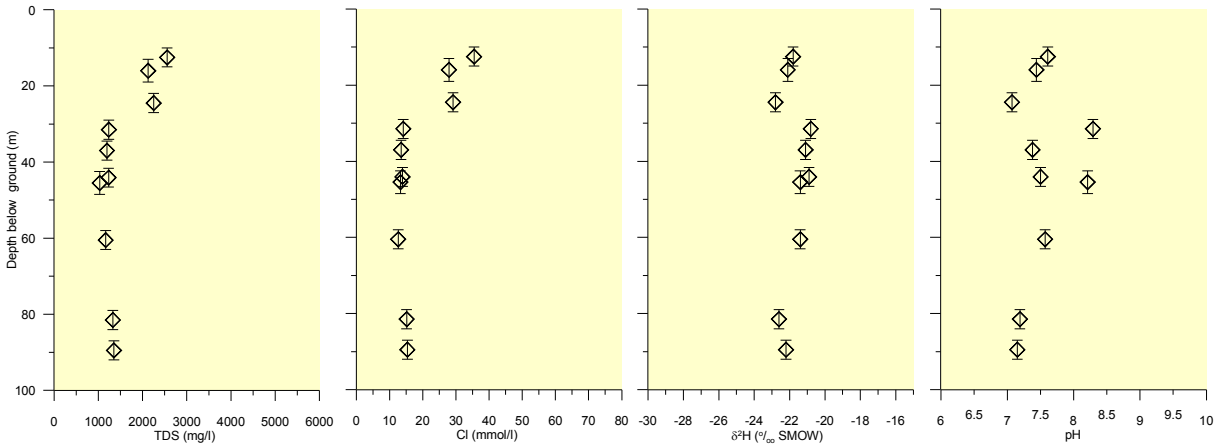

Figure 6.14 TDS, chloride, δ^2H and pH profiles sampled at the Ashbourne investigation site, February 2006. The average watertable depth was ~8 m below ground for February 2006 when sampling was completed. The error bars represent the piezometer screen length from which the sample was taken.

The pH profile from 12.5–89.5 m ranges from 7.1–8.3, typically with lower pH at greater depth. Samples from 31.5–45.5 m have a distinctly higher pH than at other depths.

The graphs in Figure 6.15 show the concentrations of major ions (Ca^{2+}, Mg^{2+}, Na^{+}, K^{+}, SO_4^{2-} and HCO_3^{-}) against chloride and their proximity to the respective seawater ion/chloride relationship. These show that the majority of samples from 30–90 m depth have a similar composition, generally clustered close to the seawater dilution line, except in the graphs of Ca^{2+} versus Cl^{-} and HCO_3^{-} versus Cl^{-}. The increases of Ca^{2+} and HCO_3 over Cl^{-}, compared to the seawater ratio, indicate a degree of calcite dissolution in samples through the entire range of depths sampled. Samples from the 12.5, 16 and 24.5 m depth piezometers have significantly higher concentrations of all the major ions than those at greater depths.

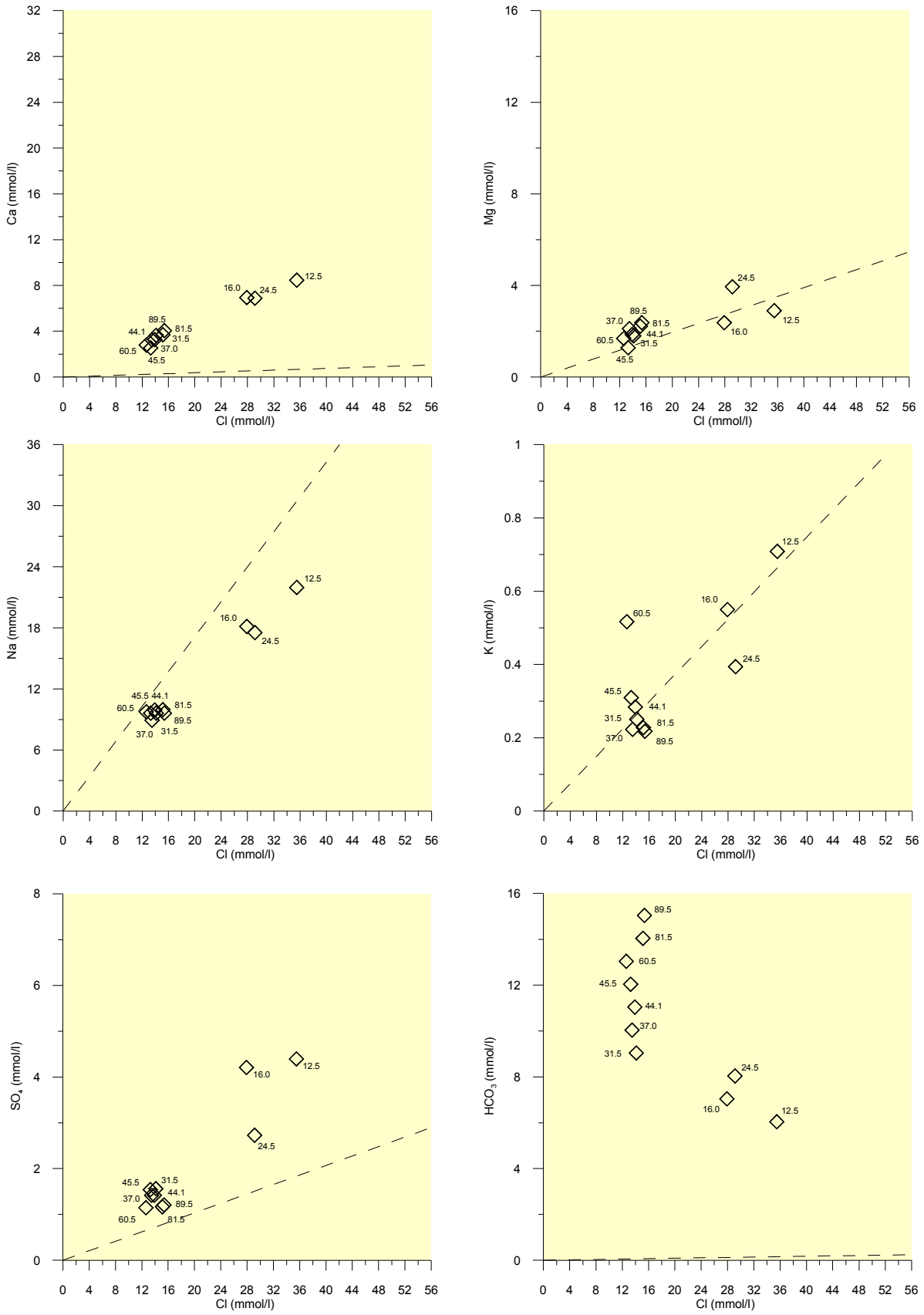

Figure 6.15 Composition diagrams of major ions versus chloride sampled at the Ashbourne investigation site, February 2006. The dashed line is the dilution line for seawater. Piezometer mid-screen depths are shown beside each point.

Groundwater at less than 30 m depth appears to be chemically distinct from the deeper groundwater. The standing water levels at this investigation site (Fig. 5.13) indicate an upward hydraulic gradient between piezometers at greater depths (60.5, 81.5 and 89.5 m) and the shallower piezometers (12.5, 16 and 24.5 m). The upward gradient and distinct difference in chemistry is consistent with the presence of a confining layer at some depth between 25–40 m, creating separate flow systems above and below the confining layer. The drill logs for this investigation site indicate a transition from weathered to unweathered metasiltstone at 27–30 m. This transition may represent the boundary between upper and lower flow systems.

The interpretation of the Cl^- and δ^2H depth profiles indicates separate recharge processes for the upper and lower flow systems, with groundwater in the upper system experiencing a greater degree of transpiration prior to recharge.

The isotopic signatures of the groundwater samples from the Ashbourne investigation site (Fig. 6.4) all plot close to the local meteoric water line, but are significantly enriched in $\delta^{18}O$ and δ^2H compared to the isotopic signature of rainfall for the catchment and the mean for Adelaide rainfall. This indicates that rain falling in the FRC undergoes significant evaporation prior to recharging the groundwater system encountered at the Ashbourne investigation site. The plot of δ^2H versus chloride (Fig. 6.5) shows that groundwater from 12.5, 16 and 24.5 m have a similar δ^2H value but greater Cl^- concentrations than water from depths below 25 m. This suggests that water recharging the groundwater at these depths is subject to significantly more transpiration than water recharging the groundwater in the deeper system. This may be due to slower vertical flow in the upper system, allowing more time for plant root water uptake, or due to different vegetation coverage to that in the recharge area for the deeper groundwater flow system or changes in vegetation with time.

6.3.2 CARBON-14 AND CHLOROFLUOROCARBONS (CFCs)

The CFC-12 concentrations for the Ashbourne investigation site (Fig. 6.16) indicate a linear age gradient in the depth range from 12–25 m, increasing from ~22 years at 12.5 m to 39 years at 24.5 m. This age gradient can be extended upward to the watertable, at a depth of ~8 m, where a CFC-12 concentration of ~240 pg/kg and age of zero years is assumed. This results in a linear age gradient of ~2.3 y/m between the watertable and 24.5 m depth. The linear nature of the age gradient suggests that a vertical ‘piston’ flow through media of uniform hydraulic conductivity exists through this depth range.

Below 24.5 m depth, the CFC-12 data support the assumption that a confining layer exists at some depth between 25–40 m. At ~44–45.5 m there appears to be younger groundwater than at 24.5 m, which is only expected if there are separate flow systems above and below a confining layer or some preferential pathway through the fractures.

The ^{14}C activities (Fig. 6.17) are all fairly similar, ~70 pmC, in groundwater between 37–89 m, suggesting rapid vertical flow through this depth range. Above 25 m, ^{14}C activities are significantly higher (81–93 pmC), supporting the suggestion that there are separate flow systems above and below a confining layer between 25–40 m. The CFC-12 and ^{14}C data for the 60.5 m piezometer are omitted from Figures 5.16–5.17 as the sample was contaminated during or after sampling.

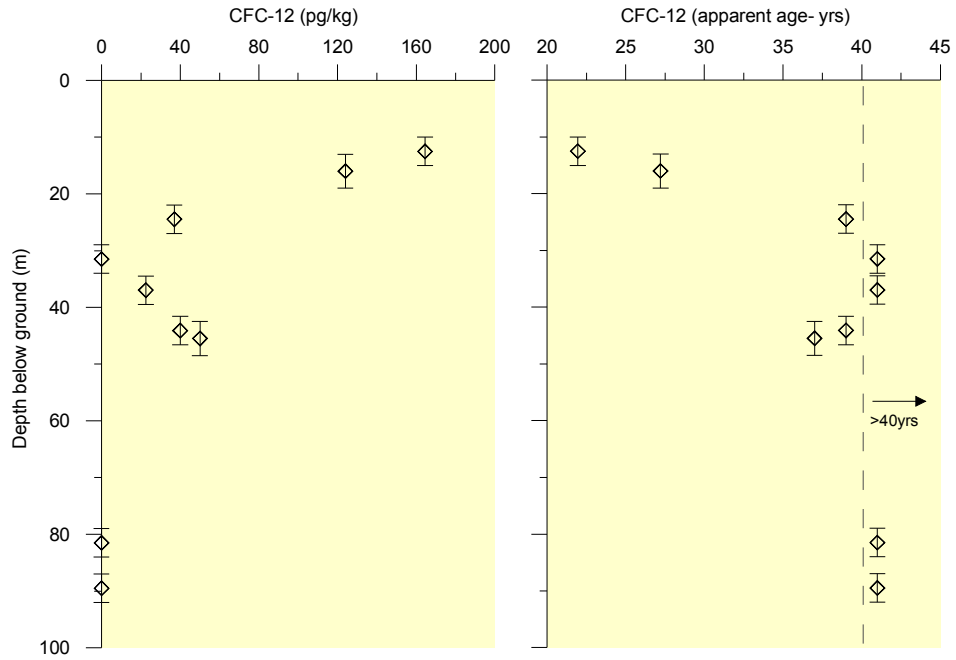

Figure 6.16 Depth profiles of CFC-12 concentrations and CFC-12 apparent ages of groundwater from the nested piezometers at the Ashbourne investigation site. The average watertable depth was 8 m below ground for February 2006 when sampling was completed. The error bars represent the piezometer screen length from which the sample was taken.

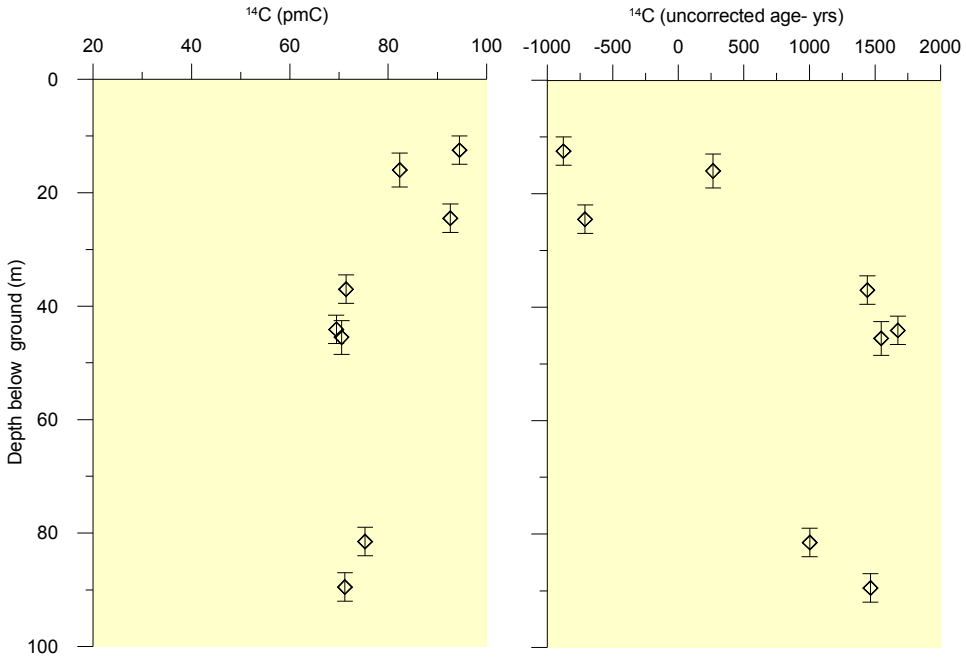

Figure 6.17 Depth profiles of ^{14}C activities and ^{14}C apparent ages from the nested piezometers at the Ashbourne investigation site, February 2006. The error bars represent the piezometer screen length from which the sample was taken.

Corrected ^{14}C ages (Table 6.3) support the suggestion of upper and lower groundwater systems separated by a confining layer between 25–40 m depth. The relatively low ages (<500 years) derived for samples from less than 25 m depth suggest that, within the resolution of the method, these are samples of modern groundwater. Between 37–90 m depth, the corrected ages are significantly greater and are of a consistent age throughout this depth range.

Table 6.3 Uncorrected and corrected ^{14}C ages for samples from the Ashbourne investigation site. Corrected ages are derived using the Fontes and Garnier (1979) correction model. Data on the sample $\delta^{13}C$ and HCO_3, and CO_2 molar concentrations are used in the correction model. The values of both the $\delta^{13}C$ and ^{14}C activities of the FRA carbonates and soil CO_2 are also used in the correction model. Values used here were: $\delta^{13}C_{carbonate}$ = -7.8$^{o}/_{oo}$, $\delta^{13}C_{soilCO2}$ = -13$^{o}/_{oo}$, $A_{carbonate}$ = 0 pmC, $A_{soilCO2}$ = 85 pmC.

Sample	Depth	A (pmC)	$\delta^{13}C$	HCO_3 (M)	CO_2 (M)	Uncorrected age (y)	Corrected age [F & G model] (y)
A1	12.5	94.5	-17.20	0.00000	0.00250	-875	-698
A2	16.0	82.3	-17.15	0.00000	0.00250	265	250
A3	24.5	92.6	-17.10	0.00000	0.00250	-711	440
A5	37.0	71.4	-16.80	0.00000	0.00250	1441	1482
A6	44.1	69.4	-16.50	0.00000	0.00250	1674	1395
A8	60.5	54.1	-15.00	0.00000	0.00250	3740	1405
A9	81.5	75.3	-16.30	0.00000	0.00250	1002	966
A10	89.5	71.2	-16.20	0.00000	0.00250	1465	1221

7. VERTICAL FLOW RATES AND AQUIFER RECHARGE

7.1 BURRA CREEK CATCHMENT

7.1.1 CARBON-14 AND CHLOROFLUOROCARBONS (CFCs)

The complex nature of the groundwater flow systems at the Burra site has made it difficult to estimate a reliable recharge rate. Due to a reversed vertical age gradient (younger age with increasing depth) in the shallow system, the vertical CFC-12 age/depth gradient in the local to intermediate flow system below the perched watertable was used. The age/depth gradient of this flow system is 0.48 y/m (12 years per 25 m). Using equation 4.6, the average equivalent fracture aperture (2*b*) obtained from the nested piezometers is equal to 204 μm, with a groundwater velocity through the fractures of 13 m/d. A mean fracture spacing of 2*B* = 0.2 m and an average bulk hydraulic conductivity of *K* = 2.6 m/d was applied according to outcrop measurements and single-well aquifer tests, respectively.

Applying the vertical plate model, the average vertical flow rate(V_w) in the fracture is 0.05 m/d and the aquifer recharge rate (Q_v) is 15 mm/y. Values of matrix diffusion coefficient and matrix porosity were assumed to be $D = 10^{-4}$ m^2/y and θ_m =0.015, respectively, and are typical of a slate, which is the main lithological unit at the Burra site. The accuracy of the vertical flow rate and recharge estimates depends largely on the estimated fracture spacing, matrix porosity and matrix diffusion coefficient and, to a lesser extent, the hydraulic conductivity and fracture aperture (Cook & Simmons 2000).

The application of the ^{14}C data to estimate recharge was not possible because of the effects of water–rock interactions, which meant the groundwater samples were a mixture of more recent carbon with very old ‘dead’ carbon from rock sources and gave a much older and unrealistic age gradient. However, as discussed in Section 6.1.2, the ^{14}C data supported the hydrochemistry results in defining the boundary between the shallow and deeper flow systems.

If the aquifer system at the Burra investigation site was representative of an homogenous unconfined sedimentary aquifer then, using equation 4.2, the recharge rate determined from the measured CFC-12 concentrations in the piezometers located between 8.3–59.5 m depth would be between ~5–75 mm/y, assuming a porosity value of 0.05.

Figure 7.1 compares the measured CFC-12 concentrations from the Burra, Bull Creek and Ashbourne investigation sites to results from an equivalent porous media model for recharge rates of 10, 20, 35, 50 and 70 mm/y using a porosity value of 0.05.

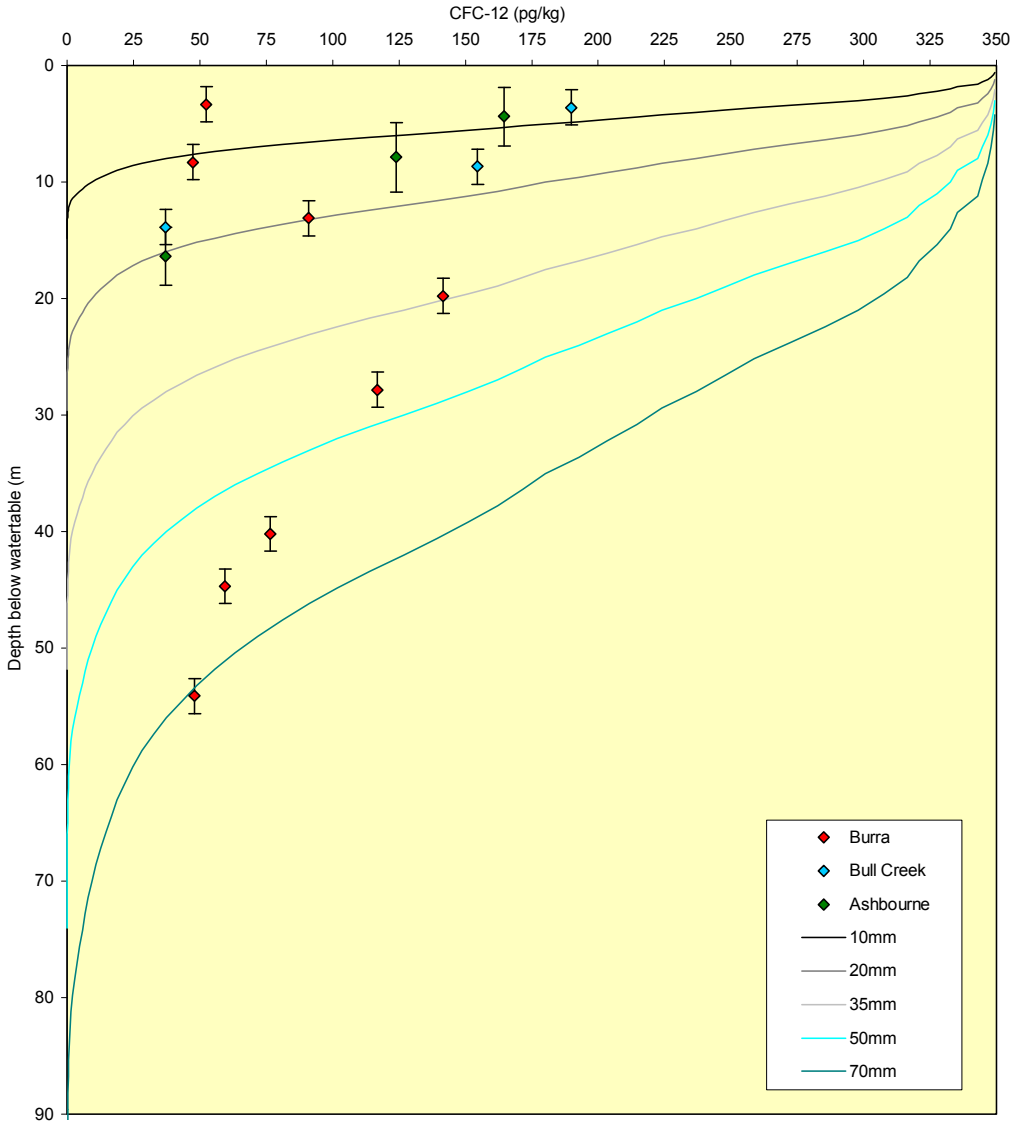

Figure 7.1 **Comparison of measured CFC-12 concentrations at the Burra, Bull Creek and Ashbourne investigation sites with results from an equivalent porous media recharge model below the watertable. The error bars represent the length of screen of the piezometer from which the sample was taken.**

7.1.2 CHLORIDE MASS BALANCE

Figure 7.2 shows the recharge estimates according to the CMB method in the upper part of the BCC. These estimates are shown for points in the catchment where there are groundwater extraction wells for which chloride concentration data are available. Annual precipitation values nearest to the bore locations were obtained from an interpolation of rainfall isohyet data produced by BoM. Precipitation is between 300–500 mm/y on the higher western margin of the catchment but less than 300 mm/y in the lower eastern part of the catchment, where it descends out onto the Murray Basin. The chloride concentration in rainfall is assumed to be 4.0 mg/L, according to measured chloride concentrations from collected rainfall at the Mount Torrens stream gauging station (2002–05), and an annual runoff rate equal to 10% of precipitation. The chloride concentration of the rainfall sample

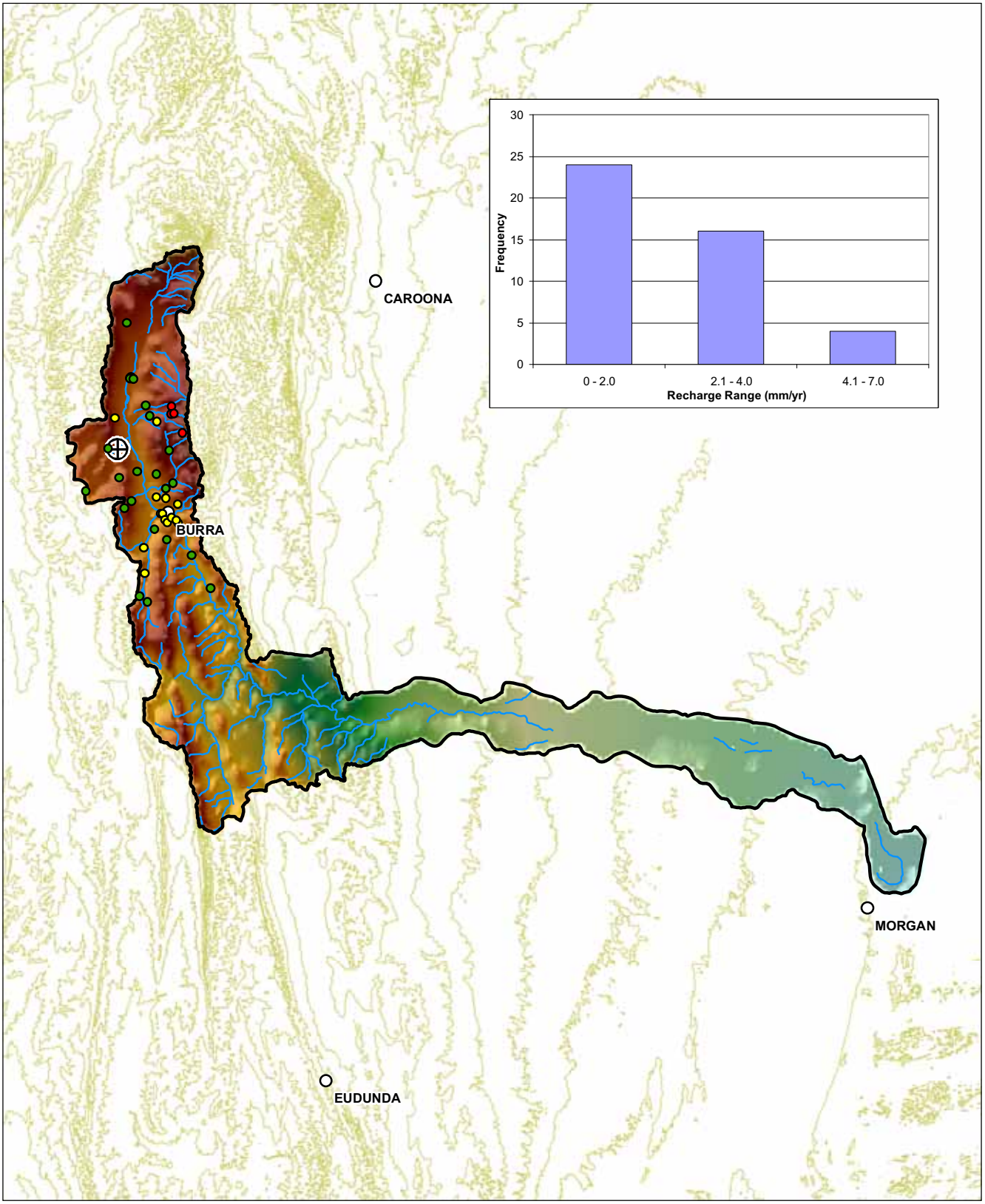

Figure 7.2 Burra Creek Catchment Recharge Estimates (Chloride Mass Balance)

GW sample locations

Recharge estimate (mm/yr)

- 0 - 2.0
- 2.1 - 4.0
- 4.1 - 7.0
- Catchment boundary
- Burra investigation site
- Town

Elevation (m ASL)

Value

High : 850

Low : 10

Streams

Topographic contours (40 m)

Produced By: Mount Lofty Ranges Team
Knowledge and Information Division
Department of Water, Land and Biodiversity Conservation

Datum: Geocentric Datum of Australia 1994 (GDA 94).

Date: 18th July 2006

N

0 5 10 15 20 25 Km

Government of South Australia
Department of Water, Land and Biodiversity Conservation

collected at the site in March 2006 was significantly less (1.5 mg/L). Chloride concentrations measured from bores in the catchment ranged from about 300–3800 mg/L and were sampled as early as 1944. Greater than 85% of the recharge estimates were less than 3 mm/y, indicating a very small proportion (0.6–1.2%) of rainfall recharges the aquifer system.

The recharge estimates according to the CMB method at the Burra investigation site ranged from ~0.5 mm/y in the shallower system (8–33 m) to 1.2 mm/y in the deeper flow system (45–90 m; Fig. 7.3). These differences reflect the observed changes in chloride and TDS concentrations between the upper and lower systems, as discussed in Section 6.1.1. The chloride concentrations in the shallower piezometers are significantly higher than concentrations in the deeper piezometers and hence recharge estimates are approximately twice as much for the deeper system as for the shallower system.

The differences in recharge estimates between the shallow and deeper flow system may reflect the effects of recent land clearing on the equilibrium of chloride between the matrix and the fractures. The removal of vegetation would result in higher recharge and potentially flush salt, stored due to processes of evapotranspiration, from the soil zone. Using equation 4.8, the approximate time taken for the chloride in the matrix to reach equilibrium with that of the fractures would be 100 years. This assumes an effective diffusion coefficient (D) of 10^{-4} m^2/y and fracture spacing ($2B$) of 0.2 m. Land clearing would have been occurring in the Burra catchment 100 years ago with the operation of the town's copper mine, which would suggest that equilibrium has been reached in the aquifer system. If the fracture spacing were 0.1 m then the time to reach equilibrium would be 50 years. This simple model is very sensitive to fracture spacing and the effective diffusion coefficient of the matrix.

7.2 ANGAS RIVER CATCHMENT

7.2.1 CARBON-14 AND CHLOROFLUOROCARBONS (CFCs)

The CFC and ^{14}C data from the Bull Creek site showed a fairly linear increase in age with depth, implying uniform recharge to the shallow and deep aquifer systems. Using equation 4.6, the average equivalent fracture aperture ($2b$), determined from aquifer tests carried out on the nested piezometers, is = 108 μm with a groundwater velocity through the fractures of 4 m/d. A mean fracture spacing of $2B$ = 0.05 m and an average bulk hydraulic conductivity of K = 1.6 m/d was applied according to outcrop measurements and the single-well aquifer tests conducted at the site, respectively.

The vertical CFC-12 age gradient for the shallow flow system at the Bull Creek investigation site is 2.7 y/m (40 years per 14.8 m). Applying the vertical plate model, and using the results from the aquifer tests together with rock outcrop measurements, the average vertical flow rate (V_w) in the fracture is 0.024 m/d and the aquifer recharge rate (Q_v) is 19 mm/y.

Values of matrix diffusion coefficient and matrix porosity were assumed to be D = 10^{-3} m^2/y and θ_m = 0.05, respectively. These values are at the high end of the scale for siltstone and slate, which provide the highest groundwater velocity, and hence recharge rate, according to the measured concentrations. The values are similar to those used in the investigation by Love et al. (2002) in the Clare Valley where the targeted geology type was the Saddleworth

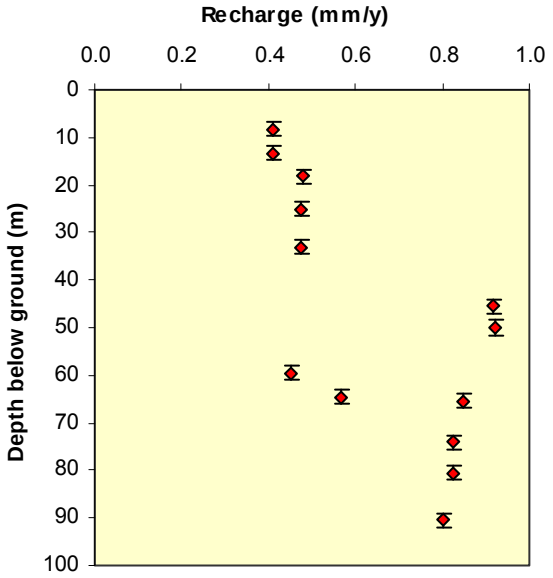

Figure 7.3 Vertical distribution of recharge estimates according to the CMB method at the Burra investigation site. The error bars represent the piezometer screen length from which the sample was taken.

Formation. The latter is dominated by siltstone, shale and dolomite and has similar characteristics to the Kanmantoo Group at the Bull Creek site.

According to ^{14}C data there is a thermonuclear component (^{14}C peaked in the atmosphere in 1964) in the first three piezometers, which implies that the age of the groundwater is modern (<40 years). Therefore, it can be inferred that the vertical ^{14}C groundwater age/depth gradient from the watertable to 20.5 m depth is 2.8 y/m (42 years per 14.8 m). Assuming the same physical characteristics of the aquifer as applied in the CFC calculations, the average vertical flow rate (V_w) in the fracture is 0.023 m/d and the aquifer recharge rate (Q_v) is 18 mm/y, which is very similar to the CFC results.

As discussed in 7.21, the accuracy of these estimates depends largely on the estimated fracture spacing, matrix porosity and matrix diffusion coefficient and to a lesser extent the hydraulic conductivity (Cook & Simmons 2000). Using the measured CFC-12 concentrations in an equivalent porous media model for recharge rates of 10, 20, 35, 50 and 70 mm/y and a porosity value of 0.05, the estimate of recharge is 9–18 mm/y (Fig. 7.1). This is similar to the estimate according to the vertical plate model, but the estimate largely depends on the estimated value of porosity.

7.2.2 CHLORIDE MASS BALANCE

Figure 7.4 shows the recharge estimates according to the CMB method in the ARC and FRC. These estimates are shown for points in the catchment where there are groundwater extraction wells for which chloride concentration data are available. Annual precipitation values nearest to the bore locations were obtained from an interpolation of rainfall isohyet data produced by BoM. Annual precipitation ranges from ~850 mm/y on the higher northwestern margin of the FRC to 450 mm/y in the lower southeastern part of the two catchments. The chloride concentration in rainfall is assumed to be 5.5 mg/L according to measured chloride concentrations from collected rainfall at the Echunga pluviometer (2003–05), and an annual runoff rate equal to 10% of precipitation. Chloride concentrations

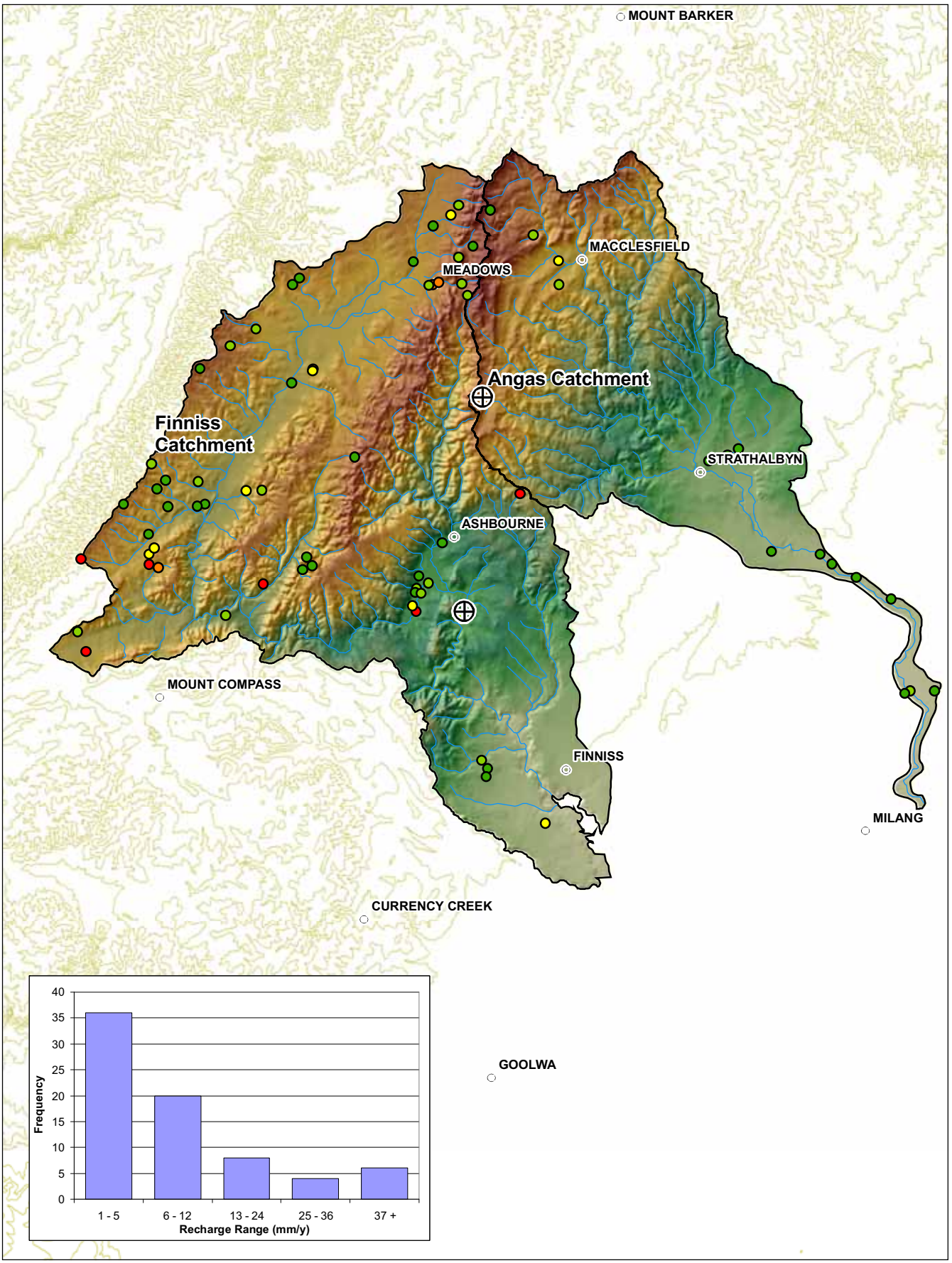

Figure 7.4 Angas and Finniss River Catchments Recharge Estimates (Chloride Mass Balance)

GW sample locations

Recharge estimate (mm/y)

- 1 - 2
- 3 - 5
- 6 - 10
- 11 - 15
- 16 +
- Ashbourne and Bull Creek investigation sites
- Catchment boundary

Elevation (m ASL)

Value

High : 500

Low : 0

Streams

Topographic contours (40 m)

Town

Produced By: Mount Lofty Ranges Team
Knowledge and Information Division
Department of Water, Land and Biodiversity Conservation

Datum: Geocentric Datum of Australia 1994 (GDA 94).

Date: 17th July 2006

N

0 2 4 6 8 10 km

Government of South Australia
Department of Water, Land and Biodiversity Conservation

M:\Projects_GWMt_Lofty_Ranges\EMLR 2006\Angas\Angas_Finniss_CMB_Recharge.mxd 18 July 2006 G. Green

measured from bores in the two catchments ranged from about 50–2700 mg/L. Recharge estimated by the CMB method ranged from 1–59 mm/y across the two catchments. More than 80% of the recharge estimates were less than 13 mm/y, indicating that only 1.5–3% of rainfall recharges the aquifer system.

The recharge estimates according to the CMB method at the Bull Creek investigation site ranged from ~2.1–4.8 mm/y (Fig. 7.5). The 15.4 m piezometer has significantly higher Cl^- concentration than at other depths. As discussed in section 6.2.1, it is surmised that this is due to water at that depth having been exposed to a higher degree of transpiration. Therefore, the CMB method estimates a lower recharge rate during the period in time that water at that depth was recharged. The Cl^- concentrations at all other depths at this site are fairly uniform and result in a range of recharge estimates from 3.8–4.8 mm/y.

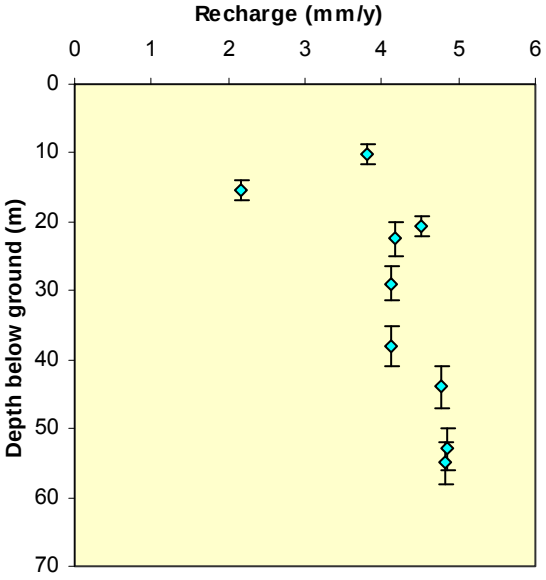

Figure 7.5 Vertical distribution of recharge estimates according to the CMB method at the Bull Creek investigation site. The error bars represent the piezometer screen length from which the sample was taken.

7.3 FINNISS RIVER CATCHMENT

7.3.1 CARBON-14 AND CHLOROFLUOROCARBONS (CFCs)

The CFC and ^{14}C data together with the hydrochemistry results from the Ashbourne site indicate that there is a shallow and deeper flow system separated by a confining layer. The vertical CFC-12 age gradient for the shallow flow system at the Ashbourne investigation site is 2.3 y/m (39 years per 16.5 m). Using equation 4.6, the average equivalent fracture aperture ($2b$), determined from aquifer tests carried out on the nested piezometers, is equal to 144 μm with a groundwater velocity through the fractures of 6 m/d. A mean fracture spacing of $2B$ equal to 0.34 m and an average bulk hydraulic conductivity of K = 1.1 m/d was used. Applying the vertical plate model, the average vertical flow rate (V_w) in the fracture is 0.18 m/d and the aquifer recharge rate (Q_v) is 22 mm/y.

Values of matrix diffusion coefficient and matrix porosity were assumed to be $D = 10^{-3}$ m^2/y and θ_m = 0.08, respectively. These values are at the high end of the scale for siltstone, which

provides the highest groundwater velocity, and hence recharge rate, according to the measured concentrations.

According to ^{14}C data there is a thermonuclear component (^{14}C peaked in the atmosphere in 1964) at 12.5 and 24.5 m depth, which implies that the age of the groundwater is modern (<40 years). Therefore, it can be inferred that the vertical ^{14}C groundwater age/depth gradient from the watertable to 24.5 m depth is 2.5 y/m (42 years per 16.5 m). Assuming the same physical characteristics of the aquifer as applied in the CFC calculations, the average vertical flow rate (V_w) in the fracture is 0.26 m/d and the aquifer recharge rate (Q_v) is 32 mm/y, which is very similar to the CFC results.

As discussed in Section 7.2.1, the accuracy of these estimates depends largely on the estimated fracture spacing, matrix porosity and matrix diffusion coefficient and to a lesser extent the hydraulic conductivity (Cook & Simmons 2000). Using the measured CFC-12 concentrations in an equivalent porous media model for recharge rates of 10, 20, 35, 50 and 70 mm/y and a porosity value of 0.05, the estimate of recharge is 10–21 mm/y (Fig. 7.1). This is similar to the estimate according to the vertical plate model, but the estimate largely depends on the estimated value of porosity.

7.3.2 CHLORIDE MASS BALANCE

At the Ashbourne investigation site, recharge estimates resulting from the CMB method range from 0.7–2.0 mm (Fig. 7.6). The recharge rate derived for the three shallow piezometers (12.5, 16.0 and 24.5 m) are significantly lower than for water at greater depths. As discussed in Section 6.3.1, it is thought that water at these depths overlies a confining layer that separates them from a deeper aquifer system with distinctly different hydrochemical characteristics. The CMB recharge estimates for these shallower piezometers range from 0.7–0.9 mm, while the estimates for the deeper system range from 1.6–2.0 mm. These results suggest that the upper and lower groundwater systems at this site have different recharge zones, implying that the deeper groundwater must flow laterally to this location, and that the recharge rate of the deeper system is significantly greater than that of the shallow system.

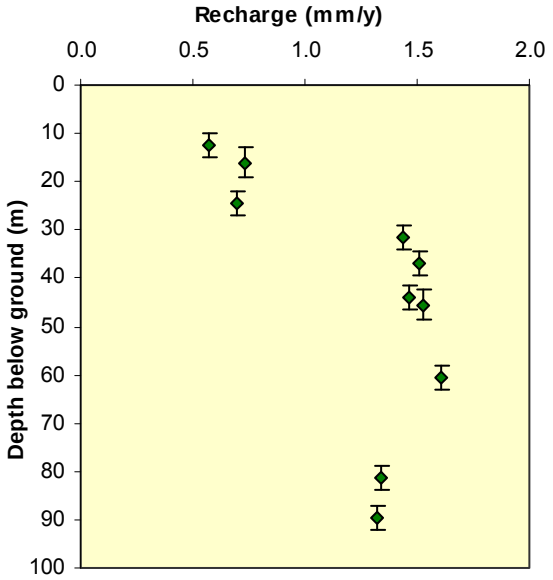

Figure 7.6 Vertical distribution of recharge estimates according to the CMB method at the Ashbourne investigation site. The error bars represent the piezometer screen length from which the sample was taken.

8. HORIZONTAL FLOW VELOCITIES

This chapter describes the horizontal flow velocities according to measured radon concentrations at the Burra, Bull Creek and Ashbourne investigation sites.

8.1 BURRA CREEK CATCHMENT

Radon concentrations measured in the piezometers from 25–65.5 m depth prior to purging (10–20 Bq/L) indicate that there is some active groundwater movement through the screens. However, from 74–90.5 m depth, the radon concentrations are less than 10 Bq/L, indicating that the groundwater flow in these piezometers is much slower (Fig. 8.1). Attempts to sample radon from the piezometers located between 8.3–18.2 m depth were unsuccessful because the piezometers, screened in low permeability clay and mixed weathered material, went dry during sampling.

The radon concentrations increased significantly after purging the piezometers, representing water sampled directly from the aquifer. The purged radon concentrations are greater than 200 Bq/L at 25–33 and 59.5–64.5 m, whilst between 45.5–50 m and below 65 m the concentrations are less than 100 Bq/L (Fig. 8.1). The variation in purged radon concentrations most likely reflects differing mineralogy and the physical characteristics of the fracture(s) intersecting the piezometer screens.

The ratios of unpurged to purged radon concentrations are less than 0.2 from 25–90.5 m, except at 50 m depth where the ratio is 0.7 (Fig. 8.1). Using equation 4.9, the calculated horizontal flow velocities at each of the sampled piezometers were all less than 3 m/y apart from at 50 m depth, which had a horizontal flow velocity of 33 m/y. Given these velocities refer to flow within the piezometers, the corresponding horizontal flows within the aquifer would be 0.75 and 8.25 m/y, respectively. The latter suggests that there is a significant fracture(s) intersecting the piezometer screen at 50 m depth but, as it is an order of magnitude higher than the other samples, it may be a result of inadequate pumping for the purged radon sample.

8.2 ANGAS RIVER CATCHMENT

Radon concentrations measured in the piezometers at 22.5, 29 and 44 m depth prior to purging were less than 20 Bq/L, whilst unpurged radon samples at 38 and 53 m depth were 172 and 63 Bq/L, respectively (Fig. 8.2). These radon concentrations suggest that there is some active horizontal groundwater movement through the piezometers screens. The high concentration at 38 m may represent a mixture of unpurged and purged groundwater during sampling. Attempts to sample radon from the piezometers located between 10–20.5 m depth were unsuccessful because they were purged dry as the screens are completed in low permeability material composed of clay and weathered siltstone.

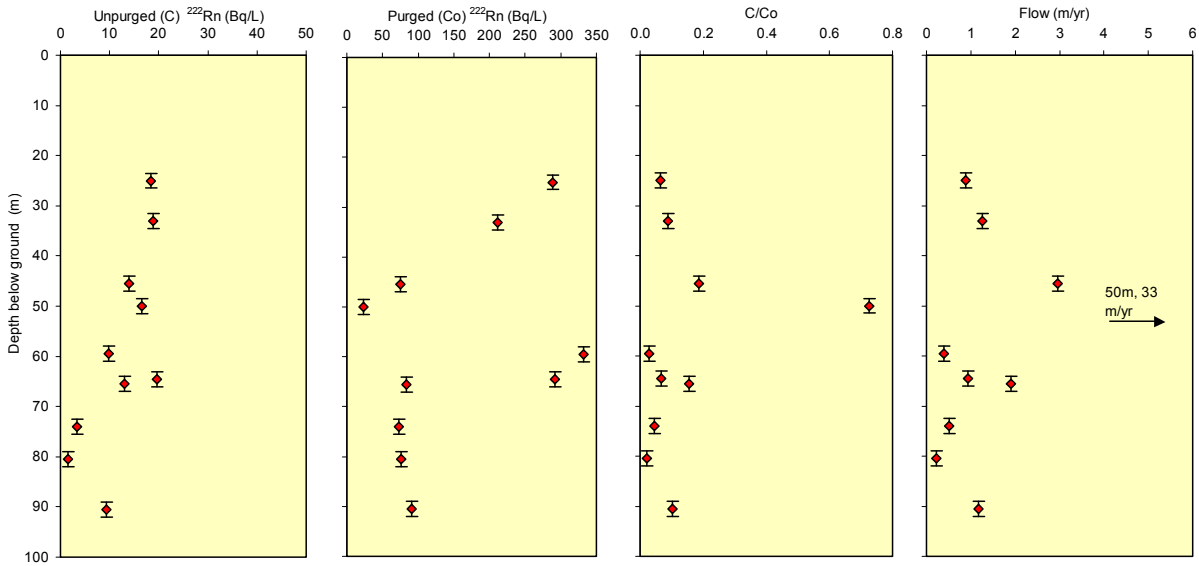

Figure 8.1 **^{222}Rn concentrations of unpurged and purged piezometers sampled during October 2005 and March 2006 (25–64.5 m), ratio of unpurged (C)/purged (Co) and horizontal flow rates within the piezometers at the Burra investigation site. Error bars show length of screen interval.**

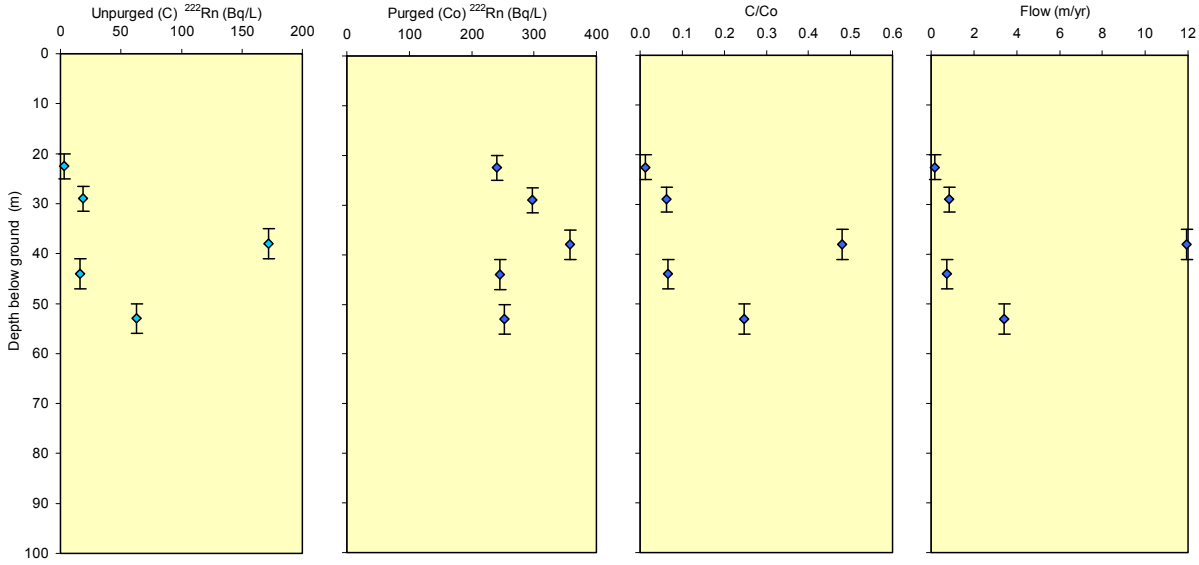

Figure 8.2 **^{222}Rn concentrations of unpurged and purged piezometers sampled during October 2005 and January 2006 (53 m), ratio of unpurged (C)/purged (Co) and horizontal flow rates within the piezometers at the Bull Creek investigation site. Error bars show length of screen interval.**

After purging the piezometers from 20.5 to 53 m depth, the radon concentrations increased significantly (greater than 240 Bq/L), representing water sampled directly from the aquifer (Fig. 8.2). As discussed in Section 7.1, the variation in purged radon concentrations most likely reflects differing mineralogy and the physical characteristics of the fracture(s) intersecting the piezometer screen. The length of the screen will also have an effect (i.e. longer screens will intersect more fractures).

The ratios of unpurged to purged radon concentrations are less than 0.1 at 22.5, 29 and 44 m depth, and 0.5 and 0.2 at 38 and 53 m depth, respectively (Fig. 8.2). Using equation 4.9, the calculated horizontal flow velocities at 22.5, 29 and 44 m depth were less than 1 m/y,

whilst at 38 and 53 m depth the horizontal velocity was 12 and 3 m/y, respectively. Again, these flow rates refer to horizontal flow within the piezometers. Horizontal flow velocities within the aquifer are <0.25, 3 and 0.75 m/y for the abovementioned depths. As mentioned earlier, the sample at 38 m may represent a mixed sample and therefore the calculated horizontal flow rate is overestimated.

8.3 FINNISS RIVER CATCHMENT

Radon concentrations measured in the piezometers between 24.5–44 m depth prior to purging were greater than 100 Bq/L, whilst from 44–89.5 m depth concentrations were less than 100 Bq/L (Fig. 8.3). Attempts to sample radon from the piezometers at 12.5 and 16 m depth were unsuccessful because they were purged dry and the sample taken at 60.5 m was contaminated.

After purging, the piezometer radon concentrations increased, particularly between 24.5–37 m depth where concentrations were greater than 1200 Bq/L (Fig. 8.3). The high concentrations may be related to the confining layer between about 25–40 m depth, identified by the hydrochemistry and CFCs. The samples taken below 37 m all had radon concentrations less than 600 Bq/L.

The ratios of unpurged to purged radon concentrations are less than 0.2 between 24.5–89.5 m except for at 44 m where the ratio is 0.36 (Fig. 8.2). Using equation 4.9, the calculated horizontal flow velocities between 24.5–89.5 m are less than ~2 m/y, whilst at 44 m depth the horizontal velocity is 6 m/y. Horizontal flow within the aquifer is ~0.5 m/y between 24.5–89.5 m, and 1.5 m/y at 44 m.

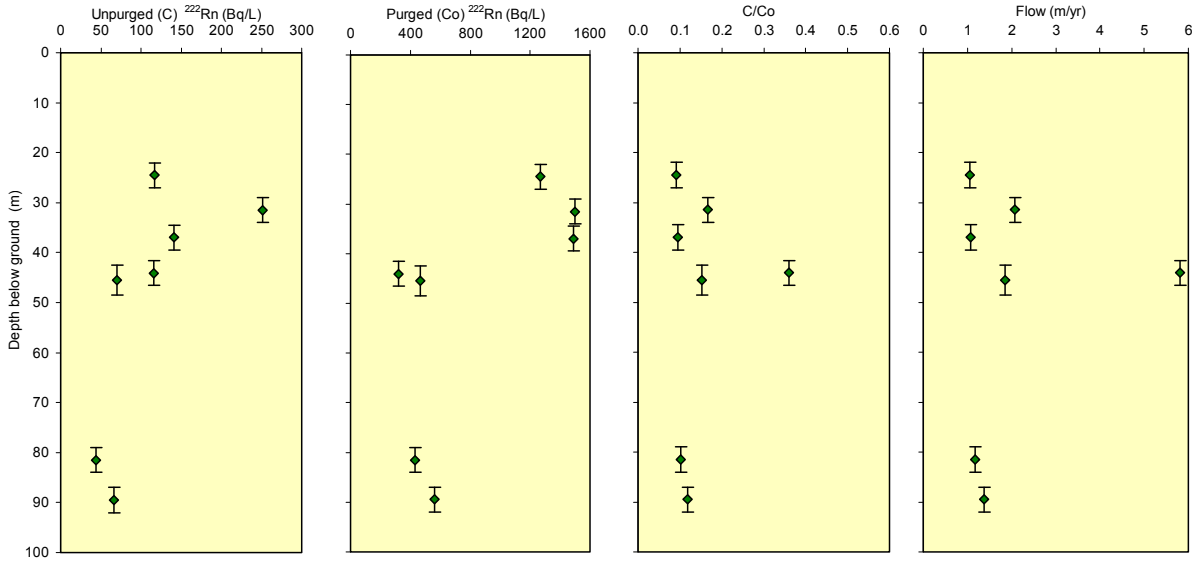

Figure 8.3 **^{222}Rn concentrations of unpurged and purged piezometers sampled during February 2006, ratio of unpurged (C)/purged (Co) and horizontal flow rates within the piezometers at the Ashbourne investigation site. Error bars show length of screen interval.**

9. GROUNDWATER FLOW AND RECHARGE

Several techniques have been used to estimate groundwater recharge rates at the Burra, Bull Creek and Ashbourne investigations sites giving a range of different estimates. On a catchment scale the CMB, calculated from over 140 bores in the BCC, showed that the majority of estimates were less than 5 mm/y. In the ARC and FRC, calculated from 74 bores, the estimates ranged from 1–59 mm/y, with more than 80% of estimates less than 13 mm/y. The CMB estimates can be considered a minimum recharge estimate.

Earlier investigations by Zulfic and Barnett (2003) estimated recharge rates using a catchment-scale water balance for the ARC and FRC as 97 and 125 mm/y, respectively. These estimates are about 12 and 15% of annual rainfall for the ARC and FRC, respectively, and are about 4–5 times greater than the estimates determined in this investigation. In comparison, a porous media model using the CFC-12 data showed that the recharge rate at the Burra, Bull Creek and Ashbourne sites is 5–75, 9–15 and 10–18 mm/y, respectively. The calculated values are quite sensitive to the chosen value of porosity, which in this case was 0.05.

The methods for determining groundwater recharge rates to the shallow and deep flow systems have assumed only piston flow and that equilibrium exist between the tracer concentrations in the fractures and the matrix. Differences in deuterium and $\delta^{18}O$ compositions can be used to distinguish between diffuse and direct recharge mechanisms (Cresswell & Herczeg 2004). Direct recharge tends to show relative enrichment in $\delta^{2}H$ and $\delta^{18}O$ because of evaporation prior to recharge, whilst diffuse recharge shows less evaporative signature because once water infiltrates below 1 m into the soil it is not affected as much by direct evaporation. The isotopic compositions of the groundwaters sampled from the shallow system at the Burra and Ashbourne sites show characteristics of direct recharge whilst diffuse mechanisms prevail for the deep systems. At the Bull Creek site, the isotopic compositions of the groundwater samples show some divergence from the meteoric water line, suggesting that direct recharge is the dominant process at the site. Horizontal flow rates at each of the investigation sites were typically low and quite variable and, hence, would require additional sampling to account for seasonal variation throughout the year.

The values used in the vertical plate recharge model for fracture spacing, fracture aperture, diffusion coefficient and matrix porosity were based according to the high end of the range of values for the rock types found at the sites and hence provided a maximum recharge value. CFC-12 data were used to estimate recharge as it most likely represents current recharge processes in the last century, when extensive land clearing began in the catchments and has a higher resolution than the ^{14}C data. A thermonuclear component in the ^{14}C concentrations confirmed the modern groundwater apparent age in the shallow flow systems at the Bull Creek and Ashbourne sites.

It is a very difficult task to accurately scale up estimates of recharge for each of the investigation sites to a catchment scale, suitable for use in the WAP, due to the complex nature of FRA. One of the main problems with the recharge estimates is the assumption that groundwater moves through the fractures and that they are interconnected over long distances. To what degree these fractures are continuous is relatively unknown and it is

intended, through further investigations prior to reassessment of the WAP, to gain a greater understanding of the physical characteristics of the geology and improve on the reliability of estimates of the recharge component in the catchment water balance and how it varies across the catchment.

10. CONCLUSIONS AND RECOMMENDATIONS

Hydrochemistry, isotopes, CFCs and radiogenic tracer profiles, together with geological mapping results and aquifer tests from the Burra, Bull Creek and Ashbourne investigation sites in the BCC, ARC and FRC, respectively, have been used to characterise groundwater flow processes and sources, and determine estimates of aquifer recharge.

Salts of marine aerosol origin dominate the chemistry of the groundwaters at each of the sites, which have undergone some evapoconcentration prior to recharge. There is little evidence for significant mineral weathering contributions except for some dissolution of carbonate-bearing minerals and water–rock interactions at the Burra site. A winter rainfall signature dominates the isotopic compositions of the samples from the Burra and Bull Creek sites whilst the samples from the Ashbourne site are slightly enriched, compared to the mean rainfall of Adelaide, suggesting evaporation prior to recharge.

At the Burra investigation site there is a local shallow flow system with a perched watertable overlying a deeper flow system divided by a semi-confining layer of clay and weathered slate between 33–45 m. In the shallow flow system, vertical circulation of groundwater is particularly slow and is of higher salinity than the deep system due to processes of evapotranspiration. The deeper flow system appears to be recharged more rapidly compared to the shallow system as indicated by the steep CFC apparent age gradient. The ^{14}C, hydrochemistry and isotope data indicated that there is connection between the shallow and deep systems. Calculations of horizontal flow in the shallow zone was not possible due to rapid drawdown in the piezometers, whilst flow in the deep system was typically less than 2 m/y at the time of sampling.

At the Bull Creek site there is good hydraulic connection between the shallow regolith zone and the FRA below. Modern groundwater (<40 years) was measured to at least 20 m depth and the ^{14}C data showed that there is a linear age gradient beyond this depth to 60 m with a ^{14}C uncorrected age of about 1500 years. At about 15 m the groundwater exhibits a strong transpiration signature implying active uptake of water by vegetation at this depth. Horizontal flow at the site, below 20 m depth, was less than 3 m/y at the time of sampling. The technique could not be conducted above this depth due to rapid drawdown in the piezometers indicating that horizontal flow is much slower in the shallow zone.

Similar to the Burra site, Ashbourne is characterised by two flow systems; a local shallow system to about 25 m, separated from an underlying deeper fractured rock system by a 15 m thick confining layer. CFC and ^{14}C results were consistent and showed that groundwater in the shallow system is less than 40 years old, whilst groundwater in the deeper system is much older (~1500 years old) with a strong vertical connection between fractures. The groundwater in the shallow system has a much higher salinity than the deep system and indicates processes of transpiration. Horizontal flow measurements made at the site were typically less than 2 m/y, at the time of sampling, between 20–90 m depth.

Estimated recharge rates for the BCC, ARC and FRC are 15, 18 and 22 mm/y, respectively. Assuming only two-thirds of the resource can be extracted, according to the CFC-12 recharge estimates, ~10, 12 and 15 mm/y are available for allocation in the BCC, ARC and FRC, respectively. The amount of water available to each user will need to be determined in accordance with the WAP.

10.1 FURTHER WORK

Further work will be done at the Burra, Bull Creek and Ashbourne investigation sites including additional sampling from the piezometers to monitor any hydrochemical change since the previous sampling cycle as well as additional pump tests and fracture mapping to quantify with more certainty the physical characteristics of the aquifer system used in the recharge models.

APPENDICES

A. CHEMISTRY RESULTS

Table A.1 **Major chemistry, isotopes, CFC-12 concentrations and ^{14}C activities of the groundwater samples at the Burra, Bull Creek and Ashbourne investigation sites, along with rainfall samples from the Finniss and Echunga Pluvio. Mean seawater is also shown**

					Field measurements							Laboratory analysis																	
Location and sample type	Unit No.	Mid-screen from ground (m)	Sample ID	Collection date	DO ppm	Field EC µS/cm	pH	Redox mV	Temp °C	Field Alkalinity (HCO_3^-) mg/L	TDS mg/L	Lab pH	Ca^{2+} mg/L	Mg^{2+} mg/L	Na^+ mg/L	K^+ mg/L	SO_4^{2-} mg/L	Cl^- mg/L	Lab Alkalinity (HCO_3^-) mg/L	Br^- mg/L	NH_4-N mg/L	NO_x-N mg/L	Sr ug/L	$\delta^{18}0$ ‰ rel SMOW	δ^2H ‰ rel SMOW	CFC-12 pg/kg	CFC-12 apparent age years	^{14}C pmC	$\delta^{13}C$ ‰ PDB
Burra GW	6630-3340	8.33	BR1	10/10/2005	4.54	5710	7.28	106	18.3	250	3320	7.4	220	184	696	15	207	1749	244	5.50	0.218	1.358	2692	-5.62	-31.5	53	36	39.2	-9.50
Burra GW	6630-3339	13.30	BR2	10/10/2005	2.91	5810	7.31	106	18.4	232	3317	7.5	222	180	694	16	211	1756	232	5.55	0.22	1.38	2501	-5.61	-32.8	48	36	39.9	-9.50
Burra GW	6630-3338	18.15	BR3	10/10/2005	3.34	5250	7.4	116	21.3	240	2934	7.7	189	163	584	16	232	1506	239	4.78	0.21	2.09	2152	-5.69	-33.9	91	30		
Burra GW	6630-3327	25.00	BR4	14/10/2005	3.97	5290	7.96	106	20.2	220	2975	7.9	222	158	603	17	250	1512	207	4.65	0.19	2.08	2151	-5.55	-34.5	142	23	36.1	-9.00
Burra GW	6630-3326	33.10	BR5	31/10/2005	3.50	5330	7.63	30	21.1	220	3127	7.7	244	165	619	20	330	1517	227	5.92	0.17	2.116	2459	-5.62	-32.9	117	26	35.9	-8.70
Burra GW	6630-3325	45.50	BR6	01/11/2005	1.63	3200	7.52	53	22.3	270	1821	7.8	107	89	379	13	150	787	294	2.67	0.07	0.128	1008	-5.57	-34.7	77	32	19.6	-7.90
Burra GW	6630-3324	50.00	BR7	28/03/2006	6.56	2804	7.81	86	18.59	178	1744	7.9	90	81	413	19	145	782	212	2.40	0.06	0.22	1033	-5.67	-33.8	59	35	19.6	-8.10
Burra GW	6630-3323	59.50	BR8	30/11/2005	4.04	5520	9.1	112	20.8	140	2939	8.3	183	155	624	18	230	1600	124	4.7	0.16	2.2	2333	-5.63	-32.5	48	36	34.4	-9.10
Burra GW	6630-3322	64.50	BR9	30/11/2005	1.29	4650	8.49	81	20.2	250	2534	7.9	167	132	513	15	186	1270	248	3.8	0.13	1.1	1910	-5.67	-34.6	38	38	18.3	-8.90
Burra GW	6630-3321	65.50	BR10	12/10/2005	-0.43	3480	7.73	-62	19.7	300	2043	7.7	172	92	398	13	268	847	249	2.59	0.14	<0.02	1339	-5.54	-35.5	<20	>41	19.6	-8.20
Burra GW	6630-3320	74.00	BR11	13/10/2005	-0.47	3350	7.89	-110	19.6	260	1937	7.9	124	97	403	14	160	872	265	2.46	0.22	<0.02	1163	-5.53	-35.4	<20	>41	19.4	-8.00
Burra GW	6630-3319	80.50	BR12	14/10/2005	-0.46	3330	8.42	-223	19.7	264	1908	8.2	123	91	402	14	147	873	254	2.68	0.18	<0.02	1064	-5.64	-34.8	<20	>41	20.5	-7.90
Burra GW	6630-3318	90.50	BR13	28/11/2005	-0.27	3510	8.38	-271	22.2	290	2009	8.0	117	100	417	20	145	900	308	2.7	0.218	1.358	2692	-5.62	-31.5	<20	>41	17.7	-8.70
Bull Creek GW	6627-11316	10.15	B1	28/09/2005	1.33	1543	7.14	-194	15.9	218	1367	7.3	101	65	545	21	79	1037	272	2.32	0.08	0.81	479	-5.24	-25.7	190	20	91.2	-15.20
Bull Creek GW	6627-11315	15.38	B2	28/09/2005	2.89	3320	6.94	-117	17	260	2122	7.2	42	31	317	9	59	500	209	1.13	0.12	<0.02	1046	-5.18	-25.4	155	24	87.8	-13.10
Bull Creek GW	6627-11314	20.53	B3	28/09/2005	1.60	1916	7.37	-59	15.3	220	1169	7.1	613	40	333	10	1310	538	273	0.83	0.04	1.01	428	-5.27	-24.7	37	40	88.5	-15.10
Bull Creek GW	6627-11304	22.50	B4	05/10/2005	-0.02	2320	7.08	-52	17.7	260	3119	7.3	488	41	336	10	1030	547	273	0.94	0.04	0.87	2958	-5.13	-26.4	22	>41	84.2	-15.50
Bull Creek GW	6627-11303	29.00	B5	05/10/2005	-0.13	3250	7.2	51	17.5	272	2726	7.4	425	43	339	10	930	548	254	1.00	0.03	0.95	2396	-5.25	-26.5	30	>41	82.3	-15.70
Bull Creek GW	6627-11302	38.00	B6	05/10/2005	-0.17	3210	7.02	73	17.5	230	2549	7.2	268	30	302	15	640	471	169	0.71	0.03	0.93	2149	-5.13	-28.5	28	>41	82.9	-16.10
Bull Creek GW	6627-11300	44.00	B7	06/10/2005	-0.12	2770	7.49	-25	18.3	182	1895	7.6	236	36	290	12	460	464	271	1.04	0.03	0.74	1545	-5.11	-26.2	24	>41	76.3	-15.90
Bull Creek GW	6627-11299	53.00	B8	18/01/2006	0.06	1878	7.43	17	18.6	216	1771	7.6	56	34	294	13	56	465	259	1.12	<0.02	0.94	954	-5.19	-25.90	21	>41	80.50	-16.5
Bull Creek GW	6627-11301	55.00	B9	17/01/2006	0.17	2183	6.97	129	19.8	220	1178	7.8	101	65	545	21	79	1037	272	2.32	<0.02	1.238	274	-5.24	-26.10	<20	>41	71.10	-16.9
Ashbourne GW	6627-11290	12.50	A1	20/02/2006	3.44	4810	7.42	78	25.6	130	2556	7.6	339	70	505	28	211	1258	141	3.40	0.06	0.020	2267	-4.02	-21.8	165	22	94.49	-17.20

Location and sample type	Unit No.	Mid-screen from ground (m)	Sample ID	Collection date	Field measurements							Laboratory analysis																	
					DO ppm	Field EC µS/cm	pH	Redox mV	Temp °C	Field Alkalinity (HCO_3^-) mg/L	TDS mg/L	Lab pH	Ca^{2+} mg/L	Mg^{2+} mg/L	Na^+ mg/L	K^+ mg/L	SO_4^{2-} mg/L	Cl^- mg/L	Lab Alkalinity (HCO_3^-) mg/L	Br^- mg/L	NH_4-N mg/L	NO_x-N mg/L	Sr ug/L	$\delta^{18}0$ ‰ rel SMOW	δ^2H ‰ rel SMOW	CFC-12 pg/kg	CFC-12 apparent age years	^{14}C pmC	$\delta^{13}C$ ‰ PDB
Ashbourne GW	6627-11296	16.00	A2	22/02/2006	3.51	3860	7.97	61	20.5	118	2127	7.4	278	58	417	22	202	989	159	2.70	0.05	0.000	1473	-4.24	-22.1	124	27	82.32	-17.15
Ashbourne GW	6627-11289	24.50	A3	20/02/2006	1.45	4100	6.84	74	19.8	222	2251	7.1	276	95.8	403	15	131	1033	294	2.90	0.05	0.000	1692	-4.07	-22.80	37	39	92.6	-17.10
Ashbourne GW	6627-11295	31.50	A4	22/02/2006	1.44	2190	8.49	63	18.6	188	1238	8.3	146	43.7	221	10	75	501	240	1.40	0.08	0.020	896	-3.96	-20.80	<20	>41		
Ashbourne GW	6627-11288	37.00	A5	20/02/2006	1.3	2120	7.1	-18	17.8	182	1195	7	130	51	205	9	68	478	253	1.30	0.06	0.010	765	-3.81	-21.10	23	>41	71.4	-16.80
Ashbourne GW	6627-11287	44.10	A6	20/02/2006	-0.2	2181	7.41	-104	18.7	182	1233	7.5	131	45	228	11	68	493	255	1.40	0.06	0.010	758	-3.81	-20.9	40	39	69.42	-16.50
Ashbourne GW	6627-11294	46.00	A7	21/02/2006	0.2	1836	8.83	51	20.1	104	1031	8.2	102	31	221	12	74	471	118	1.30	0.06	0.010	785	-3.93	-21.4	50	37	70.50	-16.60
Ashbourne GW	6627-11293	60.50	A8	21/02/2006	2.8	1936	7.53	77	19.4	204	1167	7.6	112	41	224	20	55	447	267	1.20	0.07	0.020	673	-4.14	-21.4	126	27	54.07	-15.00
Ashbourne GW	6627-11292	81.50	A9	21/02/2006	-0.08	2300	7.02	-118	18.3	212	1329	7.2	148	54	229	9	56	537	295	1.50	0.06	0.000	974	-4.03	-22.6	<20	>41	75.30	-16.30
Ashbourne GW	6627-11291	89.50	A10	21/02/2006	0.03	2360	7.03	-139	18.2	230	1353	7.2	162.0	58	221	9	58	545	299.1	1.60	0.06	0.010	1051	-4.01	-22.2	<20	>41	71.20	-16.20
BCC — rain			BCC — rain	27/03/2006							7	6.2	0.6	0.1	0.6	0.2	0.4	1.5	3.7	0.05	0.19	0.190	732						
Finniss rainfall				07/03/2003																				-4.95	-27.4				
Finniss rainfall				29/05/2003																				-5.42	-29.9				
Finniss rainfall				06/07/2005																				-5.28	-23.4				
Echunga pluvio				08/10/2003																				-5.12	-21.9				
Echunga pluvio				25/02/2005																				-2.95	-11.1				
Echunga pluvio				24/06/2005																				-5.55	-25.2				
Mean seawater											35139	8.2	412	1294	10760	399	2712	19350	145	67									

Table A.2 Measured radon concentrations from the unpurged and purged piezometers at the Burra, Bull Creek and Ashbourne investigation sites.

Location	Sample ID	Mid-screen depth from ground (m)	½ screen length (m)	Radon — unpurged date	Radon conc. (C) unpurged (Bq/L)	Radon error (C) (Bq/L)	Radon — purged date	Radon conc. (Co) purged (Bq/L)	Radon error (Co) (Bq/L)
Burra									
	BR1	8.33	1.5	10-Oct-05	42.8	1.5	10-Oct-05	69.9	2.4
	BR2	13.30	1.5	10-Oct-05	49.6	1.7	10-Oct-05	64.9	2.2
	BR3	18.15	1.5						
	BR4	25.00	1.5	27-Mar-06	18.4	0.6	27-Mar-06	289	5
	BR5	33.10	1.5	27-Mar-06	18.8	0.8	27-Mar-06	211	4
	BR6	45.50	1.5	28-Mar-06	14	0.5	28-Mar-06	75.2	1.6
	BR7	50.00	1.5	28-Mar-06	16.6	0.6	28-Mar-06	22.9	0.7
	BR8	59.50	1.5	28-Mar-06	9.8	0.4	28-Mar-06	332	6
	BR9	64.50	1.5	28-Mar-06	19.6	0.6	28-Mar-06	292	6
	BR10	65.50	1.5	12-Oct-05	13.1	0.5	12-Oct-05	83.9	2.8
	BR11	74.00	1.5	13-Oct-05	3.4	0.2	13-Oct-05	73.1	2.5
	BR12	80.50	1.5	13-Oct-05	1.6	0.2	14-Oct-05	75.8	2.6
	BR13	90.50	1.5	28-Mar-06	9.3	0.4	28-Mar-06	90.6	1.8
Bull Creek									
	B1	10.15	1.5						
	B2	15.38	1.5						
	B3	20.53	1.5						
	B4	22.50	2.5	05-Oct-05	3	0.2	05-Oct-05	241	8
	B5	29.00	2.5	05-Oct-05	18.4	0.7	05-Oct-05	297	10
	B6	38.00	3.0	05-Oct-05	172	6	05-Oct-05	358	12
	B7	44.00	3.0	05-Oct-05	16.2	0.6	06-Oct-05	245	8
	B8	53.00	3.0	18-Jan-06	62.7	1.3	18-Jan-05	253	5
	B9	55.00	3.0						
	B10	65.00	3.0						
	B11	84.00	3.0						
Ashbourne									
	A1	12.50	2.5						
	A2	16.00	3.0						
	A3	24.50	2.5	20-Feb-06	117	3.00	20-Feb-06	1270	25
	A4	31.50	2.5	20-Feb-06	251	5.00	22-Feb-06	1500	30
	A5	37.00	2.5	20-Feb-06	141	3.00	20-Feb-06	1490	30
	A6	44.10	2.5	20-Feb-06	116	3.00	20-Feb-06	322	6
	A7	45.50	3.0	21-Feb-06	70.5	1.50	21-Feb-06	464	9
	A8	60.50	2.5	21-Feb-06	81.5	1.60	21-Feb-06	75.4	1.5
	A9	81.50	2.5	21-Feb-06	44.1	1.00	21-Feb-06	432	8
	A10	89.50	2.5	21-Feb-06	66.3	1.40	21-Feb-06	563	10

B. LITHOLOGICAL LOGS

Table A.3 Lithological log for BR3 (unit number 6630-3338) at the Burra investigation site and is the same for the other two shallow piezometers BR1 and BR2

Unit No.	Permit No.	Drill date	Depth from (m)	Depth to (m)	Major lithology	Minor lithology	Description	Water cut (m)
Burra — Burra River Catchment								
6630-3338	PN106402	06/07/2005	0	0.5	Soil	Fill	Topsoil — Brown. Road fill — Brown/grey. Well cuttings from nearby well (slate — blue/grey).	
			0.5	1	Clay		Clay. Friable, low plasticity, soft. Brown.	
			1	1.5	Clay		Clay. Friable, moderate plasticity, moist and sticky. Light brown.	
			1.5	2	Clay		Clay. Friable, low plasticity. Calcrete fragments. Light brown/grey becoming brown with depth.	
			2	4	Clay	Sand	Sandy clay. Low to moderate plasticity, damp. Calcrete fragments. Brown	
			4	6	Clay		Clay. Low to moderate plasticity, damp. Calcrete fragments/grit. Brown	
			6	6.5	Clay		Clay. Low to moderate plasticity, moist to wet at base of sample. Light brown/yellow/light grey mottling	
			6.5	7	Clay		Clay. Significant calcrete, quartzite and weathered slate fragments. Wet. Brown	
			7	11	Clay		Clay. Weathered slate fragments, soft, brown/blue/grey. Minor quartz and quartzite, well rounded, white/opaque. Minor silcrete, hard, white/light yellow. Minor calcrete fragments, well cemented, hard, light brown yellow. Red brown	7
			11	13	Clay	Silt	Silty Clay. Significant weathered slate fragments, soft, brown/blue/grey. Minor muscovite. Light brown	
			13	14	Clay	Silt	Silty Clay. Significant weathered slate fragments, soft, brown/blue/grey. Minor muscovite. Very minor metasandstone fragments. Light brown	
			14	17	Clay	Silt	Silty Clay. Significant weathered slate fragments, soft, brown/blue/grey. Minor muscovite. Very minor metasandstone fragments. Light brown	

Table A.4 Lithological log for the 8 inch hole at the Burra investigation site (unit number 6630-3295)

Unit No.	Permit No.	Drill date	Depth from (m)	Depth to (m)	Major lithology	Minor lithology	Description
Burra Creek Catchment							
6630-3295	PN 102149	26/11/2004	0.0	2.0	Soil	Clay	Topsoil. Calcrete fragments and clay. Grey, white, yellowish red.
			2.0	8.0	Clay		Clay. High plasticity, moderate-low density, soft. Calcrete fragments. Yellowish red.
			8.0	10.0	Silcrete		Silcrete. Fine-grained, slight crystalline appearance. Very hard, well cemented, slightly calcareous. Pale yellow.
			10.0	16.0	Clay	Silt	Silty clay. Low plasticity, low density. Very minor muscovite. Minor weathered slate fragments, minor ferruginous fragments. Increased clay between 14 and 16 m. Pale yellow.
			16.0	18.0	Slate		Slate. Minor slaty cleavage. Weathered. Friable. Minor ferruginous fragments. Pale olive.
			18.0	23.0	Slate		Slate. Slaty cleavage. Weathered. Minor metasandstone. Fine-grained, moderate-well cemented. Minor quartz vein material (iron stained), minor ferruginous fragments. Pale olive.
			23.0	25.0	Slate		Slate. Slaty cleavage. Friable. Minor fine-grained muscovite. Iron stained fragments, iron staining on fracture surfaces. Light grey and orange-brown.
			25.0	33.0	Slate	Metasandstone	Slate. Slaty cleavage. Friable. Minor fine-grained muscovite. Minor metasandstone. Iron staining on fracture surfaces cross-cutting cleavage. Light grey and orange-brown.
			33.0	39.0	Slate		Slate. Slaty cleavage. Minor fine-grained muscovite. Iron staining on fracture surfaces cross cutting cleavage. Possibly two fracture sets, perpendicular and 45° to cleavage. Light grey.
			39.0	61.0	Slate		Slate. Slaty cleavage. Well cemented. Iron staining on fracture surfaces. Light grey.
			61.0	71.0	Slate		Slate. Slaty cleavage. Well cemented. Minor iron staining. Very minor quartz vein material between 65 and 67 m. Minor pyrite on fracture surfaces between 67–69 m. Dark grey.
			71.0	101.0	Slate		Slate. Slaty cleavage. Well cemented. Minor pyrite on fracture surfaces. Minor quartz vein material between 79 and 83 m and 87 and 89 m. Dark grey.
			101.0	107.0	Slate	Metasandstone	Slate. Slaty cleavage. Well-moderately cemented. Decreased pyrite on fracture surfaces. Dark grey. Fine-grained metasandstone, well cemented, minor laminations. Olive green.
			107.0	109.0	Slate	Metasandstone	Slate. Slaty cleavage. Well cemented. Quartz vein material (20%). Dark grey.
			109.0	119.0	Slate	Metasandstone	Slate. Slaty cleavage. Well cemented. Metasandstone, highly silicified. Quartz vein material (increases between 111 and 115 m). Dark and light grey.

Table A.5 Lithological log for the 10 inch hole at the Burra investigation site (unit number 6630-3296).

Unit No.	Permit No.	Drill date	Depth from (m)	Depth to (m)	Major lithology	Minor lithology	Description
Burra Creek Catchment							
6630-3296	PN 102412	1/12/2004	0.0	2.0	Soil	Clay	Topsoil. Calcrete fragments and clay. White, grey and weak red.
			2.0	6.0	Clay		Clay. Moderate density, low plasticity, stiff, moderate sheen. Minor calcrete fragments. Red.
			6.0	8.0	Clay		Clay. Moderate plasticity, moderate density, soft, damp, moderate sheen. Red.
			8.0	10.0	Slate		Slate. Slaty cleavage. Weathered. Iron stained, dendritic manganese. Minor silcrete fragments, minor clay. Light yellowish brown.
			10.0	23.0	Slate		Slate. Slaty cleavage. Well cemented, hard. Weathered. Iron stained, dendritic manganese. Light yellowish brown. Cobble 'layer' at approx. 18 m.
			23.0	25.0	Slate		Slate. Slaty cleavage. Well cemented, hard. Weathered. Iron staining. Minor quartz vein fragments, minor ironstone fragments. Light yellowish brown.
			25.0	27.0	Slate		Slate. Slaty cleavage. Well cemented. Moderate weathering. Iron staining on fracture surfaces. Light grey and light yellowish brown.
			27.0	33.0	Slate		Slate. Slaty cleavage. Well cemented. Decreasing weathering. Light grey.
			33.0	41.0	Slate		Slate. Slaty cleavage. Well cemented. Moderate weathering. Iron staining. Light grey and light yellowish brown.
			41.0	47.0	Slate	Metasandstone	Slate. Slaty cleavage. Well cemented, minor silicification. Minor metasandstone. Iron staining on fracture surfaces. Dark and light grey.
			47.0	59.0	Slate	Metasandstone	Slate. Slaty cleavage. Well cemented, minor silicification. Minor metasandstone. Iron staining on fracture surfaces, minor dendritic manganese. Dark and light grey.
			59.0	63.0	Slate		Slate. Slaty cleavage. Well cemented. Iron staining on fracture sets. Fracture sets at high angle to cleavage. Dark grey.
			63.0	71.0	Slate		Slate. Slaty cleavage. Well cemented. Iron staining on fracture sets. Dark grey.

Table A.6 Lithological log for B3 (unit number 6627-11314) at the Bull Creek investigation site and is the same for the other two shallow piezometers B1 and B2.

Unit No.	Permit No.	Drill date	Depth from (m)	Depth to (m)	Major lithology	Minor lithology	Description	Water cut (m)
Bull Creek — Angas River Catchment								
6627-11314	PN106405	04/07/2005	0.0	0.5	Soil		Topsoil. Fine/medium sand. Moist. Dark chocolate brown	
			0.5	1.0	Clay	Silt	Silty clay. Friable, low plasticity. Moist. Light brown/brown mottling	
			1.0	2.0	Clay		Clay. Low to medium plasticity. Moist. Light brown/dark brown	
			2.0	2.5	Siltstone	Clay	Siltstone. Very weathered. Fine grained. Some medium grained quartz sand banding. Some muscovite. Soft. Light tan/light grey. Clay present at 2–2.25 m, red-brown.	
			2.5	3.5	Siltstone		Siltstone. Weathered. Fine grained. Soft. Some muscovite. Minor quartz pieces. Light tan/light grey	
			3.5	6.0	Siltstone		Siltstone. Weathered. Micaceous. Fine grained. Medium-hard. Dark grey/blue	
			6.0	7.0	Siltstone	Quartzite	Siltstone. Weathered. Micaceous. Fine grained. Medium-hard. Dark grey/blue. Quartzite 50%, white.	
			7.0	9.0	Siltstone		Siltstone. Weathered. Micaceous. Fine grained. Soft-medium. Dark grey/blue	
			9.0	10.5	Siltstone	Quartzite	Siltstone. Weathered. Micaceous. Fine grained. Medium-hard. Dark grey/blue. Quartzite 50%, white.	
			10.5	12.5	Siltstone		Siltstone. Weathered. Micaceous. Fine grained. Hard. Some quartz. Dark grey/blue	
			12.5	19.0	Siltstone		Siltstone. Weathered. Micaceous. Fine grained. Hard. Dark grey/blue	
			19.0	22.0	Siltstone		Siltstone. Weathered. Micaceous. Fine grained. Very hard. Dark grey/blue	19

Table A.7 Lithological log for the 8 inch hole at the Bull Creek investigation site (unit number 6627-11092).

Unit No.	Permit No.	Drill date	Depth from (m)	Depth to (m)	Major lithology	Minor lithology	Description
Bull Creek — Angas River Catchment							
6627-11092	PN 102088	25/10/2004	0.0	1.0	Soil	Clay	Dark brown mainly sandy topsoil. Minor clay present.
			1.0	4.0	Sand	Clay	Brown clayey sand (topsoil) with minor micas and lumps of silty clay.
			4.0	5.0	Metasiltstone		Light grey friable metasiltstone with minor micas and iron staining. Lumps of silty clay present.
			5.0	6.0	Metasiltstone		As above minus lumps of silty clay.
			6.0	21.0	Metasiltstone		Light grey friable metasiltstone with minor micas and iron staining present.
			21.0	29.0	Metasiltstone		As above (6.0–21.0 m) but fragments of metasiltstone, not friable.
			29.0	42.0	Metasiltstone		Light grey hard metasiltstone with minor micas, minor iron staining and minor quartz fragments.
			42.0	46.0	Metasiltstone		As above but with greater quartz present, 5–10%.
			46.0	68.0	Metasiltstone		Grey well-silicified metasiltstone with minor iron staining, minor micas and minor quartz fragments and veining.
			68.0	76.0	Metasiltstone		Grey silicified hard metasiltstone with minor micas present. Iron staining absent.
			76.0	120.0	Metasiltstone		Grey to green-grey metasiltstone, silicified, hard fine-grained fragments. Minor micas (mainly muscovite) present. Iron staining and quartz veining on fragments. Pyrite on cleavage plains at 77, 83, 92–94 and 108 m. EOH

Table A.8 Lithological log for the 10 inch hole at the Bull Creek investigation site (unit number 6627-11091).

Unit No.	Permit No.	Drill date	Depth from (m)	Depth to (m)	Major lithology	Minor lithology	Description
Bull Creek — Angas River Catchment							
6627-11091	PN 102087	22/10/2004	0.0	1.0	Soil		Olive green topsoil.
			1.0	10.0	Silt	Soil	Light grey silty topsoil. High muscovite content. Minor fragments of friable metasandstone with minor iron staining.
			10.0	17.0	Metasiltstone	Soil	As above (1.0–9.0), but rock fragments of metasiltstone.
			17.0	18.0	Metasiltstone		Friable light grey metasiltstone with 10% micas (biotite and muscovite). Iron staining present.
			18.0	19.0	Clay		Grey sticky clay.
			19.0	29.0	Metasiltstone		Light grey metasiltstone with 10% micas (biotite and muscovite). Not friable. Iron staining present.
			29.0	36.0	Metasiltstone		Light grey metasiltstone as above. 10% quartz present and minor pyrite.
			36.0	61.0	Metasiltstone		Hard light grey metasiltstone. Abundant iron staining and 5–15% quartz present. EOH

UNITS OF MEASUREMENT

Units of measurement commonly used (SI and non-SI Australian legal)

Name of unit	Symbol	Definition in terms of other metric units	Quantity
day	d	24 h	time interval
gigalitre	GL	10^6 m^3	volume
gram	g	10^{-3} kg	mass
hectare	ha	10^4 m^2	area
hour	h	60 min	time interval
kilogram	kg	base unit	mass
kilolitre	kL	1 m^3	volume
kilometre	km	10^3 m	length
litre	L	10^{-3} m^3	volume
megalitre	ML	10^3 m^3	volume
metre	m	base unit	length
microgram	μg	10^{-6} g	mass
microlitre	μL	10^{-9} m^3	volume
milligram	mg	10^{-3} g	mass
millilitre	mL	10^{-6} m^3	volume
millimetre	mm	10^{-3} m	length
minute	min	60 s	time interval
second	s	base unit	time interval
year	y	365 or 366 days	time interval

δ^2H	hydrogen isotope composition
$\delta^{18}O$	oxygen isotope composition
^{14}C	carbon-14 isotope (percent modern Carbon)
$\delta^{13}C$	dissolved inorganic carbon (DIC)
CFC	chlorofluorocarbon (picograms per kilogram — pg/kg)
EC	electrical conductivity (μS/cm)
SEC	specific electrical conductivity (μS/cm)
pH	acidity
ppm	parts per million
ppb	parts per billion
TDS	total dissolved solids (mg/L)
~	approximately equal to

GLOSSARY

Act (the) — In this document, refers to the *Natural Resources Management Act* (SA) *2004*.

Ambient — The background level of an environmental parameter (e.g. a background water quality such as salinity).

Aquifer — An underground layer of rock or sediment that holds water and allows water to percolate through.

Aquifer, confined — Aquifer in which the upper surface is impervious and the water is held at greater than atmospheric pressure. Water in a penetrating well will rise above the surface of the aquifer.

Aquifer test — A hydrological test performed on a well, aimed to increase the understanding of the aquifer properties, including any interference between wells, and to more accurately estimate the sustainable use of the water resource available for development from the well.

Aquifer, unconfined — Aquifer in which the upper surface has free connection to the ground surface and the water surface is at atmospheric pressure.

Artificial recharge — The process of artificially diverting water from the surface to an aquifer. Artificial recharge can reduce evaporation losses and increase aquifer yield. *(See recharge, natural recharge, aquifer.)*

Baseflow — The water in a stream that results from groundwater discharge to the stream. (This discharge often maintains flows during seasonal dry periods and has important ecological functions.)

Bore — *See well.*

Catchment — That area of land determined by topographic features within which rainfall will contribute to runoff at a particular point.

Conjunctive use — The utilisation of more than one source of water to satisfy a single demand.

CWMB — Catchment Water Management Board.

DWLBC — Department of Water, Land and Biodiversity Conservation (Government of South Australia).

EC — Electrical conductivity. 1 EC unit = 1 micro-Siemen per centimetre (µS/cm) measured at 25°C. Commonly used to indicate the salinity of water.

EMLR — Eastern Mount Lofty Ranges.

Evapotranspiration — The total loss of water as a result of transpiration from plants and evaporation from land, and surface waterbodies.

Floodplain — Of a watercourse, means: (a) the floodplain (if any) of the watercourse identified in a catchment water management plan or a local water management plan; adopted under Part 7 of the *Water Resources Act 1997*; or (b) where paragraph (a) does not apply — the floodplain (if any) of the watercourse identified in a development plan under the *Development Act 1993*, or (c) where neither paragraph (a) nor paragraph (b) applies — the land adjoining the watercourse that is periodically subject to flooding from the watercourse.

Geological features — Include geological monuments, landscape amenity and the substrate of land systems and ecosystems.

GNIP — Global Network of Isotopes in Precipitation.

Groundwater — *See underground water.*

Heavy metal — Any metal with a high atomic weight (usually, although not exclusively, greater than 100), for example mercury, lead and chromium. Heavy metals have a widespread industrial use, and many are released into the biosphere via air, water and solids pollution. Usually these metals are toxic at low concentrations to most plant and animal life.

Hydrogeology — The study of groundwater, which includes its occurrence, recharge and discharge processes and the properties of aquifers. *(See hydrology.)*

Hydrography — The discipline related to the measurement and recording of parameters associated with the hydrological cycle, both historic and real time.

Hydrology — The study of the characteristics, occurrence, movement and utilisation of water on and below the Earth's surface and within its atmosphere. *(See hydrogeology.)*

ICP-ES — Inductively Coupled Plasma Emission Spectrometry.

Integrated catchment management — Natural resources management that considers in an integrated manner the total long-term effect of land and water management practices on a catchment basis, from production and environmental viewpoints.

IAEA — International Atomic Energy Agency.

LMWL — local meteoric water line.

MLR — Mount Lofty Ranges.

Model — A conceptual or mathematical means of understanding elements of the real world which allows for predictions of outcomes given certain conditions. Examples include estimating storm runoff, assessing the impacts of dams or predicting ecological response to environmental change.

Mount Lofty Ranges Watershed — The area prescribed by Schedule 1 of the regulations.

Natural recharge — The infiltration of water into an aquifer from the surface (rainfall, streamflow, irrigation etc.) *(See recharge area, artificial recharge.)*

Natural Resources — Soil; water resources; geological features and landscapes; native vegetation, native animals and other native organisms; ecosystems.

Permeability — A measure of the ease with which water flows through an aquifer or aquitard.

Potentiometric head — The potentiometric head or surface is the level to which water rises in a well due to water pressure in the aquifer.

Prescribed water resource — A water resource declared by the Governor to be prescribed under the Act, and includes underground water to which access is obtained by prescribed wells. Prescription of a water resource requires that future management of the resource be regulated via a licensing system.

Recharge area — The area of land from which water from the surface (rainfall, streamflow, irrigation, etc.) infiltrates into an aquifer. *(See artificial recharge, natural recharge.)*

Surface water — (a) water flowing over land (except in a watercourse), (i) after having fallen as rain or hail or having precipitated in any another manner, (ii) or after rising to the surface naturally from underground; (b) water of the kind referred to in paragraph (a) that has been collected in a dam or reservoir.

Underground water (groundwater) — Water occurring naturally below ground level or water pumped, diverted or released into a well for storage underground.

Water allocation — (a) in respect of a water licence means the quantity of water that the licensee is entitled to take and use pursuant to the licence; (b) in respect of water taken pursuant to an authorisation under s. 11 means the maximum quantity of water that can be taken and used pursuant to the authorisation.

Water allocation plan (WAP) — A plan prepared by a CWMB or water resources planning committee and adopted by the Minister in accordance with Division 3 of Part 7 of the Act.

Water licence — A licence granted under the Act entitling the holder to take water from a prescribed watercourse, lake or well or to take surface water from a surface water prescribed area. This grants the licensee a right to take an allocation of water specified on the licence, which may also include conditions on the taking and use of that water. A water licence confers a property right on the holder of the licence and this right is separate from land title.

Watercourse — A river, creek or other natural watercourse (whether modified or not) and includes: a dam or reservoir that collects water flowing in a watercourse; and a lake through which water flows; and a channel (but not a channel declared by regulation to be excluded from the this definition) into which the water of a watercourse has been diverted; and part of a watercourse.

Well — (a) an opening in the ground excavated for the purpose of obtaining access to underground water; (b) an opening in the ground excavated for some other purpose but that gives access to underground water; (c) a natural opening in the ground that gives access to underground water.

REFERENCES

Banks, EW, Wilson, T & Love, AJ (in prep.), 'Groundwater recharge investigations in the Upper Marne River Catchment, South Australia', Report, Department of Water, Land and Biodiversity Conservation, Adelaide.

Cook, PG 2003, A guide to regional groundwater flow in fractured rock aquifers CSIRO Land and Water, Australia.

Cook PG & Bohlke, J-K 1999, 'Determining timescales for groundwater flow and solute transport', in PG Cook & AL Herczeg (eds), *Environmental tracers in subsurface hydrology*, Kluwer Academic, Boston, London, pp.1-30.

Cook, PG, Love, AJ & Dighton, JC 1999, 'Inferring groundwater flow in fractured rock from dissolved radon', *Groundwater*, 37(4), pp.606-610.

Cook, PG & Simmons, CT 2000, 'Using environmental tracers to constrain flow parameters in fractured rock aquifers: Clare Valley, South Australia', in B Faybishenko (ed.), *Dynamics of fluids in fractured rocks: Concepts and recent advances*, AGU Monograph, 122, pp.337-347.

Cook, PG, Solomon, DK, Sandford, WE, Busenberg, E, Plummer, LN & Poreda, RJ 1996, 'Inferring shallow groundwater flow in saprolite and fractured rock using environmental tracers', *Water Resources Research*, 32(6), pp.1501-1509.

Coplen, TB, Herczeg, AL & Barnes, CJ 1999, 'Isotope engineering using stable isotopes of the water molecule to solve practical problems', in PG Cook & AL Herczeg (eds), *Environmental tracers in subsurface hydrology*, Kluwer Academic, Boston, London, pp.79-110.

Cresswell, RG & Herczeg, AL 2004, Groundwater recharge, mixing and salinity across the Angas–Bremer Plains, South Australia: Geochemical and isotopic constraints, CSIRO Land and Water Technical Report 29/04, Bureau of Rural Sciences Technical Report.

Dansgaard, W 1964, 'Stable isotopes in precipitation', *Tellus*, 16, pp.436-469.

Fetter, CW 2001, 'Cooper-Jacob straight line method', in *Applied Hydrogeology*, 4th edn, Prentice Hall, New Jersey, pp.174.

Fontes, JC & Garnier, JM 1979, 'Determination of the initial ^{14}C activity of the total dissolved carbon: A review of the existing models and a new approach', *Water Resources Research*, 15, pp.399-413.

Gravestock, DI & Gatehouse, CG 1995, 'Early and Middle Palaeozoic', in JF Drexel & WV Preiss (eds), *The geology of South Australia*, Vol 2, The Phanerozoic, Bulletin 54, Geological Survey, Adelaide, pp.3-61.

Harrington, GA 1999, 'Recharge mechanisms and chemical evolution in an arid groundwater system, Central Australia', PhD thesis, School of Chemistry, Physics and Earth Sciences, Flinders University of South Australia.

Harrington, GA, James-Smith, JM, Wohling, D & Van Den Akker, J 2004, Hydrogeological investigations of the Mount Lofty Ranges, progress report 5: Drilling phases 2.1 to 2.3: Research and monitoring wells at Scott Creek, Balhannah, Willunga Fault, Lobethal, Eden Valley and Ashbourne, Report DWLBC 2004/04, Department of Water, Land and Biodiversity Conservation, Adelaide.

REFERENCES

Herczeg, AL & Edmunds, WM 1999, 'Inorganic ions as tracers', in PG Cook & AL Herczeg (eds), *Environmental tracers in subsurface hydrology*, Kluwer Academic, Boston, London, pp.31-77.

Leaney, F 2006, CSIRO isotope analytical service, CSIRO, Canberra, viewed June 2006, <http://www.clw.csiro.au/services/isotope>.

Love, AJ, Cook, PG, Harrington, GA & Simmons, CT 2002, *Groundwater flow in the Clare Valley*, Report DWR 02/03/0002, Department for Water Resources, Adelaide.

Love, AJ, Simmons, CT, Cook, P, Harrington, GA, Herczeg, A & Halihan, T (in prep.), 'Estimating groundwater flow rates in fractured metasediments: Clare Valley, South Australia', International Association of Hydrogeologists SP Series.

Neretnieks, I 1981, 'Age dating of groundwater in fissured rock: Influence of water volumes in micropores', *Water Resources Research*, 17(2), pp.421-422.

Parkhurst, DL & Appelo, CAJ 1999, User's guide to PHREEQC (Version 2) — A computer program for speciation, batch-reaction, one-dimensional transport, and inverse geochemical calculations, Water Resources Investigations Report 99-4259, US Geological Survey.

Pearson, FJ Jr & Hanshaw, BB 1970, 'Sources of dissolved carbonate species in groundwater and their effects on carbon 14 dating', in *Isotope Hydrology 1970*, IAEA, Vienna, pp.271-285.

Savadamuthu, K 2003, *Surface water assessment of the Upper Finniss Catchment*, Report DWLBC 2003/18, Department of Water, Land and Biodiversity Conservation, Adelaide.

Szabo, Z, Rice, DE, Plummer, LN, Busenberg, E, Drenkard, S & Schlosser, P 1996, 'Age dating of shallow groundwater with chlorofluorocarbons, tritium/helium 3, and flow path analysis, southern New Jersey coastal plain', *Water Resources Research*, 32(4), pp.1023-1038.

Tamers, MA 1967, 'Surface-water infiltration and groundwater movement in arid zones of Venezuela', in *Isotopes in Hydrology*, IAEA, Vienna, pp.339-351.

Zulfic, D & Barnett, S 2003, *Eastern Mount Lofty Ranges groundwater assessment*, Report DWLBC 2003/25, Department of Water, Land and Biodiversity Conservation, Adelaide.